Myopia and Glaucoma

Kazuhisa Sugiyama
Nagahisa Yoshimura
Editors

Springer

Myopia and Glaucoma

Kazuhisa Sugiyama • Nagahisa Yoshimura
Editors

Myopia and Glaucoma

Springer

Editors
Kazuhisa Sugiyama
Department of Ophthalmology and Visual Science
Kanazawa University Graduate School of Medical Science
Kanazawa, Japan

Nagahisa Yoshimura
Department of Ophthalmology and Visual Sciences
Graduate School of Medicine and Faculty of Medicine Kyoto University
Kyoto, Japan

ISBN 978-4-431-55671-8 ISBN 978-4-431-55672-5 (eBook)
DOI 10.1007/978-4-431-55672-5

Library of Congress Control Number: 2015952456

Springer Tokyo Heidelberg New York Dordrecht London

Printed on acid-free paper

Springer Japan KK is part of Springer Science+Business Media (www.springer.com)

Preface

The association between myopia and glaucoma has been the subject of many clinical trials and population-based studies. Most have suggested that moderate to high myopia is associated with increased risk of primary open-angle glaucoma (POAG) and normal-tension glaucoma. Diagnosis of glaucoma involves several factors, including the level of intraocular pressure, characteristics of structural changes in the optic disc and retinal nerve fiber layer or inner retina, and functional deterioration, i.e., visual field defects. However, the clinical diagnosis of glaucoma in highly myopic eyes may be difficult.

The optic discs of myopic patients are notoriously difficult to assess, especially those coexistent with tilted discs. The discs frequently appear glaucomatous with larger diameters, greater cup-to-disc ratios, and larger and shallower optic cups. With regard to visual field defects, myopic retinal degeneration, which is common in high myopias, may cause defects that mimic glaucomatous visual field defects. It is possible that such cases of high myopia may be misclassified or misdiagnosed as POAG. Myopia, especially in moderate to high myopia, tends to present with a thin retina and choroid as the elongation of the eyeball leads to stretching of the structures, causing them to appear thinner than normal. Despite new imaging technologies with reasonable sensitivity and specificity for detecting glaucoma, each technology has some challenges associated with it when assessing myopic eyes.

We hope that this book will provide good guidance to all clinicians for diagnosing and monitoring the progression of glaucoma in myopia, especially in high myopias. It is not only a review. Our aim is to create a reference book on how to understand myopia and glaucoma better by presenting our experts' long experience, and it thus includes many of our actual clinical studies. Research findings presented here may help in understanding the mechanisms or pathogenesis of myopic glaucoma. From clinical epidemiology studies of myopia, we knew that myopia is a growing public health problem, and its prevalence and severity are increasing in various parts of the world, particularly in Asia. Epidemiological studies have suggested that there is an "epidemic" of myopia in Asia. Numerous case series, case controls, and large

population-based studies support the conclusion that there is an association between high myopia and POAG. We predict that there will be ongoing discussion and interest in this field among experts.

The course of disease in POAG with high myopia can be seen in long-term follow-ups, and common clinical features between them can be delineated only by analyzing a sufficient volume of patient data. In this book we would like to share our valuable experience through our clinical studies. This knowledge will narrow the vague area between high myopia and glaucoma for clinicians and researchers.

This book will be beneficial to all ophthalmologists both in medical school and in research centers of universities as well as in private or government hospitals and clinics. The book is written not only for ophthalmologists, however, but also will be a valuable resource for ophthalmic researchers, postgraduate students, and optometrists or certified orthoptists.

Kanazawa, Japan — Kazuhisa Sugiyama
Kyoto, Japan — Nagahisa Yoshimura

Contents

Chapter 1
An Epidemiologic Perspective

Aiko Iwase

Abstract The prevalence rates of primary open-angle glaucoma (POAG) and myopia are reported in many population-based studies. The association between myopia and POAG was discussed based on the results of population-based studies, and the importance of myopia as a strong risk factor for POAG was emphasized. A recent increase in the prevalence rate of myopia likely will lead to a future increase in the prevalence rate of POAG.

Keywords Primary open-angle glaucoma • Myopia • Prevalence rates

1.1 Introduction

Myopia, which affects about 1.6 billion people worldwide, is expected to affect 2.5 billion people by 2020 [1] and is associated with many vision-threatening eye diseases [2]. In addition to severe impairment of visual acuity associated with excessive pathologic myopia [2], the myopic refractive error, if uncorrected, also can cause visual impairment by itself, while correction of the refractive error with spectacles, contact lenses, or refractive surgery may impose a considerable socio-economic burden on individuals and society. The association of myopia and glaucoma has long been discussed, and myopia has been identified as an independent and strong risk factor for primary open-angle glaucoma (POAG) [3].

Myopic eyes have longer axial lengths and vitreous chamber depths, and it seems reasonable that these eyes tend to have a more deformed lamina cribrosa contributing to higher susceptibility to mechanical damage [4–6]. The association or relationship between myopia and POAG has long been a subject of numerous hospital-based observational studies. While that study design can highlight a particular aspect of this association, those studies are prone to selection bias, which may obscure some important causal relationships between the pathologies. In this entry, the relationship between myopia and POAG is discussed based on the results of population-based studies.

A. Iwase, M.D., Ph.D. (✉)
Tajimi Iwase Eye Clinic, 3-101-1, Honmachi, Tajimi, Gifu 507-0033, Japan
e-mail: aiko-gif@umin.net

K. Sugiyama, N. Yoshimura (eds.), *Myopia and Glaucoma*,
DOI 10.1007/978-4-431-55672-5_1

Table 1.1 Prevalence of myopia: summary data from previous population-based studies

Ethnicity	Country	Project	Age range (years)	Participation rate (%)	No. samples	Myopia (<−0.5 diopters)	Myopia (<−1.0D)	High myopia (<−5 D)	High myopia (<−6 D)
Caucasian	USA	Baltimore Eye Survey [24]	40 ≤	79.2	2,659	24.1	16.8	2.6	1.9
Caucasian	USA	Beaver Dam Eye Study [25]	43–86	83.1	4,926	26.2	26.5	3.8	
Caucasian	USA	National Health and Nutrition Examination Survey [26]	20 <	84.5	12,010	41.0	33.1	6.0	
Caucasian	Australia	Blue Mountain Eye Study [27]	49 ≤	82.4	3,654	15.5	12.6	1.8	
Caucasian	The Netherlands	Rotterdam Study [28]	55–95	79.7	5,673		17.6	4.0	
Caucasian	Australia	Melbourne Visual Impairment Project [29]	40≤	83	3,271	16.9	15.8	2.5	
Caucasian	Germany	Gutenberg Health Study [30]	35–74	92.9	13,959	35.1	26.2		3.5
Mongolian	Mongolia	(Hovsgol) [31]	40 ≤		1,617	17.2			2.7
Japanese	Japan	Tajimi Study [32]	40 ≤	78.1	3,120	41.8	32.5	8.1	5.5
Chinese	Taiwan	Shihpai Eye Study [33]	65 ≤	66.6	1,361	19.4	15.0	2.4	
Chinese	China	Beijing Eye Study [34]	40–101	83.4	4,319	21.8	16.9	3.3	2.6
Chinese	China	Handan Eye Study [35]	30 ≤	85.9	6,491	26.7		1.8	
Korean	Korea	Namil Study [36]	40 ≤		1,215	20.5			1.0
Chinese	Singapore	Tanjong Pagar Study [37]	40–79	71.8	1,232	38.7	28.0		6.9
Chinese	China	Liwan Study [19]	50 ≤		1,269	32.3			
Malaysian	Singapore	Singapore Malay Eye Survey [38]	40–80	78.7	3,280	30.5	20.0	3.9	
Indonesian	Indonesia	Sumatora [39]	41 ≤		358	34.1	26.1		1.7

Indian	India	Andhra Pradesh Eye Disease Study [40]	40 ≤	85.4	2,522	34.6		4.5	
Indian	Singapore	Singapore Indian Eye study [41]	40	75.6	3,400	28.0	20.4	4.1	
Indian	India	Central India Eye and Medical Study [42]	30<	83.1	5,885	17.0	13.0	1.8	0.9
Burmese	Myanmar	Meiktila Eye Study [43]	40 ≤	75.1	1,863	50.9	42.7		6.5
Indian	India	Chennai Glaucoma Study (rural) [44]	40 ≤	81.8	3,924	36.5			
Indian	India	Chennai Glaucoma Study (urban) [45]	40 ≤	80.2	3,850	23.2			
Iranian	Iran	The Yazd Eye Study [46]		90.4	2,098	36.5			2.3
Bengalese	Bangladesh	Bangladesh National Blindness and Low vision Survey [47]	30 ≤	90.9	1,1624	22.1	12.5	1.8	
Hispanic	USA	Proyecto VER [48]	40 <	72	4,774		18.0	2.5	
Hispanic	USA	Los Angeles Latino Eye Study [49]	40 ≤	82	6,357		16.8	2.4	
Hispanic	Spain	Segovia Study [50]	40–79	89.6	510	25.4			
Black	USA	Baltimore Eye Survey [24]	40 ≤	79.2	2,200	20.9			0.9
Afro-Caribbean	West Indies	Barbados Eye Study [51]	40–84	84	4,036	21.9			

1.2 Prevalence of Myopia

The prevalence rates of myopia have been reported to differ among ethnic groups. For example, Chinese and Japanese populations have higher prevalence rates of myopia than Caucasian, black, or Hispanic populations (Table 1.1). However, the prevalence rates of myopia also differ among the Asian countries. Both genetic and environmental factors have been implicated in the etiology of myopia [7, 8], and variations in genetic and environmental factors combined among ethnic groups should be mainly responsible for differences in the prevalence rates of myopia among countries. It is noteworthy that the prevalence rates of myopia and high myopia in Japanese are the highest in the world [9].

1.3 Prevalence of POAG

The prevalence rates of POAG reported in various countries are summarized in Table 1.2. The prevalence rates of POAG, which seem to be much less dependent on environmental factors than myopia, also differ among ethnic groups, i.e., African-American populations have the highest prevalence rates followed by Hispanic and Japanese populations. The prevalence rates of POAG generally are relatively low in Caucasians.

1.4 Relationship Between Intraocular Pressure and Refraction

Needless to say, high intraocular pressure (IOP) is a definitive risk factor for POAG. As summarized in Table 1.3, the distribution of IOP values also differs among ethnic groups with African-American and Caucasian populations having relatively higher mean values. Unexpectedly, there is a paucity of information on the relationship between refraction and IOP. In two population-based studies performed by the Japan Glaucoma Society (Tajimi Study and Kumejima Study), higher myopia was associated significantly with higher IOP [10, 11], which also agreed with the results reported in a large Japanese study [12] and a population-based study performed in Northern China (Beijing Eye Study) [13].

This significant correlation between IOP, the most important risk factor for POAG, and myopic refraction, another important risk factor for POAG, highlights the importance of refractive status in managing patients with POAG in Japan.

Table 1.2 Prevalence of OAG and NTG: summary data from previous population-based studies

Ethnicity	Country	Project	Age range (years)	Prevalence of OAG (crude)	NTG/OAG (%)	Prevalence of NTG (%) (crude)
Caucasian	UK	(Hollows and Graham) [52]	40–74	0.4	35.0	0.2
Caucasian	Ireland	Roscommon Glaucoma Survey [53]	50 ≤	1.9	36.6	0.7
Caucasian	USA	Baltimore Eye Survey [54]	40 ≤	**1.4**		
Caucasian	USA	Beaver Dam Eye Study [55]	43–86	2.1	32.0	
Caucasian	Australia	Blue Mountain Eye Study [56]	59 ≤	**3.0**		
Caucasian	The Netherlands	Rotterdam Study [57]	55–95	1.1	39.0	0.4
Caucasian	Italy	Casteldaccia Eye Study [58]	40 ≤	1.2	38.5	
Caucasian	Italy	Egna-Neumarkt Study [59]	40 ≤	2.0	28.6	0.6
Caucasian	Australia	Melbourne Visual Impairment Project [60]	40 ≤	**1.8**		1.4
Mongolian	Mongolia	(Hovsgol) [61]	40 ≤	0.4		
Mongolian	Mongolia	Kailu [62]	40 <	1.4	64.0	0.9
Japanese	Japan	Japan nationwide [12]	40 <	2.5	79.0	2.0
Japanese	Japan	Tajimi Study [63]	40 ≤	**3.9**	92.3	3.6
Japanese	Japan	Kumejima Study [64]	40 ≤	4.0	82.1	3.3
Korean	Korea	Namil Study [65]	50 ≤	3.6	77.8	2.8
Chinese	China	Beijing Eye Study [66]	40–101	2.5		
Chinese	**China**	**Handan Eye Study** [67]	**30 <**	**1.2**	**90.0**	**1.0**
Chinese	China	Liwan Study [68]	50–102	**2.1**	85.0	1.8
Chinese	Singapore	Tanjong Pagar Study [69]	40–79	**1.2**		
Malay	Singapore	Singapore Malay Eye Survey [70]	40–80	**2.5**	84.6	2.7
Bengalese	Bangladesh	Bangladesh Study [71]	35 ≤	1.2		
Thai	Thailand	(Rom Klao) [72]	50 ≤	2.3		
Indian	India	Aravind Comprehensive Eye Survey [73]	40 ≤	**1.2**	75.0	0.9

(continued)

Table 1.2 (continued)

Ethnicity	Country	Project	Age range (years)	Prevalence of OAG (crude)	NTG/OAG (%)	Prevalence of NTG (%) (crude)
Indian	India	Andhra Pradesh Eye Disease Study (rural) [14]	40 ≤	**1.6**	63.0	1.0
Indian	India	West Bengal Glaucoma Study [74]	50 ≤	3.4		
Indian	India	Chennai Glaucoma Study (rural) [75]	40 <	**1.6**	67.2	1.1
Indian	India	Chennai Glaucoma Study (urban) [75]	40 ≤	**3.5**	82.0	2.9
Indian	Singapore	Singapore Indian Eye Study [76]	40	**1.3**	82.6	1.1
Burmese	Myanmar	Meiktila Eye Study [77]	50 ≤	**2.0**		
Hispanic	USA	Proyecto VER [78]	40 <	2.0	80.0	1.6
Hispanic	USA	Los Angeles Latino Eye Study [79]	40 ≤	**4.7**	82.0	3.9
Hispanic	Spain	Segovia Study [80]	40–79	2.0		
Multiethnic	South Africa	(Western Cape) [81]	40 ≤	1.5		
Multiethnic	West Indies	Barbados Eye Study [82]	40–84	7.1		
Black	West Indies	(St Lucia) [83]	30 ≤	8.8	36.0	
Black	USA	Baltimore Eye Survey [54]	40 ≤	4.2		
Black	Tanzania	(Kongwa District) [84]	40 ≤	3.1	75.0	
Black	South Africa	(KwaZulu-Natal) [85]	40 ≤	2.8	57.1	1.6

1.5 Myopia and POAG

Previous population-based studies have not always yielded consistent results regarding the relationship between myopia and POAG, while those performed in Asian countries including Japan have consistently found a significant association between myopia and POAG [14–20]. Marcus et al. [3] reported in a meta-analysis that the pooled odds ratio (OR) of the association between myopia and POAG was 1.92 (95 % confidence interval [CI], 1.54–2.38) based on 11 population-based

Table 1.3 IOP: summary of previous population-based studies

Ethnicity	Country	Study	Age range (years)	IOP
Caucasian	United Kingdom	(Hollows and Graham) [52]	40–74	15.9
Caucasian	Ireland	Roscommon Glaucoma Survey [53]	50 ≤	14.6
Caucasian	USA	Baltimore Eye Survey [86]	40 ≤	17.2
Caucasian	USA	Beaver Dam Eye Study [87]	43–86	15.3
Caucasian	Australia	Blue Mountain Eye Study [88]	59 ≤	16
Caucasian	The Netherlands	Rotterdam Study [89]	55–95	14.7
Caucasian	Italy	Casteldaccia Eye Study [58]	40 ≤	15.1
Caucasian	Italy	The Egna-Neumarkt Study [59]	40 ≤	15.1
Caucasian	Australia	The Melbourne Visual Impairment Project [60]	40 ≤	14.3
Mongolian	Mongolia	(Hovsgol) [61]	40 ≤	15.9
Mongolian	Mongolia	Kailu [62]	40 <	15.0
Japanese	Japan	Japan nationwide [12]	40 <	13.1
Japanese	Japan	Tajimi Study [63]	40 ≤	14.6
Japanese	Japan	Kumejima Study [11]	40 ≤	14.8
Korean	Korea	Namil Study [65]	50 ≤	13.5
Chinese	China	Beijing Eye Study [66]	40–101	16.1
Chinese	China	Handan Eye Study [90]	30 <	15.0
Chinese	China	Liwan Study [91]	50–102	15.2
Chinese	Singapore	Tanjong Pagar Study [92]	40–79	15.3
Malaysian	Singapore	Singapore Malay Eye Survey [93]	40–80	15.5
Bengalese	Bangladesh	Bangladesh Study [71]	35 ≤	15
Thai	Thailand	(Rom Klao) [72]	50 ≤	13.4
Indian	India	Aravind Comprehensive Eye Survey [73]	40 ≤	15.4
Indian	India	Andhra Pradesh Eye Disease Study (rural) [14]	40 ≤	14.5
Indian	India	West Bengal Glaucoma Study [74]	50 ≤	13.8
Indian	India	Chennai Glaucoma Study (rural) [75]	40 <	14.3
Indian	India	Chennai Glaucoma Study (urban) [75]	40 ≤	16.2
Indian	Singapore	Singapore Indian Eye Study (SINDI) [76]	40-	15.6
Burmese	Myanmar	Meiktila Eye Study	50 ≤	14.5
Hispanic	USA	Proyecto VER [94]	40 <	15.6
Hispanic	USA	Los Angeles Latino Eye Study [95]	40 ≤	14.5
Hispanic	Spain	Segovia Study [80]	40–79	14.3
Multiethnic	South Africa	(Western Cape) [81]	40 ≤	17
Multiethnic	West Indies	Barbados Eye Study [96]	40–84	18.1
Black	West Indies	(St Lucia) [83]	30 ≤	17.7
Black	USA	Baltimore Eye Survey [86]	40 ≤	16
Black	Tanzania	(Kongwa District) [84]	40 ≤	15.7
Black	South Africa	(KwaZulu-Natal) [85]	40 ≤	14.2

All participants or normal right eyes (male)

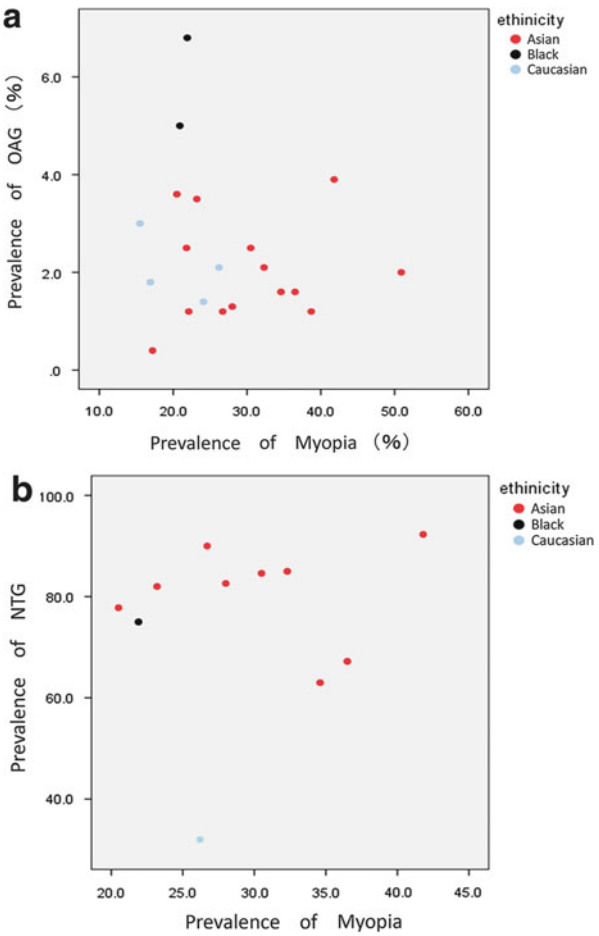

Fig. 1.1 (**a**) Prevalence of OAG versus prevalence of myopia. (**b**) Prevalence of NTG versus prevalence of myopia

studies, and the pooled ORs of the association between low myopia (> -3.0 diopters) and moderate to high myopia (≤ -3.0 diopters) were 1.65 (CI, 1.26–2.17) and 2.46 (CI, 1.93–3.15), respectively, based on seven population-based studies. The pooled ORs for low and moderate to high myopia were similar to those in the Tajimi Study, i.e., 1.85 (CI, 1.03–3.31) and 2.60 (CI, 1.56–4.35), respectively [16]. A significant relationship between myopia and POAG in Japanese patients also was confirmed by the Kumejima Study [11], in which the mean refraction was much less myopic than that in the Tajimi Study [20]. A large Swedish study [21] reported that the correlation between the prevalence rate of myopia and that of POAG was more evident in a subpopulation with IOP less than 15 mmHg, which suggested that the association between myopia and POAG would be more evident in the eyes with a normal IOP (normal-tension glaucoma [NTG]). A similar tendency also is seen in Fig. 1.1 where the prevalence rates of myopia reported in

population-based studies are plotted separately against those of POAG and NTG (POAG with IOP < 22 mmHg at screening).

The prevalence of myopia has been increasing gradually worldwide. For example, the prevalence of myopia in US citizens aged 12–54 years was significantly ($P < 0.001$ for all comparisons) higher in 1999–2004 than in 1971–1972 (41.6 % vs. 25.0 %, respectively), in Caucasians (43.0 % vs. 26.3 %) and in African-Americans (33.5 % vs. 13.0 %) [22]. Further, the prevalence of myopia is higher in younger than older generations, which indicates that the prevalence of myopia in adult populations will increase further in the future [3, 9]. Since myopia is a strong risk factor for POAG, the increased prevalence of myopia should result in an increased prevalence of POAG in the future. POAG contributes to global blindness to a degree that is second only to cataract [23]. These facts clearly indicate the importance of determining in future studies the underlying pathology associated with myopia and POAG.

References

1. Eye Diseases Prevalence Research Group (2004) The prevalence of refractive errors among adults in the United States, Western Europe, and Australia. Arch Ophthalmol 122:495–505. doi:10.1001/archopht.126.8.1111
2. Curtin BJ (1985) The myopias. Harper & Row, Philadelphia, pp 3–15
3. Marcus MW, de Vries MM, Junoy Montolio FG et al (2011) Myopia as a risk factor for open-angle glaucoma: a systematic review and meta-analysis. Ophthalmology 118:1989–1994. doi:10.1016/j.ophtha.2011.03.012
4. Scott R, Grosvenor T (1993) Structural model for emmetropic and myopic eyes. Ophthalmic Physiol Opt 13:41–47
5. Jonas JB, Gusek GC, Naumann GO (1988) Optic disk morphometry in high myopia. Graefes Arch Clin Exp Ophthalmol 226:587–590
6. Jonas JB, Dichtl A (1997) Optic disc morphology in myopic primary open-angle glaucoma. Graefes Arch Clin Exp Ophthalmol 235:627–633
7. Pan CW, Ramamurthy D, Saw SM (2012) Worldwide prevalence and risk factors for myopia. Ophthalmic Physiol Opt 32:3–16
8. Jacobi FK, Pusch CM (2010) A decade in search of myopia genes. Front Biosci 15:359–372
9. Sawada A, Tomidokoro A, Araie M et al (2008) Refractive errors in an elderly Japanese population: the Tajimi study. Ophthalmology 115:363–370.e3. doi:10.1016/j.ophtha.2007.03.075
10. Kawase K, Tomidokoro A, Araie M et al (2008) Ocular and systemic factors related to intraocular pressure in Japanese adults: the Tajimi study. Br J Ophthalmol 92:1175–1179. doi:10.1136/bjo.2007.128819. Epub 2008 Jul 31
11. Tomoyose E, Higa A, Sakai H et al (2010) Intraocular pressure and related systemic and ocular biometric factors in a population-based study in Japan: the Kumejima study. Am J Ophthalmol 150:279–286. doi:10.1016/j.ajo.2010.03.009. Epub 2010 Jun 8
12. Shiose Y, Kitazawa Y, Tsukahara S et al (1991) Epidemiology of glaucoma in Japan – a nationwide glaucoma survey. Jpn J Ophthalmol 35:133–155
13. Xu L, Li J, Zheng Y et al (2005) Intraocular pressure in Northern China in an urban and rural population: the Beijing eye study. Am J Ophthalmol 140:913–915. doi:10.1136/bjo.2007.128819. Epub 2008 Jul 31

14. Garudadri C, Senthil S, Khanna RC et al (2010) Prevalence and risk factors for primary glaucomas in adult urban and rural populations in the Andhra Pradesh eye disease study. Ophthalmology 117:1352–1359. doi:10.1016/j.ophtha.2009.11.006. Epub 2010 Feb 25
15. Ramakrishnan R, Nirmalan PK, Krishnadas R et al (2003) Glaucoma in a rural population of southern India: the Aravind Comprehensive eye survey. Ophthalmology 110:1484–1490
16. Suzuki Y, Iwase A, Araie M et al (2006) Risk factors for open-angle glaucoma in a Japanese population: the Tajimi study. Ophthalmology 113:1613–1617
17. Xu L, Wang Y, Wang S et al (2007) High myopia and glaucoma susceptibility: the Beijing eye study. Ophthalmology 114:216–220
18. Casson RJ, Gupta A, Newland HS et al (2007) Risk factors for primary open-angle glaucoma in a Burmese population: the Meiktila eye study. Clin Experiment Ophthalmol 35:739–744
19. Perera SA, Wong TY, Tay WT et al (2010) Refractive error, axial dimensions, and primary open-angle glaucoma: the Singapore Malay eye study. Arch Ophthalmol 128:900–905. doi:10.1001/archophthalmol.2010.125
20. Yamamoto S, Sawaguchi S, Iwase A et al (2014) Primary open-angle glaucoma in a population associated with high prevalence of primary angle-closure glaucoma: the Kumejima study. Ophthalmology 121(8):1558–1565. doi:10.1016/j.ophtha.2014.03.003
21. Grødum K, Heijl A, Bengtsson B (2001) Refractive error and glaucoma. Acta Ophthalmol Scand 79:560–566
22. Vitale S, Sperduto RD, Ferris FL 3rd (2009) Increased prevalence of myopia in the United States between 1971–1972 and 1999–2004. Arch Ophthalmol 127:1632–1639. doi:10.1001/archophthalmol.2009.303
23. Resnikoff S, Pascolini D, Etya'ale D et al (2004) Global data on visual impairment in the year 2002. Bull World Health Organ 82:844–851
24. Katz J, Tielsch JM, Sommer A (1997) Prevalence and risk factors for refractive errors in an adult inner city population. Invest Ophthalmol Vis Sci 38:334–340
25. Wang Q, Klein BE, Klein R et al (1994) Refractive status in the Beaver Dam eye study. Invest Ophthalmol Vis Sci 35:4344–4347
26. Vitalen S, Ellwein L, Cotch MF et al (2008) Prevalence of refractive error in the United States, 1999–2004. Arch Ophthalmol 106:1066–1072. doi:10.1001/archopht.126.8.1111
27. Attebo K, Ivers RQ, Mitchell P (1999) Refractive errors in an older population: the Blue mountain eye study. Ophthalmology 106:1066–1072. doi:10.1016/S0161-6420(99)90251-90258
28. Ikram MK, Leeuwen RV, Vingerling JR et al (2003) Relationship between refraction and prevalent as well as incident age-related maculopathy: the Rotterdam study. Invest Ophthalmol Vis Sci 44:3778–3783. doi:10.1167/iovs.03-0120
29. Wensor M, McCarty CA, Taylor HR (1999) Prevalence and risk factors of myopia in Victoria, Australia. Arch Ophthalmol 117:658–663. doi:10.1001/archopht.117.5.658
30. Wolfram C, Höhn R, Kottler U et al (2014) Prevalence of refractive errors in the European adult population: the Gutenberg Health Study (GHS). Br J Ophthalmol 98:857–861. doi:10.1136/bjophthalmol-2013-304228
31. Wickremasinghe S, Foster PJ, Uranchimeg D et al (2004) Ocular biometry and refraction in Mongolian adults. Invest Ophthalmol Vis Sci 45:776–783
32. Cheng CY, Hsu WM, Liu JH et al (2003) Refractive errors in an elderly Chinese population in Taiwan: the Shihpai eye study. Invest Ophthalmol Vis Sci 44:4630–4638
33. Xe L, Li J, Cui T et al (2005) Refractive error in urban and rural adult Chinese in Beijing. Ophthalmology 112:1676–1683. doi:10.1016/j.ophtha.2005.05.015
34. Liang YB, Wong TY, Sun LP et al (2009) Refractive errors in a rural Chinese adult population: the Handan eye study. Ophthalmology 116:2119–2127. doi:10.1016/j.ophtha.2009.04.040. Epub 2009 Sep 10
35. Yoo YC, Kim JM, Park KH et al (2013) Refractive errors in a rural Korean adult population: the Namil study. Eye 27:1368–1375. doi:10.1038/eye.2013.195. Epub 2013 Sep 13

36. Wong TY, Foster PJ, Hee J et al (2000) Prevalence and risk factors for refractive errors in adult Chinese in Singapore. Invest Ophthalmol Vis Sci 41:2486–2494
37. He M, Huan W, Li Y et al (2009) Refractive error and biometry in older Chinese adults: the Liwan eye study. Invest Ophthalmol Vis Sci 50:5130–5136. doi:10.1167/iovs.09-3455. Epub 2009 Jun 24
38. Saw SM, Gazzard G, Koh D et al (2002) Prevalence rates of refractive error in Sumatra, Indonesia. Invest Ophthalmol Vis Sci 43:3174–3180
39. Dandona R, Dandona L, Naduvilath TJ et al (1999) Refractive errors in an urban population in Southern India: the Andhra Pradesh eye disease study. Invest Ophthalmol Vis Sci 40:2810–2818
40. Pan CW, Wong TY, Lavanya R et al (2011) Prevalence and risk factors for refractive errors in Indians: the Singapore Indian eye study (SINDI). Invest Ophthalmol Vis Sci 52:3166–3173. doi:10.1167/iovs.10-6210
41. Nangia V, Jonas JB, Sinha A et al (2012) Prevalence of undercorrection of refractive error in rural Central India. The Central India eye and medical study. Acta Ophthalmol 90:e166–e167. doi:10.1111/j.1755-3768.2010.02073.x. Epub 2011 Apr 6
42. Warrier S, Wu HM, Newland HS et al (2008) Ocular biometry and determinants of refractive error in rural Myanmar: the Meiktila eye study. Br J Ophthalmol 292:1591–1594. doi:10.1136/bjo.2008.144477. Epub 2008 Oct 16
43. Raju P, Ramesh SV, Arvind H et al (2004) Prevalence of refractive errors in a rural South Indian population. Invest Ophthalmol Vis Sci 45:4268–4272
44. Prema R, George R, Sathyamangalam Ve R et al (2008) Comparison of refractive errors and factors associated with spectacle use in a rural and urban South Indian population. Indian J Ophthalmol 56:139–144. doi:10.4103/0301-4738.39119
45. Ziaei H, Katibeh M, Solaimanizad R et al (2013) Prevalence of refractive errors; the Yazd eye study. J Ophthalmic Vis Res 8:227–236
46. Bourne RR, Dineen BP, Ali SM et al (2004) Prevalence of refractive error in Bangladeshi adults: results of the National Blindness and Low Vision Survey of Bangladesh. Ophthalmology 111:1150–1160. doi:10.1016/j.ophtha.2003.09.046
47. Uribe JA, Swenor BK, Muñoz B et al (2011) Uncorrected refractive error in a Latino population: Proyecto VER. Ophthalmology 118:805–811. doi:10.1016/j.ophtha.2010.09.015. Epub 2010 Dec 13
48. Tarczy-Hornoch K, Ying-Lai M, Varma R et al (2006) Myopic refractive error in adult Latinos: the Los Angeles Latino eye study. Invest Ophthalmol Vis Sci 47:1845–1852
49. Antón A, Andrada MT, Mayo A et al (2009) Epidemiology of refractive errors in an adult European population: the Segovia study. Ophthalmic Epidemiol 16:231–237. doi:10.3109/09286580903000476
50. Sy W, Yoo YJ, Nemesure B et al (2005) Nine-year refractive changes in the Barbados eye studies. Invest Ophthalmol Vis Sci 46:4032–4039
51. Hollows FC, Graham PA (1966) Intra-ocular pressure, glaucoma, and glaucoma suspects in a defined population. Br J Ophthalmol 50:570–586. doi:10.1136/bjo.50.10.570
52. Coffey M, Reidy A, Wormald R et al (1993) Prevalence of glaucoma in the west of Ireland. Br J Ophthalmol 77:17–21. doi:10.1136/bjo.77.1.17
53. Tielsch JM, Sommer A, Katz J et al (1991) Racial variations in the prevalence of primary open-angle glaucoma: the Baltimore eye survey. JAMA 266:369–374. doi:10.1001/jama.03470030069026
54. Klein BE, Klein R, Sponsel WE et al (1992) Prevalence of glaucoma: the Beaver Dam eye study. Ophthalmology 99:1499–1504
55. Mitchell P, Smith W, Attebo K et al (1996) Prevalence of open-angle glaucoma in Australia: the Blue Mountains eye study. Ophthalmology 103:1661–1669
56. Dielemans I, Vingerling JR, Wolfs RC et al (1994) The prevalence of primary open-angle glaucoma in a population-based study in The Netherlands: the Rotterdam Study. Rotterdam Study Ophthalmol 101:1851–1855

57. Giuffre G, Giammanco R, Dardanoni G, Ponte F (1995) Prevalence of glaucoma and distribution of intraocular pressure in a population: the Casteldaccia eye study. Acta Ophthalmol Scand 73:222–225
58. Bonomi L, Marchini G, Marraffa M et al (1998) Prevalence of glaucoma and intraocular pressure distribution in a defined population: the Egna-Neumarkt study. Ophthalmology 105:209–215
59. Wensor MD, McCarty CA, Stanislavsky YL et al (1998) The prevalence of glaucoma in the Melbourne visual impairment project. Ophthalmology 105:733–739
60. Foster PJ, Baasanhu J, Alsbirk PH et al (1996) Glaucoma in Mongolia: a population-based survey in Hovsgol province, northern Mongolia. Arch Ophthalmol 114:1235–1241
61. Song W, Shan L, Cheng F (2011) Prevalence of glaucoma in a rural northern China adult population: a population-based survey in Kailu County, Inner Mongolia. Ophthalmology 118:1982–1988. doi:10.1016/j.ophtha.2011.02.050
62. Iwase A, Suzuki Y, Araie M et al (2004) The prevalence of primary open-angle glaucoma in Japanese: the Tajimi study. Ophthalmology 111:1641–1648. doi:10.1016/j.ophtha.2004.03.029
63. Yamamoto S, Sawaguchi S, Iwase A et al (2014) Primary open-angle glaucoma in a population associated with high prevalence of primary angle-closure glaucoma: the Kumejima study. Ophthalmology 121:1558–1565. doi:10.1016/j.ophtha.2014.03.003. Published online 21 Apr 2014
64. Kim CS, Seong GJ, Lee NH et al (2011) Prevalence of primary open-angle glaucoma in central South Korea the Namil study. Ophthalmology 118:1024–1030. doi:10.1016/j.ophtha.2010.10.016. Epub 2011 Jan 26
65. Wang YX, Xu L, Yang H et al (2010) Prevalence of glaucoma in North China: the Beijing Eye Study. Am J Ophthalmol 150:917–924. doi:10.1016/j.ajo.2010.06.037. Epub 2010 Oct 20
66. Liang Y, Friedman DS, Zhou Q et al (2011) Prevalence of primary open angle glaucoma in a rural adult Chinese population: the Handan eye study. Invest Ophthalmol Vis Sci 52:8250–8257. doi:10.1167/iovs.11-7472
67. He M, Foster PJ, Ge J et al (2006) Prevalence and clinical characteristics of glaucoma in adult Chinese: a population-based study in Liwan District, Guangzhou. Invest Ophthalmol Vis Sci 47:2782–2788. doi:10.1167/iovs.06-0051
68. Foster PJ, Oen FT, Machin D et al (2000) The prevalence of glaucoma in Chinese residents of Singapore: a cross-sectional population survey of the Tanjong Pagar district. Arch Ophthalmol 118:1105–1111. doi:10.1001/archopht.118.8.1105
69. Shen SY, Wong TY, Foster PJ et al (2008) The prevalence and types of glaucoma in Malay people: the Singapore Malay eye study. Invest Ophthalmol Vis Sci 49:3846–3851. doi:10.1167/iovs.08-1759
70. Rahman MM, Rahman N, Foster PJ et al (2004) The prevalence of glaucoma in Bangladesh: a population based survey in Dhaka division. Br J Ophthalmol 88:1493–1497. doi:10.1136/bjo.2004.043612
71. Bourne RR, Sukudom P, Foster PJ et al (2003) Prevalence of glaucoma in Thailand: a population based survey in Rom Klao District, Bangkok. Br J Ophthalmol 87:1069–1074. doi:10.1136/bjo.87.9.1069
72. Ramakrishnan R, Nirmalan PK, Krishnadas R (2003) Glaucoma in a rural population of southern India: the Aravind comprehensive eye survey. Ophthalmology 110:1484–1490. doi:10.1016/S0161-6420(03)00564-5
73. Garudadri C, Senthil S, Khanna RC et al (2010) Prevalence and risk factors for primary glaucomas in adult urban and rural populations in the Andhra Pradesh Eye Disease Study. Ophthalmology 117:1352–1359
74. Raychaudhuri Alahiri SK, Bandyopadhyay M et al (2005) A population based survey of the prevalence and types of glaucoma in rural West Bengal: the West Bengal Glaucoma Study. Br J Ophthalmol 89:1559–1564. doi:10.1136/bjo.2005.074948

75. Vijayal GR, Baskaran M et al (2008) Prevalence of primary open-angle glaucoma in an urban south Indian population and comparison with a rural population. Chennai Glaucoma Study Ophthalmol 115(648–654), e1. doi:10.1016/j.ophtha.2007.04.062
76. Narayanaswamy A, Baskaran M, Zheng Yingfeng A et al (2013) The prevalence and types of glaucoma in an urban Indian population: The Singapore Indian Eye Study. Invest Ophthalmol Vis Sci 54:4621–4627. doi:10.1167/IOVS.13-11950
77. Casson RJ, Newland HS, Muecke J et al (2006) Prevalence of glaucoma in rural Myanmar: the Meiktila Eye Study. Br J Ophthalmol 91:710–714. doi:10.1136/bjo.2006.107573
78. Quigley HA, West SK, Rodriguez J et al (2001) The prevalence of glaucoma in a population-based study of Hispanic subjects: Proyecto VER. Arch Ophthalmol 119:1819–1826. doi:10.1001/archopht.119.12.1819
79. Varma R, Ying-Lai M, Francis BA et al (2004) Prevalence of open-angle glaucoma and ocular hypertension in Latinos: the Los Angeles Latino Eye Study. Ophthalmology 111:1439–1448. doi:10.1016/j.ophtha.2004.01.025
80. Antón A, Andrada MT, Mujica V et al (2004) Prevalence of primary open-angle glaucoma in a Spanish population: the Segovia study. J Glaucoma 13:371–376
81. Salmon JF, Mermoud A, Ivey A et al (1993) The prevalence of primary angle closure glaucoma and open angle glaucoma in Mamre, western Cape, South Africa. Arch Ophthalmol 111:1263–1269. doi:10.1001/archopht.1993.01090090115029
82. Leske MC, Connell AM, Schachat AP et al (1994) The Barbados Eye Study: prevalence of open angle glaucoma. Arch Ophthalmol 112:821–829. doi:10.1001/archopht.1994.01090180121046
83. Mason RP, Kosoko O, Wilson MR et al (1989) National survey of the prevalence and risk factors of glaucoma in St. Lucia, West Indies: Part I. Prevalence findings. Ophthalmology 96:1363–1368
84. Buhrmann RR, Quigley HA, Barron Y et al (2000) Prevalence of glaucoma in a rural East African population. Invest Ophthalmol Vis Sci 41:40–48
85. Rotchford AP, Johnson GJ (2002) Glaucoma in Zulus: a population-based cross-sectional survey in a rural district in South Africa. Arch Ophthalmol 120:471–478. doi:10.1001/archopht.120.4.471
86. Sommer A, Tielsch JM, Katz J et al (1991) Relationship between intraocular pressure and primary open angle glaucoma among white and black Americans: the Baltimore Eye Survey. Arch Ophthalmol 109:1090–1095. doi:10.1001/archopht.1991.01080080050026
87. Klein BE, Klein R, Linton KL (1992) Intraocular pressure in an American community. The Beaver Dam Eye Study. Invest Ophthalmol Vis Sci 33:2224–2228
88. Rochtchina E, Mitchell P, Wang JJ (2002) Relationship between age and intraocular pressure: the Blue Mountains Eye Study. Clin Experiment Ophthalmol 30:173–175
89. Dielemans I, Vingerling JR, Algra D et al (1995) Primary open-angle glaucoma, intraocular pressure, and systemic blood pressure in the general elderly population: the Rotterdam Study. Rotterdam Study Ophthalmol 102:54–60
90. Zhou Q, Liang YB, Wong TY et al (2012) Intraocular pressure and its relationship to ocular and systemic factors in a healthy Chinese rural population: the Handan Eye Study. Ophthalmic Epidemiol 19:278–284. doi:10.3109/09286586.2012.708084
91. Wang D, Huang W, Li Y et al (2011) Intraocular pressure, central corneal thickness, and glaucoma in Chinese adults: the Liwan Eye Study. Am J Ophthalmol 152:454–462.e1. doi:10.1016/j.ajo.2011.03.005
92. Foster PJ, Machin D, Wong TY et al (2003) Determinants of intraocular pressure and its association with glaucomatous optic neuropathy in Chinese Singaporeans: the Tanjong Pagar Study. Invest Ophthalmol Vis Sci 44:3885–3891
93. Wong TT, Wong TY, Foster PJ et al (2009) The relationship of intraocular pressure with age, systolic blood pressure, and central corneal thickness in an Asian population. Invest Ophthalmol Vis Sci 50:4097–4102. doi:10.1167/iovs.08-2822. Epub 2009 May 20

94. Casson RJ, Abraham LM, Newland HS et al (2008) Corneal thickness and intraocular pressure in a nonglaucomatous Burmese population: the Meiktila Eye Study. Arch Ophthalmol 126:981–985. doi:10.1001/archopht.126.7.981
95. Memarzadeh F, Ying-Lai M, Azen SP et al (2008) Associations with intraocular pressure in Latinos: the Los Angeles Latino Eye Study. Am J Ophthalmol 146:69–76. doi:10.1016/j.ajo.2008.03.015. Epub 2008 May 16
96. Leske MC, Connell AM, Wu SY et al (1997) Distribution of intraocular pressure: the Barbados Eye Study. Arch Ophthalmol 115:1051–1057. doi:10.1001/archopht.1997.01100160221012

Chapter 2
Clinical Features in Myopic Glaucoma

Koji Nitta and Kazuhisa Sugiyama

Abstract Optical coherence tomography (OCT) imaging of optic nerve head and macula has been widely used in recent years to detect and monitor glaucoma. However, there are many cases with myopic glaucoma in which both myopic changes and glaucomatous changes are thought to be present, and it is often difficult to clearly distinguish the two types of changes. Myopic glaucoma often demonstrates thinning of the macular ganglion cell complex (i.e., retinal nerve fiber layer + retinal ganglion cell layer + inner plexiform layer) in the papillomacular bundle using OCT. In addition, myopic glaucoma patients seem to be susceptible to visual field defects near the fixation point. The rate of visual field loss progression in patients with general enlargement type was significantly faster than those with myopic type. Using OCT imaging, myopic disc changes often showed deformation of lamina cribrosa due to elongation of peripapillary sclera in the X–Y direction. However, structural changes in non-myopic glaucomatous eyes are thought to occur due to pressing force on the lamina cribrosa in the Z direction. A significantly lower incidence of disc hemorrhage in myopic glaucomatous eyes was reported as compared with non-myopic glaucomatous eyes. The difference in structural changes in lamina cribrosa between myopic and non-myopic glaucoma may affect the frequency of disc hemorrhage and visual field deterioration. Peripapillary gamma zone was related to myopic conus, and beta zone was correlated with glaucomatous peripapillary chorioretinal atrophy.

Keywords Myopic optic neuropathy • Peripapillary chorioretinal atrophy • Optical coherence tomography • Disc hemorrhage

K. Nitta, M.D., Ph.D. (✉)
Fukui-ken Saiseikai Hospital, 7-1 Wadanaka-machi, Funabashi, Fukui 918-8503, Japan
e-mail: k-nitta@fukui.saiseikai.or.jp

K. Sugiyama, M.D., Ph.D.
Department of Ophthalmology, Kanazawa University Graduate School of Medical Science, Kanazawa, Ishikawa, Japan

K. Sugiyama, N. Yoshimura (eds.), *Myopia and Glaucoma*,
DOI 10.1007/978-4-431-55672-5_2

2.1 Introduction

Myopic glaucoma is considered to be a disease composed of "myopic optic neuropathy" and "glaucomatous optic neuropathy," which are often difficult to clearly differentiate. Previously, myopia and glaucoma were discussed as separate entities. However, optical coherence tomography (OCT) enabled detailed structural analysis of the optic disc and its surroundings, with various new findings being reported. The possible influences of myopia on glaucomatous optic disc and its surrounding structures including peripapillary chorioretinal atrophy have been discussed. A qualitative image of the optic disc and its surrounding morphology would therefore be useful for clinical research into myopic glaucoma, so clinical features of myopic glaucoma are described in this section.

2.2 "Myopic Neuropathy" and Visual Field Defects

In myopic eyes, the optic disc becomes tilted as the axial length elongates in early adulthood. When posterior staphyloma develops in early middle age, optic disc structural changes usually occur as well. These changes result in the fragility of the supporting tissue in the *lamina c*ribrosa and in dynamic imbalance due to structural changes in the surroundings of the optic nerve head. Even if there are no typical fundus findings of pathological myopia (such as myopic chorioretinal atrophy), a visual field defect can develop due to these morphological changes. Rudnicka and Edgar used standard automatic perimetry (SAP) and found that if patients had myopia of more than −5D and axial lengths above 26 mm, the mean deviation (MD) and mean sensitivity decreased as the axial length elongated [1]. The authors examined the correlation between the axial length and retinal sensitivity in normal eyes using the Humphrey Visual Field Analyzer. In 25 of 52 total test points, short wavelength automatic perimetry showed a significant decrease in retinal sensitivity as the axial length enlarged. SAP showed 13 such test points [2]. Ohno-Matsui et al. examined patients with high myopia (i.e., refractive error < -8D or axial length ≥ 26.5 mm) with a follow-up of at least 10 years. They found that 13.2 % of the patients developed new visual field defects, and the progression of visual field defects was observed in over 60 % of patients. The scleral curvature temporal to the optic disc was the only factor significantly associated with the progression of the visual field defects [3]. This scleral curvature corresponded to types VII and IX in the classification of posterior staphyloma proposed by Curtin [4]. An independent disease concept has been proposed to establish this disease as "myopic optic neuropathy."

OCT enables high penetration imaging of structural changes of the optic nerve and its surroundings. Using swept-source OCT, Ohno-Matsui et al. observed that the subarachnoid space around the optic nerve was enlarged in highly myopic eyes compared with that in emmetropic eyes. In addition, highly myopic eyes had

thinner sclera in the subarachnoid space and shorter distances between the vitreous space and cerebrospinal space [5]. In 16.2 % of highly myopic eyes, peripapillary pits (disc pits or conus pits) were found at the border of the optic disc or in the scleral crescent adjacent to the disc [6]. In these types of myopic eyes, structural changes might be causing the visual field defect. Akagi et al. found that when nonglaucomatous myopic eyes had more severe scleral bending in the area with peripapillary chorioretinal atrophy, there was significant thinning of the retinal nerve fiber layer in the same area. In addition, when nonglaucomatous myopic eyes had more severe scleral bending, the visual field defect was significantly more severe [7].

Kiumehr et al. reported that a focal lamina cribrosa defect was observed in 34 % of eyes diagnosed with glaucoma [8]. Park et al. examined the presence or absence of focal lamina cribrosa defects in glaucomatous eyes using OCT. The results showed that the frequency of disc hemorrhage was the greatest risk factor for focal lamina cribrosa defects [9]. OCT imaging of the retinal nerve fiber layer around the optic disc and macula has been widely used in recent years to detect and monitor glaucoma. However, there are many myopic glaucoma cases in which myopic changes and glaucomatous changes are both thought to be present, and it is often difficult to clearly distinguish the two types of changes.

2.3 Morphological Characteristics of the Myopic Optic Disc

Glaucomatous optic discs can be classified into four types by disc morphology [10]. Focal ischemic type is characterized by disc rim notching. Myopic type is characterized by temporal tilting of the disc. Senile sclerotic type is characterized by peripapillary chorioretinal atrophy with shallow cupping. The general enlargement type is characterized by concentric deep cupping. Nakazawa et al. examined normal-tension glaucoma (NTG) patients and grouped them using this classification. The results indicated that the visual field defect progressed most rapidly in patients with the general enlargement type, and the rate of progression differed significantly between the general enlargement type and the myopic type [11]. In some myopic discs, structural changes were caused by axonopathy associated with lamina cribrosa deformation, occurring since a young age due to myopia. If these patients were managed as myopic glaucoma, the structural changes might have slowed or stopped.

2.4 Myopic Glaucoma May Develop Visual Field Defects Near the Fixation Point at an Early Stage

Nakazawa et al. examined the relationship between advanced glaucoma and disc morphology. They found that a significantly high proportion of patients with a myopic type disc had a worse visual acuity of 0.3 or less [12]. Myopic glaucoma might be associated with early development of a central field defect. Glaucoma usually causes visual field defects such as the Bjerrum area defect and nasal steps. In the natural history of glaucoma, these defects enlarge, combine with each other, and gradually extend to the central area. The common type of visual field defect progression pattern often occurs over a long period of time from the onset of glaucoma until the development of the central visual field defect.

Progression of central visual field defects lead to a decrease in the quality of vision (QOV). Thus, when patients develop scotoma near the fixation point in the early stages, the central 10–2 and 30–2 threshold tests should be used alternately during the follow-ups. Thinning of the macular ganglion cell complex (i.e., retinal nerve fiber layer + retinal ganglion cell layer + inner plexiform layer) is often observed in the papillomacular bundle using OCT. Such patients will be susceptible to a visual field defect near the fixation point. Kimura et al. observed an early retinal nerve fiber layer defect (RNFLD) at the papillomacular bundle region in over 40 % of highly myopic glaucomatous eyes. This percentage was significantly higher than non-myopic glaucomatous eyes [13]. Structural changes observed by OCT often precede functional changes determined by perimetry. If myopic glaucomatous eyes have an RNFLD in the papillomacular bundle, they could be more susceptible to a visual field defect near the fixation point. Therefore, ophthalmologists should manage myopic glaucoma patients at an early stage, before the development of impaired visual acuity and central visual field defects.

2.5 Myopic Glaucoma and Disc Hemorrhage (DH)

The greatest risk factor of glaucoma progression is the presence of DH in the surroundings of the optic disc. The Collaborative Normal-Tension Glaucoma Study Group reported that the hazard ratio for the progression of visual field defects was 2.72 in patients with DH [14]. Ishida et al. examined the relationship between disc hemorrhage in NTG eyes and the progression of visual field defects. The results showed that the 5 year cumulative probability of visual field loss progression was significantly greater in eyes with DH (89 %) than in eyes without (40 %). There was a significant relationship between the location of DH and the area of the progression of the visual field [15]. Moreover, De Moraes et al. divided the perimetry test results into six sectors based on Garway-Heath mapping, correspondingly divided the optic nerve into six areas, and examined the changes in visual field progression before and after DH. The mean deviation slope of visual field

progression for the corresponding DH sector were -2.0 ± 1.0 dB/year before DH and -3.7 ± 3.6 dB/year after DH ($p < 0.01$), indicating a rapid increase in rate after DH. The visual field sector with the fastest progression rate was the location of the future DH in 85 % of the cases. The sector with the fastest progression rate corresponded to the region of DH in 92 % of the cases [16].

However, significantly lower DH incidences as well as lower progression rates of visual field loss in myopic glaucomatous eyes were reported as compared to non-myopic glaucomatous eyes during follow-ups [17], as well as lower progression rates of visual field loss [18, 19]. The reason for the difference in DH occurrence and visual field loss progression between the myopic and non-myopic glaucomatous eyes might be due to the difference in mechanism of glaucoma development and progression. Using OCT imaging, myopic disc changes often showed deformation of lamina cribrosa due to the elongation of peripapillary sclera in the X–Y direction [20, 21]. In non-myopic glaucomatous eyes, structural changes are thought to occur due to the pressing force on the lamina cribrosa in the Z direction. The pressing force is mainly directing a pressing force from the intraocular pressure and the pressure gradient between the intraocular pressure and cerebrospinal pressure.

The cause of DH has not yet been established. However, it is speculated that the following process causes DH. As retinal nerve fiber bundles are lost and the lamina cribrosa moves posteriorly, capillaries of the anterior lamina cribrosa become very stretched to maintain the connection with the anterior portion in the retina near the disc. Consequently, capillaries become occluded and subsequently become atrophied. A portion of the stretched capillaries ruptures, resulting in DH. Therefore, DH is thought to be caused by mechanical damage of capillaries due to structural changes such as those of the lamina cribrosa [22]. The differences of structural changes in the optic disc, including lamina cribrosa and its surrounding between myopic and non-myopic glaucomatous eyes, may affect the frequency of disc hemorrhage and deterioration rate of visual field loss.

2.6 Differences Between Myopic Conus and Peripapillary Chorioretinal Atrophy (PPA)

An elongated axial length stretches the choroid and retina laterally. As a result, the myopic optic disc tends to develop tilted discs with crescent conus (Fig. 2.1) (Kim et al. [23]). A significant correlation between the enlarged area of the PPA and visual field defect progression has been reported [24]. Glaucomatous PPA and myopic conus are often confused as different or the same entities. Jonas et al. proposed that they can be differentiated based on histological examination [25]. They found that only retinal nerve fiber layers existed in the area of myopic conus, and no overlying choroid, Bruch's membrane, or deep retinal layers remained. This region was defined as a gamma zone (Fig. 2.2). A beta zone was

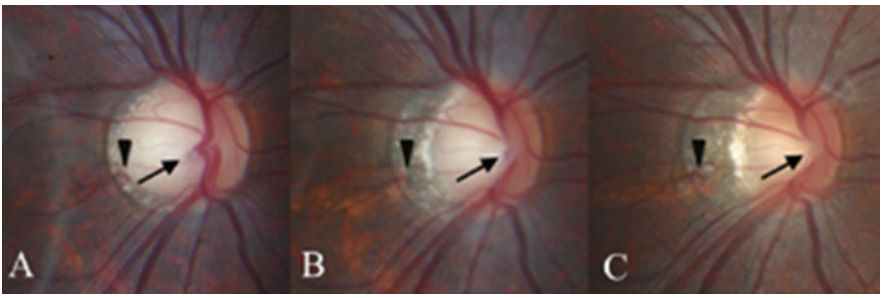

Fig. 2.1 Disc photograph of a 16-year-old male patient with crescent-type peripapillary chorioretinal atrophy (PPA) who was followed-up for 6 years. (**a**) Baseline disc photograph shows a small area of PPA and a large disc. (**b**) Two years later, an enlarged PPA and disc tilt were observed. Cilioretinal vessels in the 8 o'clock sector (*arrowhead*) remained at the prior disc margin. (**a**) Six years later, a larger area of PPA and more prominent disc tilt were observed. Note the progressive nasalization and the nasal rotation of the central retinal vessel trunk [23]

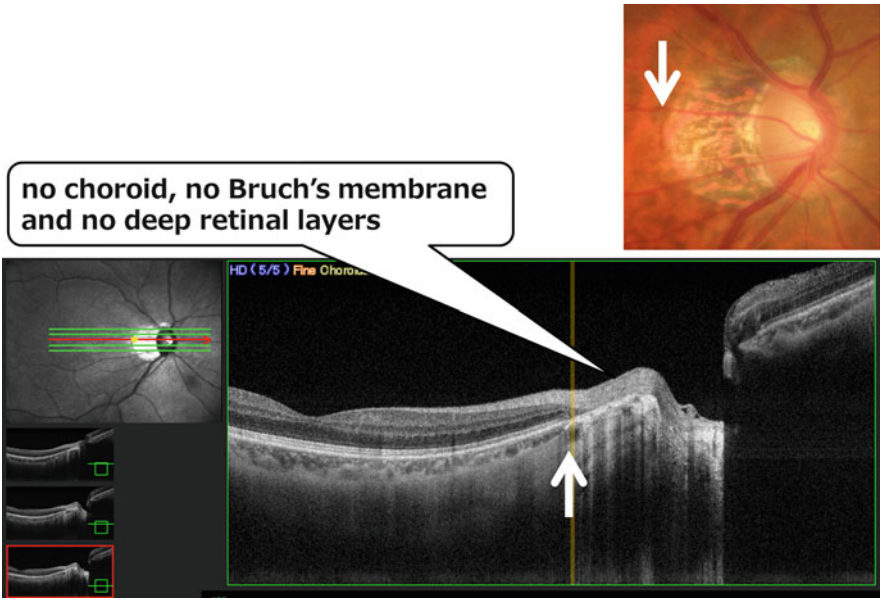

Fig. 2.2 Gamma zone PPA, spectral domain optical coherence tomography images. In the gamma zone, only the retinal nerve fiber layer bundle and the underlying scleral tissues are apparent, with very short terminal fragments of retinal layers and choroidal tissues observed just inside the gamma zone margin (*white arrows*)

defined as a region of PPA in which retinal layers and Bruch's membrane remained, except the retinal pigment epithelium (Fig. 2.3). In some cases, the gamma zone and beta zone cannot be differentiated by the color tone of the atrophic area in fundus photographs (Fig. 2.4). In highly myopic eyes, morphology of myopic conus

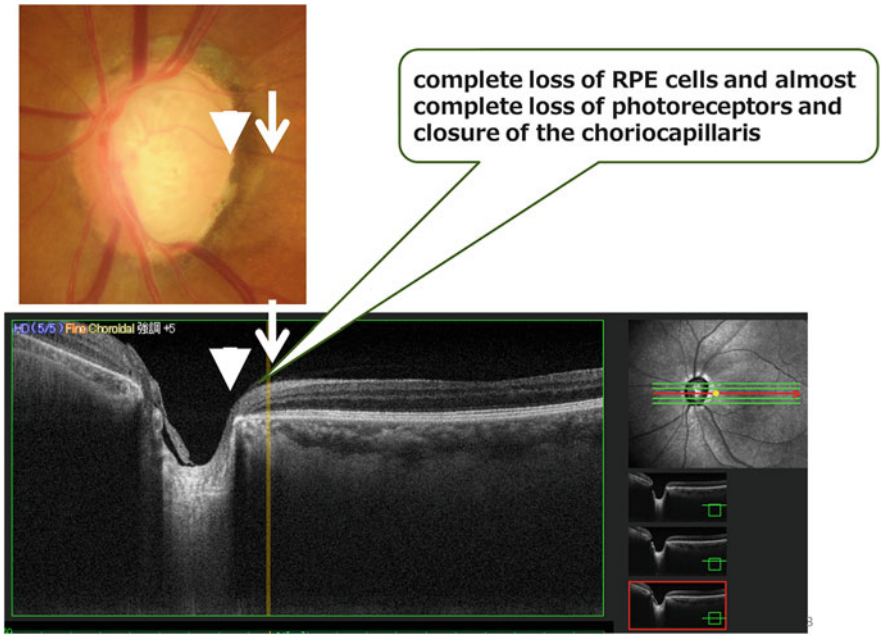

Fig. 2.3 Beta zone PPA, spectral domain optical coherence tomography images. In the beta zone, thin choroidal tissues are visible up to the disc margin (*arrowhead*). Retinal layers also extend to the disc margin in a tapering configuration across the limits of the PPA (*arrows*)

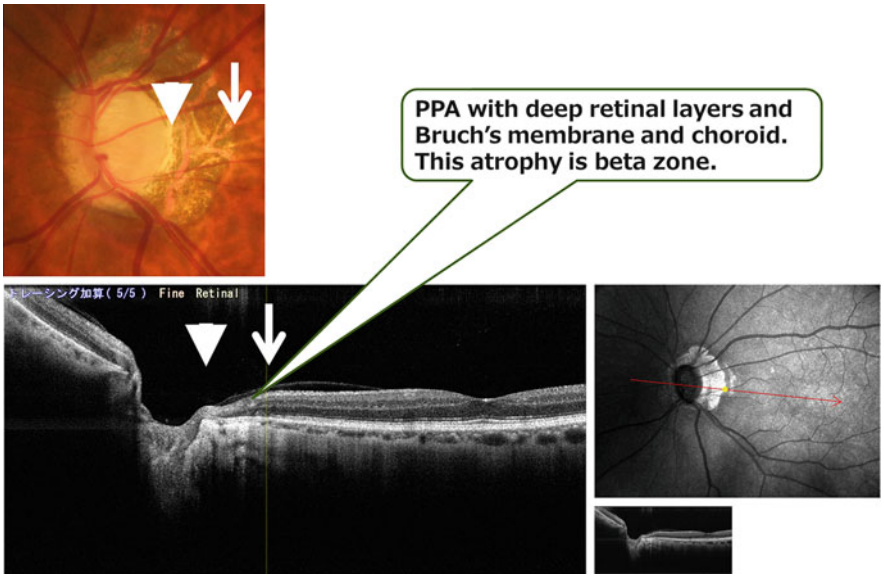

Fig. 2.4 Hard differentiation by the color tone of the PPA area in fundus photographs. Although this disc photograph appears as gamma zone PPA, the OCT image suggests the PPA is beta zone, with deep retinal layers and Bruch's membrane and choro

manifested as high incidences of RPE loss and photoreceptor loss [26]. Hayashi et al. found that a high percentage of myopic eyes lacked Bruch's membrane in the PPA area, and a high percentage of glaucomatous eyes had curved Bruch's membrane in this same area [27]. The peripapillary gamma zone was strongly related to axial globe elongation and myopic conus [28]. The beta zone was correlated with glaucomatous PPA and not with globe elongation. Thus, the myopic conus lacks Bruch's membrane corresponding to the gamma zone, and glaucomatous PPA histologically has Bruch's membrane corresponding to the beta zone. These zones can be clearly distinguished by OCT (Figs. 2.2 and 2.3).

2.7 Conclusions

There are many myopic glaucoma cases where both myopic changes and glaucomatous changes are thought to be present. Ophthalmologists should manage myopic glaucoma patients during relatively early stages before the development of impaired visual acuity and central visual field defects. The difference in structural changes in the optic disc, including lamina cribrosa and its surroundings, between myopic and non-myopic glaucomatous eyes may affect the frequency of disc hemorrhage and deterioration rate of the visual field loss. The myopic conus lacks Bruch's membrane corresponding to the gamma zone, and glaucomatous PPA has Bruch's membrane corresponding to the beta zone.

References

1. Rudnicka AR, Edgar DF (1995) Automated static perimetry in myopes with peripapillary crescents-Part I. Ophthalmic Physiol Opt 15(5):409–412
2. Nitta K, Saito Y, Sugiyama K (2006) The influence on the static visual field of peripapillary chorioretinal atrophy-relation to axial length. Nihon Ganka Gakkai Zasshi 110(4):257–262
3. Ohno-Matsui K, Shimada N, Yasuzumi K et al (2011) Long-term development of significant visual field defects in highly myopic eyes. Am J Ophthalmol 152(2):256–265. e1. doi:10.1016/j.ajo.2011.01.052
4. Curtin BJ (1985) Basic science and clinical management. In: Curtin BJ (ed) The myopias. Harper & Row, New York, pp 301–308
5. Ohno-Matsui K, Akiba M, Moriyama M et al (2011) Imaging the retrobulbar subarachnoid space around the optic nerve by swept-source optical coherence tomography in eyes with pathologic myopia. Invest Ophthalmol Vis Sci 52(13):9644–9650. doi:10.1167/iovs.11-8597
6. Ohno-Matsui K, Akiba M, Moriyama M et al (2012) Acquired optic nerve and peripapillary pits in pathologic myopia. Ophthalmology 119(8):1685–1692. doi:10.1016/j.ophtha.2012.01.047
7. Akagi T, Hangai M, Kimura Y et al (2013) Peripapillary scleral deformation and retinal nerve fiber damage in high myopia assessed with swept-source optical coherence tomography. Am J Ophthalmol 155(5):927–936. doi:10.1016/j.ajo.2012.12.014
8. Kiumehr S, Park SC, Syril D et al (2012) In vivo evaluation of focal lamina cribrosa defects in glaucoma. Arch Ophthalmol 130(5):552–559. doi:10.1001/archopthalmol.2011.1309

9. Park SC, Hsu AT, Su D et al (2013) Factors associated with focal lamina cribrosa defects in glaucoma. Invest Ophthalmol Vis Sci 54(13):8401–8407. doi:10.1167/iovs.13-13014
10. Nicolela MT, Drance SM (1996) Various glaucomatous optic nerve appearances: clinical correlations. Ophthalmology 103:640–649
11. Nakazawa T, Shimura M, Ryu M et al (2012) Progression of visual field defects in eyes with different optic disc appearances in patients with normal tension glaucoma. J Glaucoma 21 (6):426–430. doi:10.1097/IJG.0b013e3182182897
12. Nakazawa T, Fuse N, Omodaka K et al (2010) Different types of optic disc shape in patients with advanced open-angle glaucoma. Jpn J Ophthalmol 54(4):291–295. doi:10.1007/s10384-010-0816-y
13. Kimura Y, Hangai M, Morooka S et al (2012) Retinal nerve fiber layer defects in highly myopic eyes with early glaucoma. Invest Ophthalmol Vis Sci 53(10):6472–6478
14. Collaborative Normal-Tension Glaucoma Study Group (1998) Comparison of glaucomatous progression between untreated patients with normal-tension glaucoma and patients with therapeutically reduced intraocular pressures. Am J Ophthalmol 126(6):487–497
15. Ishida K, Yamamoto T, Sugiyama K et al (2000) Disk hemorrhage is a significantly negative prognostic factor in normal-tension glaucoma. Am J Ophthalmol 129(6):707–714
16. De Moraes CG, Prata TS, Liebmann CA et al (2009) Spatially consistent, localized visual field loss before and after disc hemorrhage. Invest Ophthalmol Vis Sci 50(10):4727–4733. doi:10.1167/iovs.09-3446
17. Araie M, Shirato S, Yamazaki Y et al (2012) Risk factors for progression of normal-tension glaucoma under β–blocker monotherapy. Acta Ophthalmol 90(5):e337–e343. doi:10.1111/j.1755-3768.2012.02425.x
18. Sohn SW, Song JS, Kee C (2010) Influence of the extent of myopia on the progression of normal-tension glaucoma. Am J Ophthalmol 149(5):831–838. doi:10.1016/j.ajo
19. Chao DL, Shrivastava A, Kim DH et al (2010) Axial length does not correlate with degree of visual field loss in myopic Chinese individuals with glaucomatous appearing optic nerves. J Glaucoma 19(8):509–513. doi:10.1097/IJG.0b013e3181d12dae
20. Lopilly Park HY, Lee NY, Choi JA et al (2014) Measurement of scleral thickness using swept-source optical coherence tomography in open-angle glaucoma patients with myopia. Am J Ophthalmol 157:876–884, E-pub
21. Vurgese S, Panda-Jonas S, Jonas JB (2012) Scleral thickness in human eyes. PLoS One 7(1): e29692. doi:10.1371/journal.pone.0029692
22. Nitta K, Sugiyama K, Higashide T et al (2011) Does the enlargement of retinal nerve fiber layer defects relate to disc hemorrhage or progress visual field loss in normal-tension glaucoma? J Glaucoma 20(3):189–195. doi:10.1097/IJG.0b013e3181e0799c
23. Kim TW, Kim M, Weinreb RN et al (2012) Optic disc change with incipient myopia of childhood. Ophthalmology 119:21–26.e1-3. doi:10.1016/j.ophtha
24. Uchida H, Ugurlu S, Caprioli J (1998) Increasing peripapillary atrophy is associated with progressive glaucoma. Ophthalmology 105:1541–1545
25. Jonas JB, Jonas SB, Jonas RA et al (2012) Parapapillary atrophy: histological gamma zone and delta zone. PLoS One 7(10):e47237. doi:10.1371/journal.pone.0047237
26. Manjunath V, Shah H, Fujimoto JG et al (2011) Analysis of peripapillary atrophy using spectral domain optical coherence tomography. Ophthalmology 118(3):531–536. doi:10.1016/j.ophtha.2010.07.013
27. Hayashi K, Tomidokoro A, Lee KY et al (2012) Spectral-domain optical coherence tomography of β-zone peripapillary atrophy: influence of myopia and glaucoma. Invest Ophthalmol Vis Sci 53(3):1499–1505. doi:10.1167/iovs.11-8572
28. Jonas J, Dichtl A (1997) Optic disc morphology in myopic primary open-angle glaucoma. Graefes Arch Clin Exp Ophthalmol 235(10):627–633

Chapter 3
Glaucoma Diagnosis in Myopic Eyes

Masanori Hangai

Abstract This chapter discusses on several difficulties for early glaucoma diagnosis in myopic eyes. Varying deformation of the myopic optic disc and large peripapillary atrophy makes glaucoma diagnosis difficult. A large part of spectral-domain optical coherence tomography (SD-OCT) devices do not include normative database for high myopia. Measurement of circumpapillary retinal nerve fiber layer sometimes fails due to the steep peripapillary scleral slope and large peripapillary atrophy. The difference in retinal nerve fiber layer profiles between highly myopic and non-highly myopic (normative database) causes false-positive errors. To help glaucoma diagnosis in myopic eyes, this chapter also discusses on the usefulness of macular layer structure. Macular shape is less affected by the myopic changes of the fundus. Macular layer shape is vertically symmetrical, which remains with aging. Recent speckle noise-free spectral-domain OCT images allow us to observe and measure individual retinal layers in the macula. These advantages characteristic to the macula greatly enhance our ability to detect early glaucomatous structural changes in myopia. Thus, it is crucial to understand the characteristics of the fundus structure that underlie the current problems in glaucoma diagnosis in high myopes.

Keywords Tilted disc • Peripapillary atrophy • Macula • Ganglion cell layer • Retinal nerve fiber layer

3.1 Introduction

Glaucoma is a progressive disease in which the number of retinal ganglion cells (RGCs) decreases faster and more focal than in normal physiological loss with aging. It is thought that glaucomatous RGC loss results from damage to RGC axons at the level of the optic disc lamina cribrosa. This RGC loss, called glaucomatous optic neuropathy (GON), presents clinically as progressive visual field (VF) defects associated with structural changes on biomicroscopic appearance, such as optic disc neuroretinal rim loss and retinal nerve fiber layer (RNFL) defects, which are the

M. Hangai, M.D., Ph.D. (✉)
Department of Ophthalmology, Saitama Medical University, 38 Morohongo, Moroyama-machi, Iruma-gun, Saitama 350-0495, Japan
e-mail: hangai@saitama-med.ac.jp

K. Sugiyama, N. Yoshimura (eds.), *Myopia and Glaucoma*,
DOI 10.1007/978-4-431-55672-5_3

conventional indicators of GON. It is known that such detectable structural changes precede the detection of VF defects with standard automated perimetry (SAP) 24-2 or 30-2 [1–7]. This early stage is called preperimetric glaucoma and can be explained by the fact that histological and empirical studies show considerable loss of RGCs (>50 %) occurring before VF defects are detectable [8–10]. Therefore, investigators have focused on the development of reproducible and accurate methods to detect glaucomatous structural changes.

Myopia affects approximately 1.6 billion people worldwide and is expected to increase in prevalence, particularly in East Asia [11–14], to 2.5 billion by the year 2020 [11, 12]. Myopia, especially high myopia, is a risk factor for developing glaucoma [15]. Glaucomatous VF defects in patients with high myopia are more likely to threaten fixation, even in early glaucoma [16–18]. Thus, because the myopic population is at greater risk of decreased quality of vision, early detection of glaucoma is necessary, particularly for myopic patients. However, it is often difficult to evaluate the myopic optic disc, which shows variably deformed shapes, comprising tilting, cyclotorsion, pale appearance, shallow and/or large cups, extremely large or small disc, and large areas of peripapillary atrophy (PPA) [19–22]. To enhance our ability to accurately detect glaucomatous structural changes in myopic eyes, we need another structural diagnostic marker, one which is also damaged in GON.

Glaucomatous loss of RGCs leads to thinning of the RNFL due to RGC axon loss and thinning of the ganglion cell layer (GCL) due to RGC soma loss. The advent of spectral-domain optical coherence tomography (SD-OCT) technology has opened new avenues to direct assessment of glaucomatous damage to macular retinal layers. The technique has allowed thickness parameters, such as those of the circumpapillary RNFL (cpRNFL), and the combined macular inner retinal layer, which comprises the RNFL and ganglion cell layer (GCL), to be established. Multiple B-scan averaging, a noise reduction method, successfully generated a B-scan with improved visualization of each retinal layer, which is the current standard for B-scan images [23, 24]. We will now consider whether these macular retinal layers can be a structural diagnostic marker for glaucoma diagnosis that is less affected by myopia.

This chapter focuses on the anatomical peculiarities of myopic eyes that cause difficulties in glaucoma diagnosis and explores promising indicators of GON in myopia.

3.2 Why Is It Difficult to Detect Glaucoma in Highly Myopic Eyes?

Glaucoma diagnosis is evaluated on the basis of optic disc appearance and VF defects. Common features of the glaucomatous optic disc are localized or diffuse thinning of the neuroretinal rim and a difference greater than 0.2 or 0.3 between the

vertical cup/disc ratios of paired eyes. However, the inter-eye vertical cup/disc ratio is not a definitive criterion because there is variation between individuals in the size of the optic disc [25, 26]. RNFL defects can be a useful indicator of glaucomatous damage only when other diseases that lead to such defects can be ruled out. Importantly, glaucoma can be confirmed when these structural findings correspond with VF defects. However, this is not the case for preperimetric glaucoma.

Occasionally, VF defects cannot be detected in SAP 24-2 or 30-2 tested eyes that have undergone examination with the Humphrey Visual Field Analyzer (Carl Zeiss Meditec, Dublin, CA), utilizing the 24-2 Swedish interactive threshold algorithm (SITA) standard program, despite an evident glaucomatous appearance in the optic disc, or RNFL defects [27]. The diagnosis of such early glaucoma (termed preperimetric glaucoma) cases depends on the evaluation of glaucomatous structural abnormalities alone.

Although optic disc evaluation is so critically important, it is often difficult to evaluate optic disc appearance in highly myopic eyes, because the optic disc shape and peripapillary structures are highly deformed by myopic elongation of the eyeball; this deformation is generally more severe with higher myopia and shows highly variable patterns: extremely large or small disc, varying tilting, varying cyclotorsion, and varying peripapillary atrophy (PPA; Fig. 3.1) [19–22]. The problem for glaucoma diagnosis in these patients is the difficulty in distinguishing

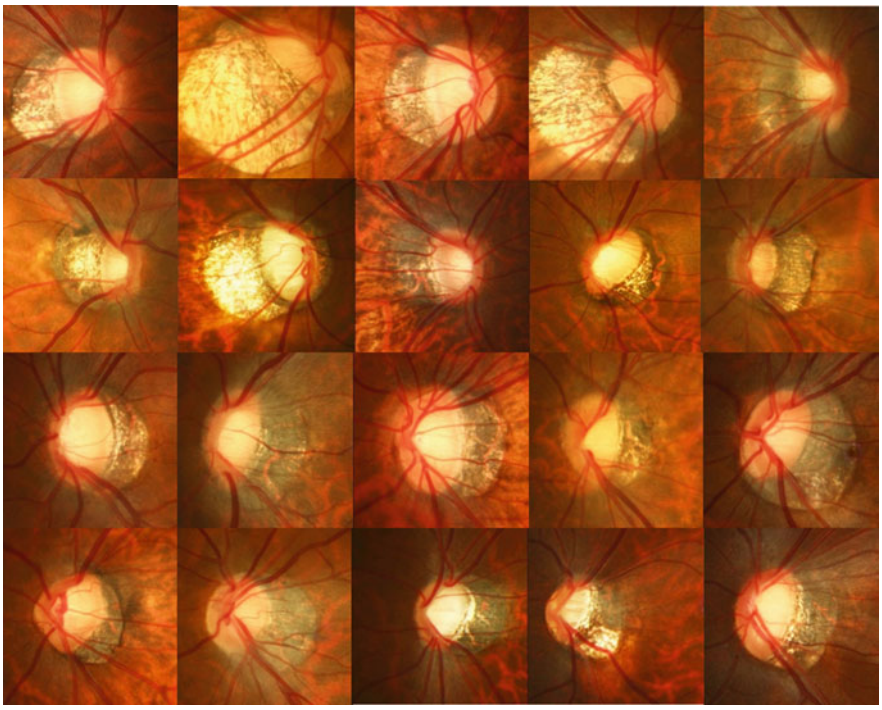

Fig. 3.1 Variable deformation of the optic disc and peripapillary appearance in highly myopic eyes (Nakano et al. [28])

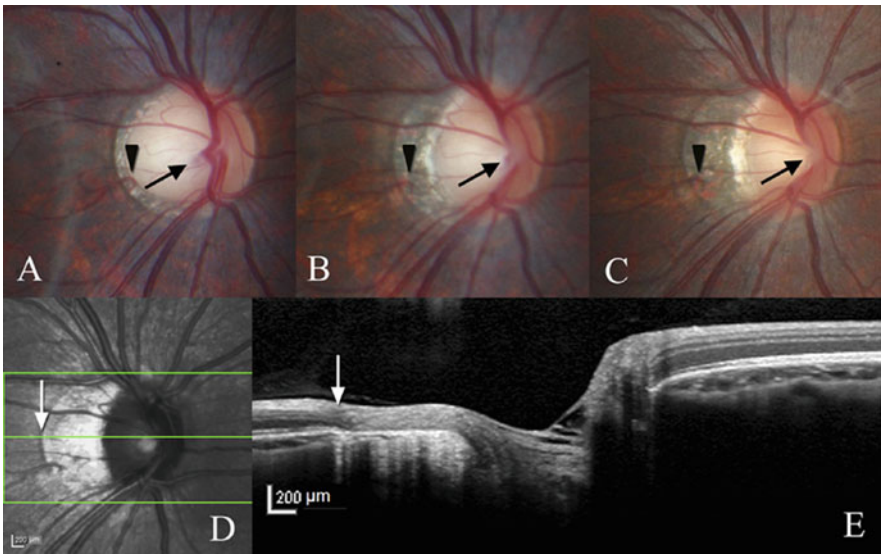

Fig. 3.2 Progressive tilting and formation of peripapillary atrophy in children who exhibited myopic shift. (**a–c**) Color disc photographs (**a**) at 12 years, (b) 14 years, and (**c**) 18 years old. (**d** and **e**) Spectral-domain optical coherence tomography images of the optic disc in (**c**) (Kim et al. [29])

glaucomatous changes from the variable optic disc deformations that result from myopia.

Recently, it has been shown that tilting of the optic disc and enlargement of PPA are acquired features that are progressive in children who exhibit myopic shift (Fig. 3.2) [29]. Thus, variable myopic deformation of the optic disc may be acquired from peripapillary scleral stretching associated with myopic eyeball elongation [29]. Furthermore, excessive myopic shift does not appear to affect only the optic disc and peripapillary structure, but it also causes lamina cribrosa (LC) abnormalities, such as LC thinning [30], greater LC pore area [31], horizontal LC tilting [32], and a higher incidence of LC defects [33, 34].

PPA has been found to be more complicated in structure than previously thought. A study using SD-OCT revealed that PPA is comprised of two components: aging-related RPE atrophy with intact Bruch's membrane (BM) and a gap between the scleral ring and BM termination resulting from scleral stretching associated with myopic elongation of the globe in children (Fig. 3.3) [35, 36].

These optic disc and peripapillary deformations not only make GON diagnosis difficult but also are themselves associated with glaucomatous damage. Optic disc tilt and cyclotorsion have been found in several studies to be highly prevalent in normal-tension glaucoma (NTG) patients with myopia. In addition, the direction of optic disc cyclotorsion was associated with the location of VF defects [37, 38]. Moreover, the presence of LC defects, which have recently been shown to be related to glaucomatous damage [39] and glaucomatous VF progression [40], has been associated with myopic optic disc morphology in primary open-angle glaucoma (POAG) eyes with high myopia [34]. The rate of RNFL thinning was faster

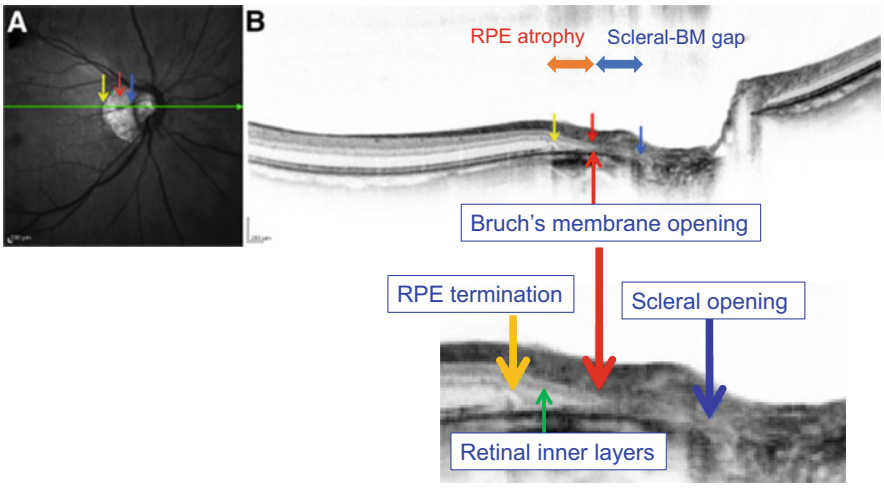

Fig. 3.3 Peripapillary atrophy is comprised of two component: aging-related retinal pigment epithelium (RPE) atrophy, including intact Bruch's membrane (BM), and a gap between scleral ring and BM termination resulting from scleral stretching associated with myopic elongation of the globe (Nonaka et al. [35])

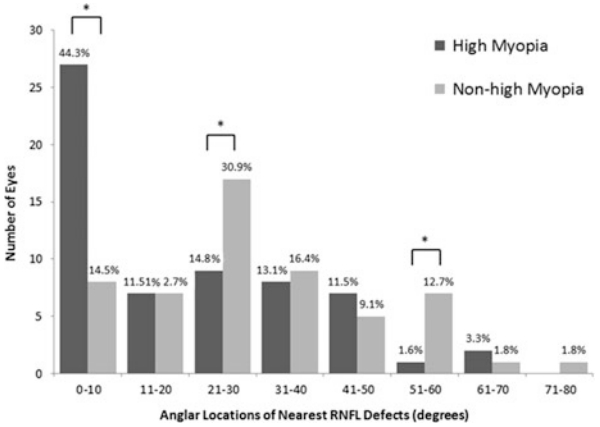

Fig. 3.4 Highly myopic eyes are more susceptible to papillomacular bundle defects in early glaucoma. *$P < 0.01$ (chi-square test). The number of eyes in which the nearest retinal nerve fiber layer defect was detected within the corresponding range was plotted for each angular location (Kimura et al. [18])

for eyes with β-zone PPA and an intact BM than for eyes without β-zone PPA or with β-zone PPA devoid of BM [41].

Higher myopia has been associated with a significantly higher incidence of cecocentral scotomas located just temporal and inferior to the fixation point in advanced glaucoma [16, 17]. Additionally, highly myopic eyes are more susceptible to papillomacular bundle defects, even in early glaucoma (Fig. 3.4) [18]. These

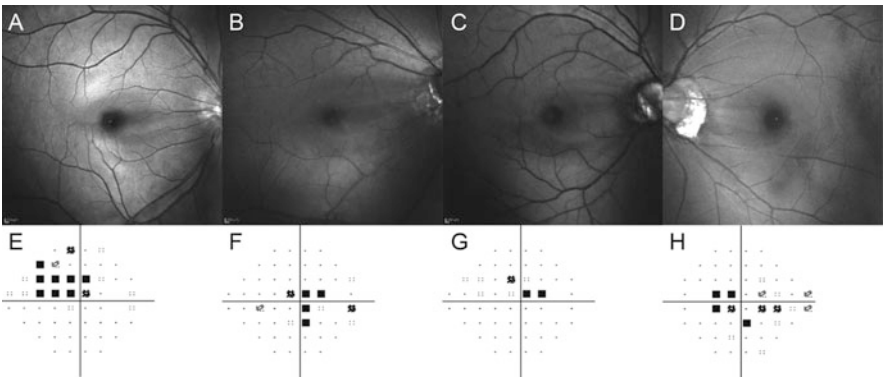

Fig. 3.5 Retinal nerve fiber layer (RNFL) defects involving the papillomacular bundle observed in highly myopic eyes. (**a–d**) Red-free imaging using HRA2 (Heidelberg Engineering, Heidelberg, Germany); (**e–h**) Humphrey Visual Field Analyzer (Carl Zeiss Meditec, Dublin, CA) with the 24-2 Swedish interactive threshold algorithm (SITA) standard program. Multiple RNFL defects can be seen. Although the locations of the paracentral scotomas varied (at $P < 0.01$), they included the temporal paracentral test points in all four cases (Kimura et al. [18])

defects are characterized by multiple narrow defects (Fig. 3.5) [18, 42]. It remains unknown whether the myopic deformation of the optic disc is related to this atypical glaucomatous damage. It should be noted that the narrow papillomacular bundle defects are not as easily found because the background RNFL reflection is weaker in the macula than in the superotemporal and inferotemporal double-hump regions. Also, early damage to the papillomacular bundles is often undetectable by SAP 24-2 or 30-2 [43]. Detection of early RNFL damage causing paracentral VF defects is also important for glaucoma diagnosis in high myopia.

3.3 Limitations in Glaucoma Detection by Inter-person Comparison with a Normative Database

SD-OCT allows the reproducible and accurate measurement of several thickness parameters, including circumpapillary RNFL (cpRNFL), and macular thickness parameters, one of which is the ganglion cell complex (GCC; RNFL + ganglion cell layer [GCL] + inner plexiform layer [IPL]) thickness, and another is the GCIPL (Carl Zeiss Meditec)/GCL + (Topcon, Tokyo, Japan) (GCL + IPL) thickness. To determine if the thickness parameters in each eye are abnormally diminished, they are statistically compared, by using confidence intervals (CIs), with the parameters of a normative database of the corresponding age range and gender. Abnormal thinning (red color) is defined as falling below the lower 99th percentile of the CI limit of the normative database, and borderline thinning (colored with yellow) as between the lower 95th and 99th percentile CI limits (Fig. 3.6). Such a method,

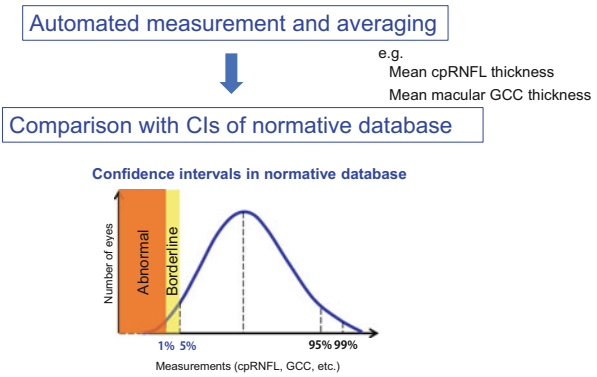

Fig. 3.6 Definition of abnormal and borderline thinning from OCT measurements compared with the confidence intervals (CIs) of the same measurements from a normative database of the corresponding age range and gender. *cpRNFL* circumpapillary retinal nerve fiber layer, *GCC* ganglion cell complex

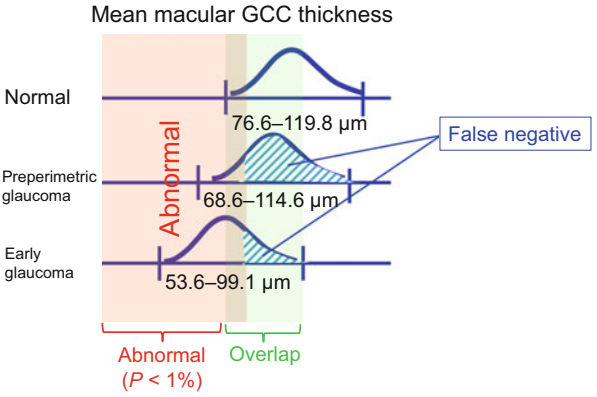

Fig. 3.7 Schematic explanation of the reasons for the poor performance of the normative database comparison strategy with regard to the differential diagnosis of normal and early diseased eyes (This scheme is based on data presented in the following article: Tan et al. [44])

based on comparison of measurements, has the following three limitations that lower the ability to identify glaucoma:

1. A large overlap exists between normal and early glaucomatous eyes.

   The range of thickness is quite large in healthy eyes. Such variation in the human body is useful for survival of humans as a species against the environmental change encountered in nature, but it makes it difficult to discriminate an abnormal structure from normal one. There is a significant overlap in the thickness distribution of retinal layers between normal and early diseased eyes, even if age, gender, and refractive errors match [44–55]. This holds true even in eyes with early VF defects. It is difficult to statistically distinguish two groups with a wide overlap. For example, Tan et al. measured macular GCC thicknesses (mean ± SD) of 76.6–119.0 (94.8 ± 7.58) μm, 68.6–114.6 (87.0 ± 9.37) μm, and 53.6–99.1 (79.4 ± 10.4) μm for normal eyes, eyes with preperimetric glaucoma, and eyes with early glaucoma, respectively [44]. When the CIs of the study subjects are compared to those of the normative database, it is evident that a large number of early diseased eyes were classified as normal (false-negative; Fig. 3.7). This is a limitation originating from the inherent variability of the

human race, and therefore it cannot be resolved by the development of more accurate measurement technologies. It follows therefore that inter-person comparison is not a suitable strategy for discriminating between normal and glaucomatous eyes.

2. The averaging of measurements within a fixed area results in an underestimation of results.

   It is difficult in practice to compare each of numerous OCT A-scans with that of the normative database. Therefore, the measurements of all the A-scans on a circumpapillary (cp) circle around the optic disc are averaged to generate the cpRNFL parameter and those within a circle of 6-mm diameter over the macula to generate the macular thickness parameters (total thickness, GCC, and GCIPL/GCL+). This averaging causes an underestimation of the degree of retinal layer thinning, because early glaucomatous damage is often localized within a smaller segment of the measurement area. For example, even if a circle area of 2-mm diameter within the macula of 6-mm diameter is thinned by 100 %, this amounts to a total loss in thickness of only 6 % within the macula. Thus, when averaged within an area, the healthy or less affected areas render the measured degree of thinning less severe. To avoid this underestimation, sector analysis has been developed. In this, the cpRNFL circle is divided into 6–36 sectors, and the macular circle of 6-mm diameter is divided into either superior and inferior semicircles, Early Treatment Diabetic Retinopathy Study (ETDRS) sectors, or glaucoma chart sectors (ETDRS sectors rotated by 45°). Sector analysis appears to effectively detect local damage in early glaucoma. However, the location of RGC damage, which differs among patients, is not necessarily limited to one sector, but often spans 2–4 sectors. As a result, the glaucomatous damage is often localized even within the sectors.

3. The effects of myopia are not considered in current normative databases.

   Prior studies have shown that decreased average cpRNFL thickness is a strong indicator of glaucoma [56–62]. Unfortunately, cpRNFL thickness is not as effective as a diagnostic marker in highly myopic eyes [63–66]. This discrepancy has been attributed to the somewhat abnormal cpRNFL profiles in highly myopic eyes, which include thinning [64, 67–69] and differences in peripapillary thickness distribution [70–72] in comparison with non-highly myopic eyes. Abnormalities in the cpRNFL profile become more prominent with increases in the degree of myopia [64, 68, 69, 72], axial length [64, 65, 69, 72], and optic disc tilting [70, 71]. Regardless of the strong effects of high myopia on cpRNFL thickness, current normative databases, except that of the RS-3000 Advance (Nidek, Gamagori, Japan), do not include data specific to refractive errors greater than -6 diopters. Similarly, although the glaucoma diagnostic software in these SD-OCT instruments uses CIs from age- and gender-matched eyes for identifying abnormal thinning, none of them compare measurements with CIs from a normative database of eyes with corresponding refractive errors.

The first and second limitations addressed above hold true regardless of the presence, absence, or severity of myopia. In particular, a large overlap between normal and early diseased eyes due to the wide distribution of normal thickness values clearly indicates the difficulty in perfectly discriminating normal from early glaucomatous eyes. Underestimation resulting from area averaging further decreases the ability to discriminate for all the thickness parameters, as does the third limitation mentioned, which is specific to myopic eyes. Thus, we need to interpret the results of statistical comparisons with CIs from normative databases with these limitations in mind.

3.4 Segmental Errors Caused by Deformation of the Peripapillary Structure

Myopic deformation of peripapillary structures leads to failures in cpRNFL thickness measurement in some highly myopic eyes (7.1 %) [28]. Specifically, two types of deformation are responsible for cpRNFL segmentation (software generation of boundary lines) failure: steep peripapillary scleral slope and large PPA. The cpRNFL varies in height in eyes with high myopia, being most commonly highest in the nasal quadrant and lowest in the temporal quadrant, giving the structure a dome-like appearance in cpRNFL B-scan (Fig. 3.8) [28]. The temporal-most portion of the cpRNFL (the bottom of the dome-like appearance) appears in the inferior half of the image acquisition frame and generally shows low signal intensity [28]. This is due to the fact that signal intensity decays with deeper axial

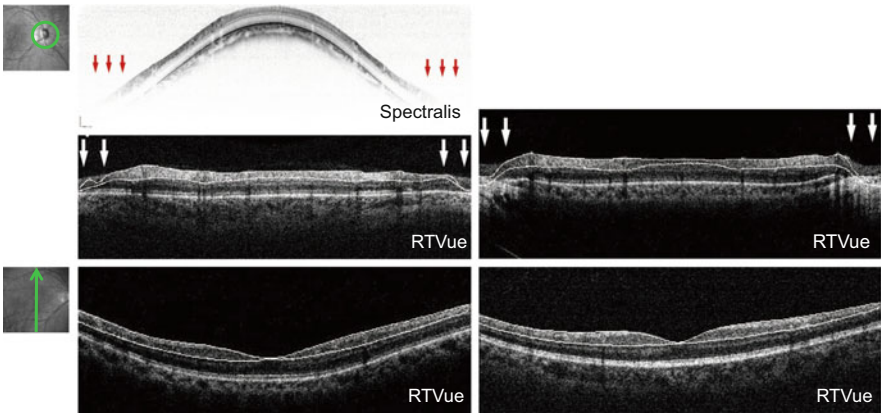

Fig. 3.8 Segmental errors caused by deformation of the peripapillary structure. There are two reasons why segmentation error occurs in the circumpapillary retinal nerve fiber layer (cpRNFL) measurement but not in the macular ganglion cell complex measurement. The *left-hand images* indicate cpRNFL segmentation errors caused by signal intensity decays stemming from deeper axial distance. The *right-hand images* show extensive PPA (Nakano et al. [28])

distance, a disadvantage of SD-OCT technology [73]. In eyes with an inferiorly tilted disc, the inferior peripapillary portion is much lower than superior one, which results in a sigmoid appearance. Consequently, the signal intensity of the inferior cpRNFL is rendered very low. Such low signal intensity can result in segmentation algorithms being unable to recognize the RNFL boundaries, straying instead into the deeper retina (Fig. 3.8) [28]. Another common cause of segmentation failure in highly myopic eyes is inclusion of PPA on the circumpapillary circle scan. In this case, the segmentation algorithm appears to be pulled away from the cpRNFL boundaries by the high scleral reflectivity within the PPA (Fig. 3.8) [28].

3.5 Differing Effects of Higher Myopia on Glaucoma Discriminating Power

We now understand that highly myopic eyes often have structural limitations, such as abnormal profiles of the cpRNFL and peripapillary steep slope. These limitations may be responsible for inaccuracies in cpRNFL measurements to detect glaucoma. A receiver operating characteristic (ROC) regression analysis [74, 75] was conducted in the following model considering the modeling covariates age, sex, visual field mean deviation (MD), axial length, and signal strength index:

$$\text{Receiver operating characteristic}\,(t) = \Phi\left[\alpha 0 + \alpha 1\,\Phi - 1\,(t) + \alpha 2\text{Age} + \alpha 3\text{Sex} + \alpha 4\text{MD} + \alpha 5\text{AL} + \alpha 6\text{SSI}\right]$$

where Φ = probit function, MD = visual field mean deviation, AL = axial length, and SSI = signal strength index.

This model revealed that the effects of longer axial length on glaucoma diagnostic performance differ depending on specific thickness parameters used. Using cpRNFL thickness, a longer axial length was likely to be associated with a poorer diagnostic performance, whereas this was not the case when macular GCC thickness was used [28].

3.6 The Usefulness of the Deviation Map in Detecting Glaucomatous Abnormalities, and Its Limitations in High Myopia

A deviation map is a display of abnormally and borderline-thinned areas on the OCT projection fundus image (Fig. 3.9). Thickness measurements are performed on each A-scan. When the measurement of each A-scan, or the average measurement of several neighboring A-points (the "superpixel"), is below the lower 99th percentile of the CI limit of the normative database, and between the lower 95th and

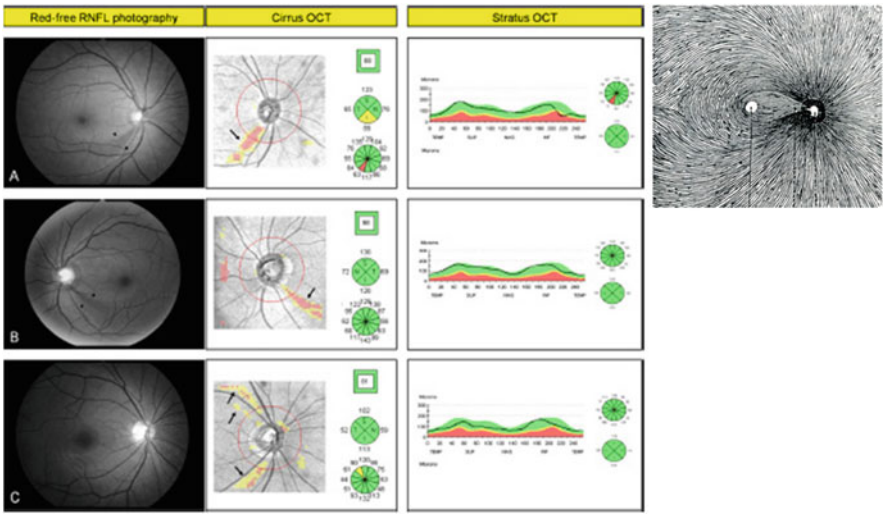

Fig. 3.9 The deviation map is accurate in detecting retinal nerve fiber layer defect in early glaucoma (Jeoung and Park [76])

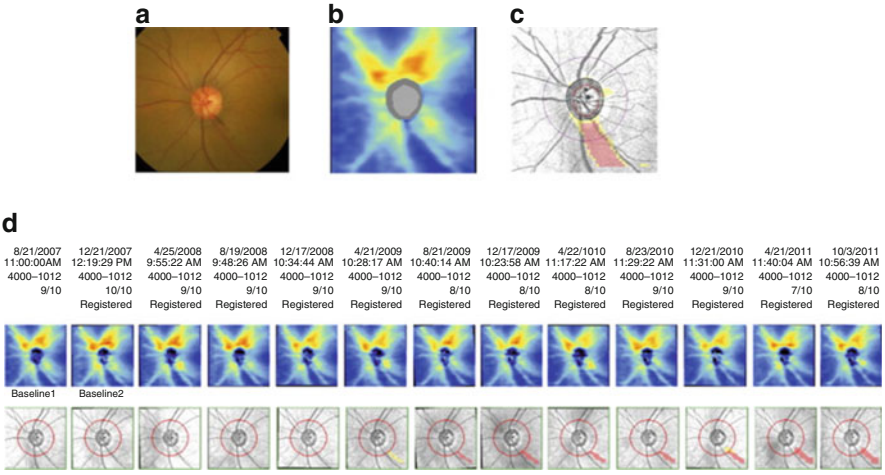

Fig. 3.10 The deviation map is an accurate indicator of glaucoma progression (Leung et al. [77])

99th percentile CI limits, it is exhibited in red (abnormal) and yellow (borderline), respectively. In the deviation map, glaucomatous RNFL damage often appears as a pattern of RNFL defects (Figs. 3.9 and 3.10) [76, 78]. These defects occur along the retinal nerve fibers that arise from the optic disc and extend radially or in an arcuate shape. Because false-positive A-scans or superpixels are rarely arranged in this unique pattern, an RNFL defect-like abnormal area in the deviation map is an excellent indicator of glaucomatous damage and its progression (Figs. 3.9 and 3.10)

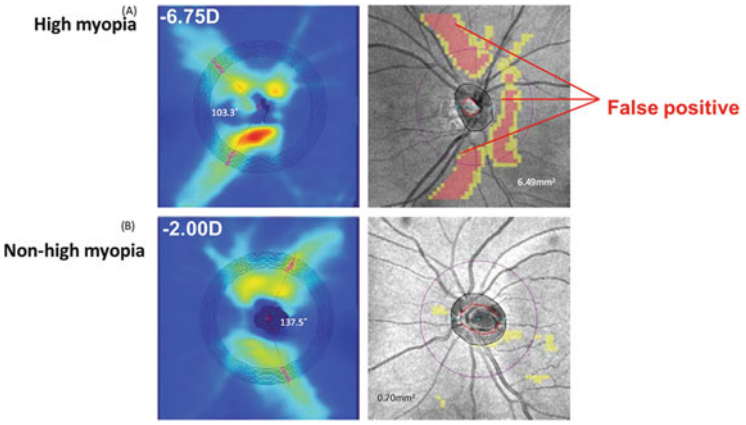

Fig. 3.11 RNFL thickness maps (*left-hand panel*) and RNFL thickness deviation maps (*right-hand panel*) of two healthy myopic eyes with spherical equivalent of (**a**) −6.75 D and (**b**) −2.00 D imaged by the Cirrus HD-OCT (Carl Zeiss Meditec). The superotemporal and inferotemporal regions become false-positive for glaucoma in highly myopic eyes when compared with a commercially available normative database (Leung et al. [79])

[76, 78]. However, we need to note that this pattern also often gives rise to false-positives in high myopia.

Compared to non-highly myopic eyes, in eyes with high myopia, the superotemporal and inferotemporal arcuate regions with the thickest RNFL (the double hump) are shifted temporally. The RNFL double-hump angle decreases by approximately 3.38° for every 1-mm increase in axial length [79]. In contrast, normative databases in commercially available SD-OCT devices often primarily contain data from non-highly myopic eyes. For this reason, superotemporal and inferotemporal regions where double humps (thickest RNFL) are located in non-highly myopic eyes are classified as abnormal thinning in highly myopic eyes (Fig. 3.11) when compared with a normative database. The abnormally thinned area has a typical RNFL pattern. However, this finding is a false-positive resulting from the application of a normative database without refractive matching. Thus, we need to exercise care in interpreting deviation maps from eyes with high myopia in OCT devices where a normative database for the condition is not available. Currently, to the best of our knowledge, such a database is only available in the RS-3000 Advance (Nidek).

3.7 From Measurement Alone to Observation of Anatomy

It is not only in SD-OCT that average measurements have been compared with normative databases, it is also a standard practice for images from the Heidelberg Retina Tomograph (HRT) confocal laser scanning ophthalmoscope (Heidelberg

Engineering, Heidelberg, Germany), the GDx-VCC scanning laser polarimeter (Carl Zeiss Meditec), and the Stratus time-domain OCT (Carl Zeiss Meditec). SD-OCT has higher axial resolution than these conventional imaging devices and much higher imaging speed than time-domain OCT. These advantages of SD-OCT are useful for increasing measurement accuracy and reproducibility [80], but not in resolving the three limitations mentioned above. Speckle noise-free B-scans, which are currently standard B-scans in all SD-OCT instruments, allow observation of single retinal layers, including the GCL, and peripapillary structures, involving optic disc margin anatomy. Because resolution is thus drastically improved in SD-OCT technologies, we should develop further diagnostic strategies based on direct observation of GON-related structural changes, rather than statistical inter-person comparison alone.

3.8 Symmetrical Macular Shape Remains with Aging

Individual macular retinal layers, including the RNFL and GCL, are highly symmetrical between superior and inferior hemispheres [27, 81]. Although each of the macular retinal layers decays with aging, the symmetrical shape remains with aging (Fig. 3.12) [81]. Macular GCL thickness increases rapidly to a peak around 1 mm superior and inferior to the foveal center (Figs. 3.13 and 3.14) [27] and gradually decreases with greater distance from the fovea (Figs. 3.13 and 3.14). Furthermore, the macular GCL is slightly thinner on the temporal than on the nasal side

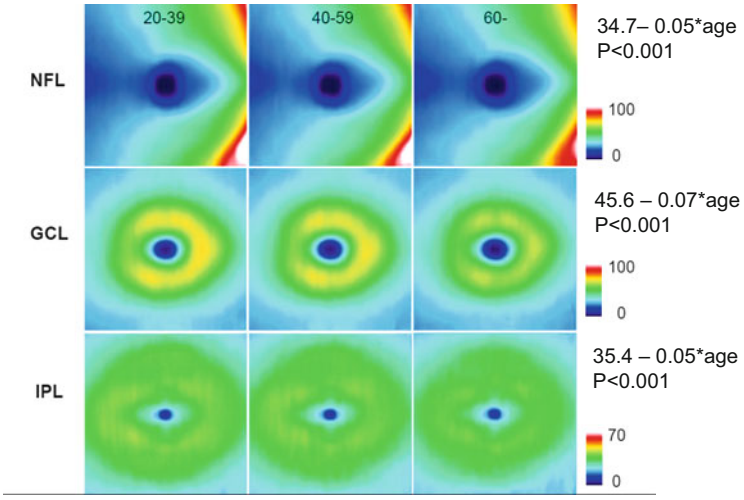

Fig. 3.12 Mean thickness maps of 80 subjects aged 20–39 years (*left*), 83 subjects aged 40–59 years (*middle*), and 93 subjects aged 60 years and older (*right*) for the nerve fiber layer (NFL), ganglion cell layer (GCL), and inner plexiform layer (IPL). *Right*, nasal; *left*, temporal. Each of the layers thins with age, but remains vertically symmetrical (Ooto et al. [81])

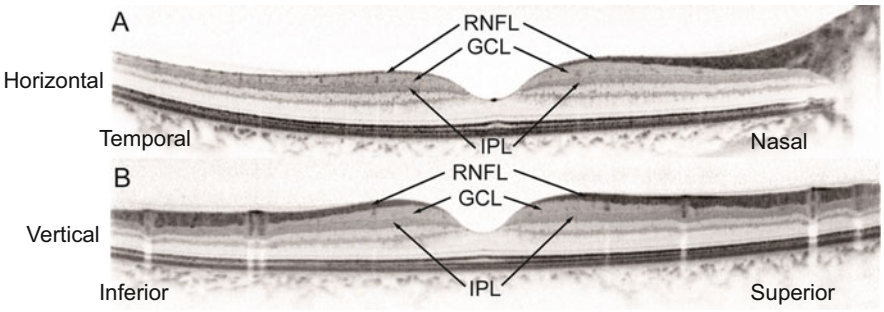

Fig. 3.13 Horizontal (**a**) and vertical (**b**) spectral-domain optical coherence tomography B-scan images Each image was generated by averaging 100 B-scans obtained by the eye-tracking SD-OCT system (Spectralis, Heidelberg Engineering, Heidelberg, Germany) (Nakano et al. [27])

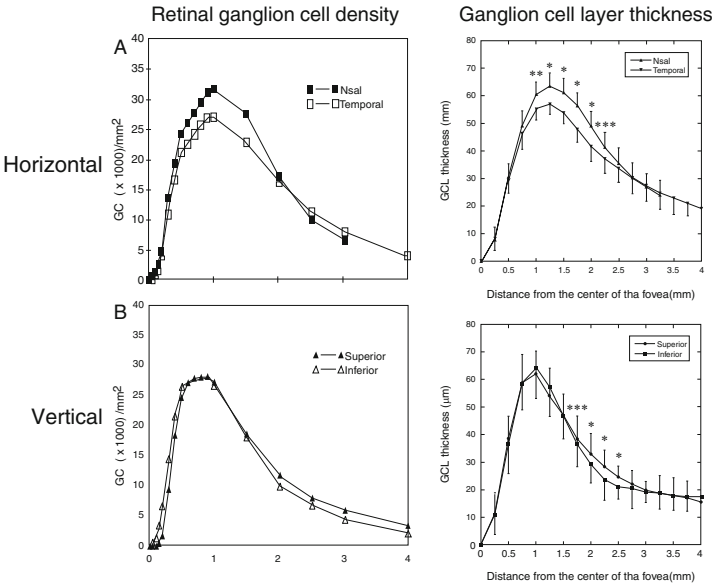

Fig. 3.14 Retinal ganglion cell density and ganglion cell layer thickness are identical in the macula (Retinal ganglion cell density graphs are from the following paper: Curcio and Allen [82]. Ganglion cell layer thickness graphs are from: Nakano et al. [27])

(Fig. 3.14) [27]. As a result, the GCL thickness map generated from three-dimensional macular raster scans shows a Landolt ring-like shape (Fig. 3.12) [81]. Importantly, this characteristic GCL structure is almost identical to the RGC density topography that has been obtained from enucleated human eyes (Fig. 3.14) [82].

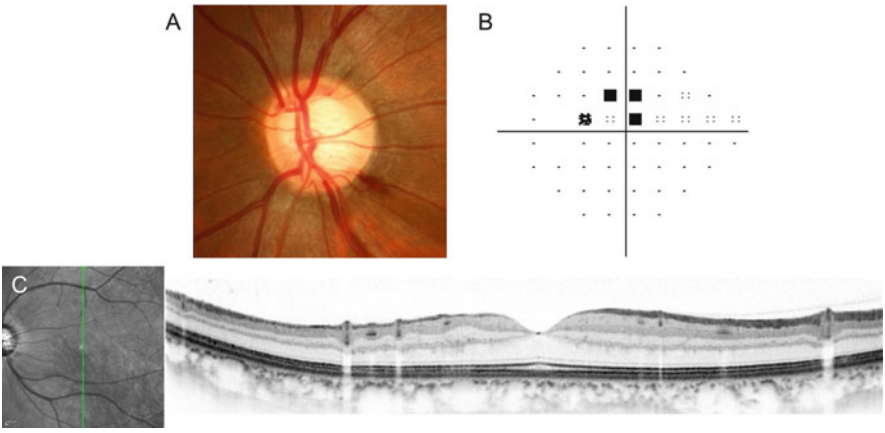

Fig. 3.15 The symmetrical ganglion cell layer structure is apparently diminished in a location corresponding to the visual field defects, optic disc neuroretinal rim thinning, and retinal nerve fiber layer defects. (**a**) Color disc photo, (**b**) pattern deviation map from standard automated perimetry 24-2, (**c**) vertical scan of spectral-domain optical coherence tomography through the fovea as shown in the infrared image

3.9 Macular Retinal Layer Thinning Seen on Glaucomatous Optic Neuropathy

In glaucoma, the symmetric GCL structure is apparently diminished in the locations of the corresponding VF defects and optic disc neuroretinal rim thinning/RNFL defects (Fig. 3.15) [28]. Thinning of the GCL is even seen in a large part of eyes with preperimetric glaucoma (Fig. 3.16) [27]. At this early stage, GCL thinning appears to be localized and abrupt.

3.10 Macular Shape Is Less Affected by the Myopic Changes of the Fundus

The photographic appearance of the optic disc, including disc size, tilting, cyclotorsion, and shape, was highly variable in highly myopic eyes, regardless of VF defect severity (Fig. 3.17) [19–22, 28]. The area of PPA also varied in size and circumference (Figs. 3.2, 3.3, and 3.4). In non-glaucomatous highly myopic eyes, macular layer structure is uniform regardless of the highly variable myopia-related optic disc deformation, which includes tilting, cyclotorsion, and PPA (Fig. 3.17) [28]. Importantly, the uniform layer structure has highly symmetrical shapes in vertical scans, even in highly myopic eyes [28]. The macula lies centrally along the globe's optical axis, whereas the optic disc is nasally shifted from the optical axis. The fact that the macula is less affected by myopic globe elongation than both the

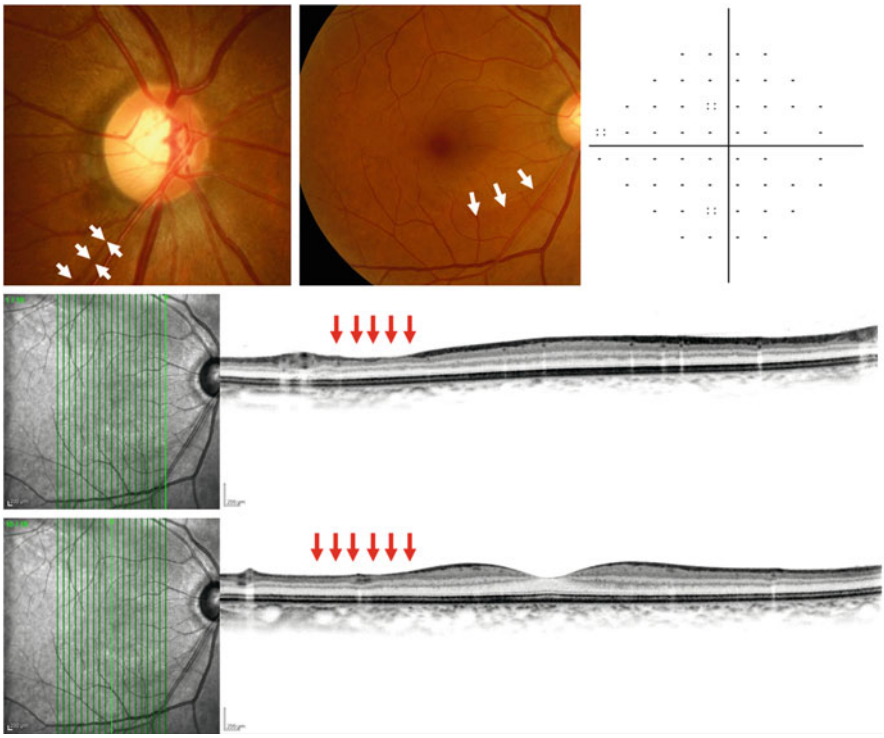

Fig. 3.16 Appearance of the macula on spectral-domain optical coherence serial vertical scans in an eye with preperimetric glaucoma

optic disc and the peripapillary sclera is probably due to this difference in position. Excessive myopic globe elongation leads to abnormal scleral extension in the macula, which causes posterior staphyloma. Posterior staphyloma in these eyes mainly shows Curtin classification type I [83], in which the macular layer symmetry remains [28]. In rare cases of type V (inferior staphyloma), type VI/VII (combined staphyloma), and type IX (septal staphyloma), the macular structure may be highly affected. Eyes with such asymmetrical deformation of posterior eye globe often have an extremely long axial length (~30 mm and sometimes more). Such cases may be better classified as pathological myopia. In the glaucoma service, highly myopic glaucomatous eyes usually have an axial length of 28 mm and less and often have symmetrical macular layer structures.

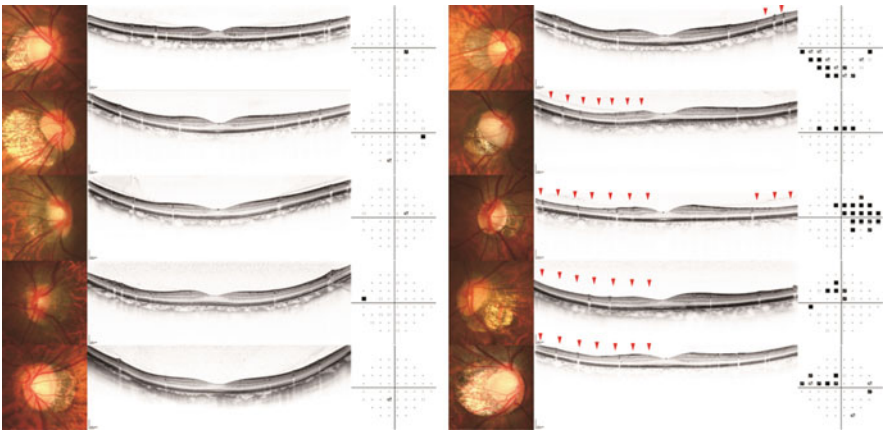

Fig. 3.17 Appearance of the optic disc and spectral-domain optical coherence tomography (SD-OCT) vertical macular scans in highly myopic eyes. The optic disc appearance and peripapillary atrophy are variable regardless of VF defect severity. In contrast, the macular appearance in SD-OCT vertical scans is uniformly symmetrical in eyes without VF defects. The retinal nerve fiber and ganglion cell layers are thinned in locations corresponding to the visual field defects

3.11 Subjective Evaluation of Macular Retinal Layers

Subjective evaluation of structural optic disc abnormalities is not favored in the field of glaucoma diagnosis research. This is because interobserver reproducibility for evaluation of the optic disc appearance is poor. However, in clinical practice, optic disc evaluation has been a gold standard criterion for glaucoma diagnosis. The advent of SD-OCT has allowed clear observation of each macular layer, including the RNFL and GCL. This has reintroduced the possibility that subjective evaluation of cross-sectional RNFL and GCL images may be a useful method for glaucoma diagnosis [27]. As discussed above, variable deformation of the optic disc makes it difficult to detect early glaucomatous changes in the optic disc, particularly in high myopia. Because the macula is highly uniform in size and shape regardless of the highly variable myopic changes of the optic disc, evaluation of the cross-sectional macular retinal layers may now be reproducible and accurate. To test this hypothesis, we asked well-trained glaucoma specialists to evaluate optic disc photos and serial vertical SD-OCT B-scans and found that in non-highly myopic eyes, interobserver agreement was excellent for both optic disc photos and SD-OCT B-scans, whereas in highly myopic eyes, interobserver agreement was poor for optic disc photos but excellent for SD-OCT B-scans [28]. In addition, in non-highly myopic eyes, classification of glaucomatous and non-glaucomatous eyes was almost perfect for both optic disc photos and SD-OCT B-scans, while in highly myopic eyes, photographic classification was less accurate than SD-OCT classification. Thus, subjective assessment of SD-OCT macular serial vertical scans may

be useful for supporting glaucoma diagnoses made using photographic disc assessment and software analysis in highly myopic eyes.

3.12 Detection of Damage Causing Paracentral Visual Field Defects

Glaucoma patients who have paracentral scotomas are at high risk of visual acuity loss [84, 85]. Moreover, paracentral VF defects can occur even in the early stages of the disease [18, 86–88]. Oversight or delay in detection of such defects causes physicians to underestimate the severity of glaucoma and progression of central vision loss. Risk factors for developing paracentral scotomas are normal-tension glaucoma (NTG) [89, 90], low maximum untreated intraocular pressures (IOPs) [91], frequent disc hemorrhage [91], systemic factors [91], and high myopia [16, 17, 42, 92, 93]. In advanced glaucoma, high myopia has been associated with significantly higher frequencies of cecocentral scotomas located just temporal and inferior to the fixation point [16, 17]. Atypical RNFL defects, including papillomacular bundle defects, are found in highly myopic eyes with primarily moderate-to-severe VF defects [42]. In this report, longer axial length, larger optic disc, and normal-tension glaucoma are risk factors for papillomacular bundle defects. Importantly, high myopia is a significant risk factor for papillomacular bundle defects and inferotemporal paracentral VF defects, even in early glaucoma [18]. Thus, it is of paramount importance to detect paracentral scotomas as early as possible, particularly in highly myopic eyes. That said, evaluation of optic disc appearance to predict paracentral VF defects is difficult, even in non-highly myopic eyes. This is much more the case in highly myopic eyes.

Unfortunately, routine SAP 24-2 or 30-2 VF testing also performs poorly in detecting early paracentral VF defects. SAP cannot detect small VF defects around 5° from a fixation point, which are detectable with SAP 10-2 [43]. This is partly because there are only five test points placed within 5° of the fixation in the SITA 24-2 or 30-2 program. In these cases, SD-OCT allows visualization of evident RNFL and GCL thinning near the fovea, which in turn motivates physicians to use the SITA 10-2 program to find VF defects at or near fixation. The macular structural parameters defined on the significance and deviation maps of retinal inner layers as measured with SD-OCT discriminated between paracentral and other VF defects better than did the cpRNFL parameters. Hence, they are potentially a predictor of paracentral VF defects [94, 95].

3.13 Intra-eye Comparison of Measurements May Outperform Inter-eye Comparison

In the subjective assessment of macular shape on serial vertical B-scans, the observers focused on symmetry between the superior and inferior hemispheres in non-glaucomatous eyes and disruption of this symmetry, caused, for example, by localized thinning of the RNFL and GCL, in glaucomatous eyes. This intra-eye comparison is justified by the fact that the human body varies widely between people. Comparison between the right and left eyes, that is, intra-person comparison, would be also free of inter-person variation. Developing intra-eye disease markers would be an effective strategy for early glaucoma diagnosis.

We developed the asymmetry index based on a logarithmic ratio of upper to lower thickness as follows [96]: We used ten vertical B-scan lines for defining the index. A horizontal line passing through the fovea and perpendicular to the direction of the horizontal scanning was used as the axis of symmetry. To compare upper (U) and lower (L) hemiretinal thickness values, we first calculated "A," the asymmetry in the thicknesses of each of eight pairs of 0.5-mm segments (x) in the upper (U) and lower (L) retinal hemispheres. We used the following equation, where Ux and Lx are the thicknesses of each parameter (RNFL, GCL, GCC, and total retina) within the xth segment from the symmetry axis in the upper (U) and lower (L) hemispheres in a single scan:

$$\begin{aligned} &\mathrm{A\ (asymmetry\ \ for\ selected\ scan\ of\ selected\ retinal\ layer\ \ for\ segment\ x)} \\ &\quad = \left|\log_{10}(\mathrm{Ux}/\mathrm{Lx})\right|. \end{aligned}$$

Then, we calculated the asymmetry index (AI) for the eight segments on each of the nasal (An $1 \sim 5$) and temporal (At $1 \sim 5$) macular scans as follows:

$$\mathrm{AI\ \ for\ each\ scan}\left(\mathrm{n1{\sim}5/t1{\sim}5}\right) = \frac{\left|\log_{10}(\mathrm{U1/L1})\right| + \left|\log 10(\mathrm{U2/L2})\right| + \cdots + \left|\log 10(\mathrm{U8/L8})\right|}{8}.$$

Finally, we calculated the asymmetry index (AI) for each eye by using the following equation:

$$\mathrm{AI\ \ for\ each\ eye} = \frac{\mathrm{An1} + \mathrm{An2} + \mathrm{An3} + \mathrm{An4} + \mathrm{An5} + \mathrm{At1} + \mathrm{At2} + \mathrm{At3} + \mathrm{At4} + \mathrm{At5}}{10}.$$

By this definition, in an eye with completely symmetrical upper and lower hemispheres, the value of AI is zero, and as asymmetry in thickness between the upper and lower hemispheres increases, the asymmetry index increases.

We found the asymmetry index had unique and favorable characteristics as an indicator of early glaucomatous damage [96]. For each retinal layer, the asymmetry indices tended to show less overlap between normal and glaucomatous eyes than did retinal layer thickness parameters (Fig. 3.18). Moreover, unlike retinal layer thickness parameters, the asymmetry indices had weak or no correlation with visual

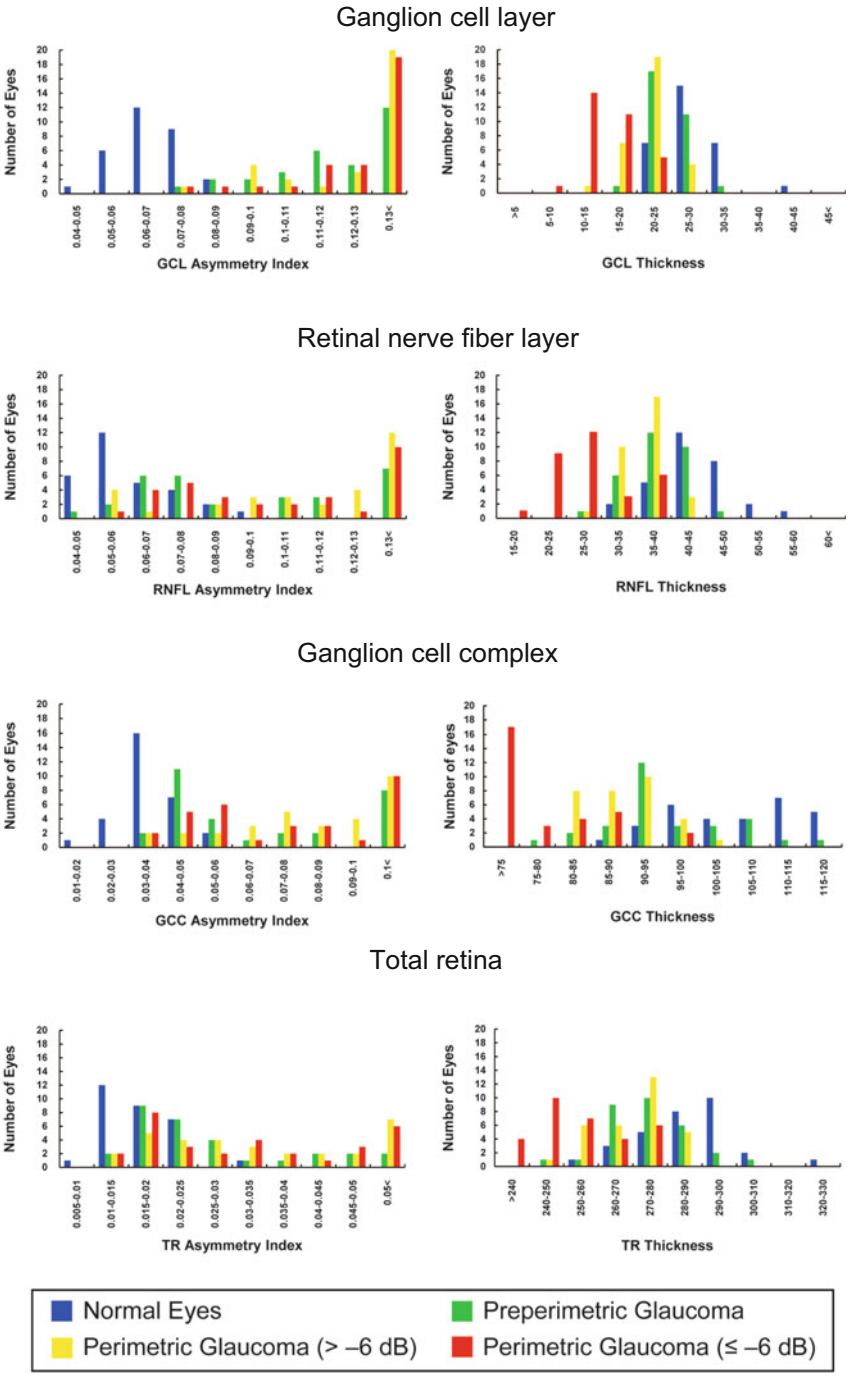

Fig. 3.18 Histograms showing the distribution of the asymmetry indices (*left*) and thicknesses (*right*) of macular retinal layers as measured using spectral-domain optical coherence tomography (Yamada et al. [96])

field MD and had good glaucoma discriminating ability (as assessed by area under the ROC curve) for each stage of glaucoma. The GCL asymmetry index in particular almost perfectly discriminated between normal eyes and eyes with glaucoma, regardless of glaucoma severity, outperforming all thickness measurements, and other asymmetry indices (Fig. 3.19). Furthermore, the GCL asymmetry index showed minimal overlap between normal and glaucomatous eyes and correlated only weakly with visual field mean deviation, which is likely to make it a better indicator of preperimetric glaucoma. This would not be expected when inter-person comparison is used.

3.14 Concluding Remarks

The optic disc and sensory retina are parts of the human body, and we need to consider the nature of human body if we are to understand the differences in the abilities of the various techniques described above to discriminate between healthy and diseased eyes. The reasons for these differences can be summarized as follows:

1. The sizes of tissues and organs vary widely. This can lead to a large overlap between healthy and early diseased eyes. Inter-person comparison is limited by this inter-person variation.
2. Almost all human motility and sensory organs exist as a symmetrical pair. Probably, because of the three-dimensionally symmetry of human vision, and the nasal shift of optic disc, retinal structures are highly vertically symmetrical. Such symmetry allows intra-person comparison.

In addition to the nature of the human body, we also need to focus on the characteristics specific to high myopia, which are as follows:

1. Myopic elongation of eye globe leads to variable deformation of the optic disc and peripapillary structures, but much less deformation in the macula. This is because the optic disc is nasally shifted, and the macula is central along the optical axis in higher primates.
2. Profiles of the cpRNFL and macular layer structures are affected by myopia and its severity. Therefore, we need to compare OCT measurements with a normative database of corresponding axial lengths/refractive errors.

These common and specific biological natures underlie the current problems in glaucoma diagnosis in high myopes. Careful consideration of these natures is essential if we are to improve the diagnosis of glaucomatous optic neuropathy in high myopia.

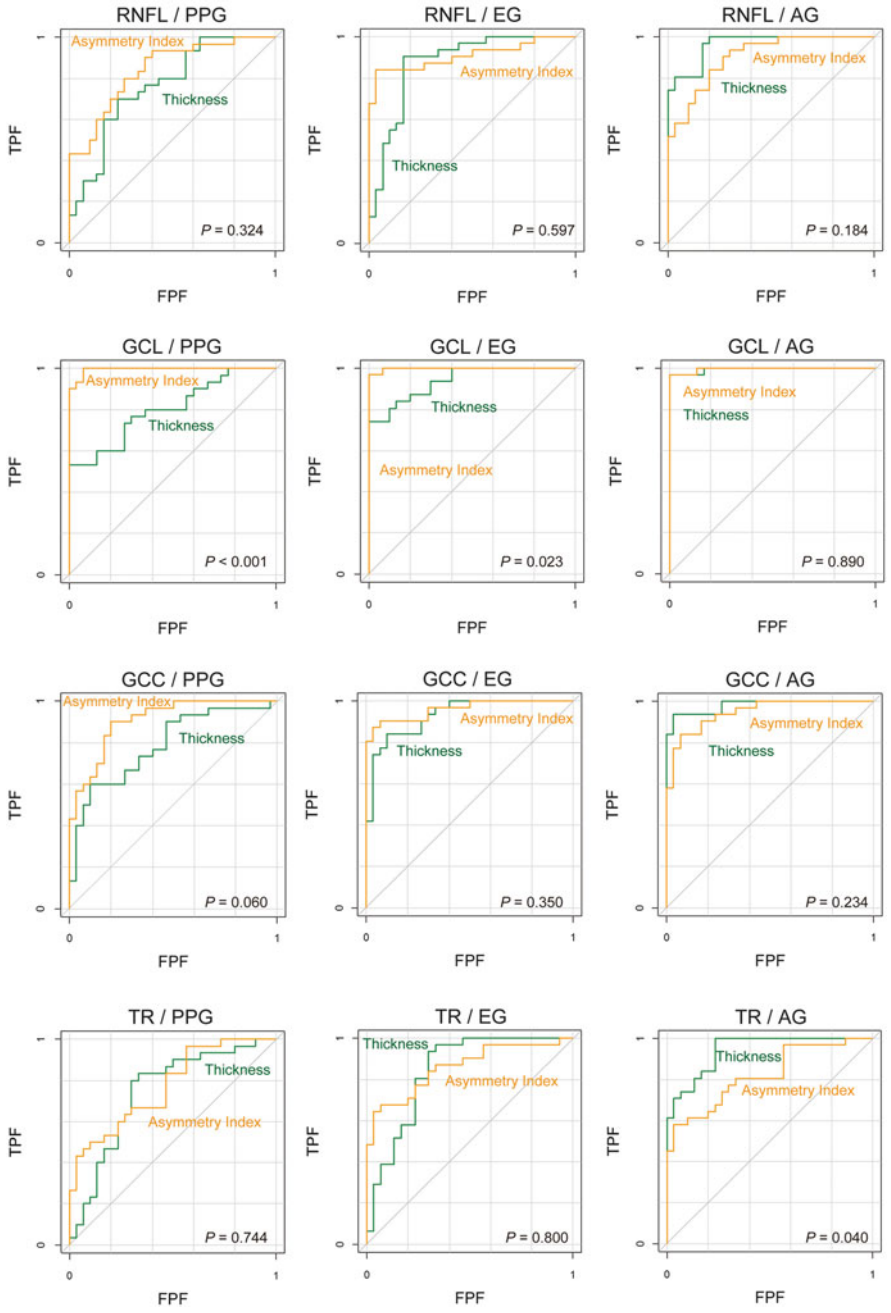

Fig. 3.19 Receiver operating characteristic curves for glaucoma diagnosis of thicknesses (*green lines*) and asymmetry indices (*orange lines*) of macular retinal layers as measured using spectral-domain optical coherence tomography. *PG* preperimetric glaucoma, *EG* early glaucoma (perimetric glaucoma with MD > -6 dB), *AG* advanced glaucoma (perimetric glaucoma with MD $\leq$ -6 dB, *right*) (Yamada et al. [96])

References

1. Harwerth RS, Carter-Dawson L, Shen F et al (1999) Ganglion cell losses underlying visual field defects from experimental glaucoma. Invest Ophthalmol Vis Sci 40:2242–2250
2. Hoyt WF, Newman NM (1972) The earliest observable defect in glaucoma? Lancet 1:692–693
3. Sommer A, Pollack I, Maumenee AE (1979) Optic disc parameters and onset of glaucomatous field loss. I. Methods and progressive changes in disc morphology. Arch Ophthalmol 97:1444–1448
4. Funk J (1991) Early detection of glaucoma by longitudinal monitoring of the optic disc structure. Graefes Arch Clin Exp Ophthalmol 229:57–61
5. Sommer A, Katz J, Quigley HA et al (1991) Clinically detectable nerve fiber atrophy precedes the onset of glaucomatous field loss. Arch Ophthalmol 109:77–83
6. Motolko M, Drance SM (1981) Features of the optic disc in preglaucomatous eyes. Arch Ophthalmol 99:1992–1994
7. Kass MA, Heuer DK, Higginbotham EJ, Ocular Hypertension Treatment Study Group et al (2002) The Ocular Hypertension Treatment Study: a randomized trial determines that topical ocular hypotensive medication delays or prevents the onset of primary open-angle glaucoma. Arch Ophthalmol 120:701–713
8. Quigley HA, Dunkelberger GR, Green WR (1989) Retinal ganglion cell atrophy correlated with automated perimetry in human eyes with glaucoma. Am J Ophthalmol 107:453–464
9. Kerrigan-Baumrind LA, Quigley HA, Pease ME et al (2000) Number of ganglion cells in glaucoma eyes compared with threshold visual field tests in the same persons. Invest Ophthalmol Vis Sci 41:741–748
10. Medeiros FA, Zangwill LM, Bowd C, Mansouri K, Weinreb RN (2012) The structure and function relationship in glaucoma: implications for detection of progression and measurement of rates of change. Invest Ophthalmol Vis Sci 53(11):6939–6946
11. Lin LLK, Shih YF, Tsai CR et al (1999) Epidemiologic study of ocular refraction among school children in Taiwan in 1995. Optom Vis Sci 76(5):275–281
12. Ling SL, Chen AJ, Rajan U et al (1987) Myopia in ten year old children: a case control study. Singapore Med J 28(4):288–292
13. Au Eong KG, Tay TH, Lim MK (1993) Race, culture and myopia in 110,236 young Singaporean males. Singapore Med J 34(1):29–32
14. He M, Xu J, Yin Q et al (2005) Need and challenges of refractive correction in urban Chinese school children. Optom Vis Sci 82(4):229–234
15. Marcus MW, de Vries MM, Montolio FG, Jansonius NM (2012) Myopia as a risk factor for open-angle glaucoma: a systematic review and meta-analysis. Ophthalmology 118(10):1989–1994
16. Mayama C, Suzuki Y, Araie M et al (2002) Myopia and advanced-stage open-angle glaucoma. Ophthalmology 109(11):2072–2077
17. Araie M, Arai M, Koseki N et al (1995) Influence of myopic refraction on visual field defects in normal tension and primary open angle glaucoma. Jpn J Ophthalmol 39(1):60–64
18. Kimura Y, Hangai M, Morooka S, Takayama K, Nakano N, Nukada M, Ikeda HO, Akagi T, Yoshimura N (2012) Retinal nerve fiber layer defects in highly myopic eyes with early glaucoma. Invest Ophthalmol Vis Sci 53(10):6472–6478
19. Jonas JB, Gusek GC, Naumann GO (1988) Optic disk morphometry in high myopia. Graefes Arch Clin Exp Ophthalmol 226(6):587–590
20. Nicolela MT, Drance SM (1996) Various glaucomatous optic nerve appearances: clinical correlations. Ophthalmology 103(4):640–649
21. Jonas JB, Dichtl A (1997) Optic disc morphology in myopic primary open-angle glaucoma. Graefes Arch Clin Exp Ophthalmol 235(10):627–633
22. Tay E, Seah SK, Chan SP et al (2005) Optic disk ovality as an index of tilt and its relationship to myopia and perimetry. Am J Ophthalmol 139(2):247–252

23. Sakamoto A, Hangai M, Yoshimura N (2008) Spectral-domain optical coherence tomography with multiple B-scan averaging for enhanced imaging of retinal diseases. Ophthalmology 115 (6):1071–1078
24. Hangai M, Yamamoto M, Sakamoto A, Yoshimura N (2009) Ultrahigh-resolution versus speckle noise-reduction in spectral-domain optical coherence tomography. Opt Express 17 (5):4221–4235
25. Jonas JB, Gusek GC, Guggenmoos-Holzmann I, Naumann GO (1988) Size of the optic nerve scleral canal and comparison with intravital determination of optic disc dimensions. Graefes Arch Clin Exp Ophthalmol 226(3):213–215
26. Jonas JB, Gusek GC, Naumann GO (1988) Optic disc, cup and neuroretinal rim size, configuration and correlations in normal eyes. Invest Ophthalmol Vis Sci 29(7):1151–1158
27. Nakano N, Hangai M, Nakanishi H, Mori S, Nukada M, Kotera Y, Ikeda HO, Nakamura H, Nonaka A, Yoshimura N (2011) Macular ganglion cell layer imaging in preperimetric glaucoma with speckle noise-reduced spectral domain optical coherence tomography. Ophthalmology 118(12):2414–2426
28. Nakano N, Hangai M, Noma H, Nukada M, Mori S, Morooka S, Takayama K, Kimura Y, Ikeda HO, Akagi T, Yoshimura N (2013) Macular imaging in highly myopic eyes with and without glaucoma. Am J Ophthalmol 156(3):511–523
29. Kim TW, Kim M, Weinreb RN, Woo SJ, Park KH, Hwang JM (2012) Optic disc change with incipient myopia of childhood. Ophthalmology 119(1):21–26
30. Jonas JB, Berenshtein E, Holbach L (2004) Lamina cribrosa thickness and spatial relationships between intraocular space and cerebrospinal fluid space in highly myopic eyes. Invest Ophthalmol Vis Sci 45(8):2660–2665
31. Akagi T, Hangai M, Takayama K, Nonaka A, Ooto S, Yoshimura N (2012) In vivo imaging of lamina cribrosa pores by adaptive optics scanning laser ophthalmoscopy. Invest Ophthalmol Vis Sci 53(7):4111–4119
32. Shoji T, Kuroda H, Suzuki M, Baba M, Hangai M, Araie M, Yoneya S (2014) Correlation between Lamina Cribrosa tilt angles, Myopia and Glaucoma using OCT with a wide bandwidth Femtosecond mode-locked laser. PLoS One 9(12):e116305
33. Takayama K, Hangai M, Kimura Y, Morooka S, Nukada M, Akagi T, Ikeda HO, Matsumoto A, Yoshimura N (2013) Three-dimensional imaging of lamina cribrosa defects in glaucoma using swept-source optical coherence tomography. Invest Ophthalmol Vis Sci 54(7):4798–4807
34. Kimura Y, Akagi T, Hangai M, Takayama K, Hasegawa T, Suda K, Yoshikawa M, Yamada H, Nakanishi H, Unoki N, Ikeda HO, Yoshimura N (2014) Lamina cribrosa defects and optic disc morphology in primary open angle glaucoma with high myopia. PLoS One 9(12):e115313
35. Nonaka A, Hangai M, Akagi T, Mori S, Nukada M, Nakano N, Yoshimura N (2011) Biometric features of peripapillary atrophy beta in eyes with high myopia. Invest Ophthalmol Vis Sci 52 (9):6706–6713
36. Kim M, Kim TW, Weinreb RN, Lee EJ (2013) Differentiation of parapapillary atrophy using spectral-domain optical coherence tomography. Ophthalmology 120(9):1790–1797
37. Park HY, Lee K, Park CK (2012) Optic disc torsion direction predicts the location of glaucomatous damage in normal-tension glaucoma patients with myopia. Ophthalmology 119(9):1844–1851
38. Choi JA, Park HY, Shin HY, Park CK (2014) Optic disc tilt direction determines the location of initial glaucomatous damage. Invest Ophthalmol Vis Sci 55(8):4991–4998
39. Kiumehr S, Park SC, Syril D, Teng CC, Tello C, Liebmann JM, Ritch R (2012) In vivo evaluation of focal lamina cribrosa defects in glaucoma. Arch Ophthalmol 130(5):552–559
40. Faridi OS, Park SC, Kabadi R, Su D, De Moraes CG, Liebmann JM, Ritch R (2014) Effect of focal lamina cribrosa defect on glaucomatous visual field progression. Ophthalmology 121 (8):1524–1530

41. Kim YW, Lee EJ, Kim TW, Kim M, Kim H (2014) Microstructure of β-zone parapapillary atrophy and rate of retinal nerve fiber layer thinning in primary open-angle glaucoma. Ophthalmology 121(7):1341–1349
42. Chihara E, Honda Y (1992) Multiple defects in the retinal nerve fiber layer in glaucoma. Graefes Arch Clin Exp Ophthalmol 230(3):201–205
43. Hangai M, Ikeda HO, Akagi T, Yoshimura N (2014) Paracentral scotoma in glaucoma detected by 10-2 but not by 24-2 perimetry. Jpn J Ophthalmol 58(2):188–196
44. Tan O, Chopra V, Lu AT et al (2009) Detection of macular ganglion cell loss in glaucoma by Fourier-domain optical coherence tomography. Ophthalmology 116(12):2305–2314, e1-2
45. Kim NR, Lee ES, Seong GJ, Kim JH, An HG, Kim CY (2010) Structure-function relationship and diagnostic value of macular ganglion cell complex measurement using Fourier-domain OCT in glaucoma. Invest Ophthalmol Vis Sci 51(9):4646–4651
46. Seong M, Sung KR, Choi EH et al (2010) Macular and peripapillary retinal nerve fiber layer measurements by spectral domain optical coherence tomography in normal-tension glaucoma. Invest Ophthalmol Vis Sci 51(3):1446–1452
47. Mori S, Hangai M, Sakamoto A, Yoshimura N (2010) Spectral-domain optical coherence tomography measurement of macular volume for diagnosing glaucoma. J Glaucoma 19 (8):528–534
48. Mwanza JC, Oakley JD, Budenz DL, Chang RT, Knight OJ, Feuer WJ (2011) Macular ganglion cell-inner plexiform layer: automated detection and thickness reproducibility with spectral domain-optical coherence tomography in glaucoma. Invest Ophthalmol Vis Sci 52 (11):8323–8329
49. Mwanza JC, Durbin MK, Budenz DL et al (2012) Glaucoma diagnostic accuracy of ganglion cell-inner plexiform layer thickness: comparison with nerve fiber layer and optic nerve head. Ophthalmology 119(6):1151–1158
50. Kotera Y, Hangai M, Hirose F, Mori S, Yoshimura N (2011) Three-dimensional imaging of macular inner structures in glaucoma by using spectral-domain optical coherence tomography. Invest Ophthalmol Vis Sci 52(3):1412–1421
51. Rolle T, Briamonte C, Curto D, Grignolo FM (2011) Ganglion cell complex and retinal nerve fiber layer measured by fourier-domain optical coherence tomography for early detection of structural damage in patients with preperimetric glaucoma. Clin Ophthalmol 5:961–969
52. Hirashima T, Hangai M, Nukada M et al (2013) Frequency-doubling technology and retinal measurements with spectral-domain optical coherence tomography in preperimetric glaucoma. Graefes Arch Clin Exp Ophthalmol 251(1):129–137
53. Arintawati P, Sone T, Akita T, Tanaka J, Kiuchi Y (2013) The applicability of ganglion cell complex parameters determined from SD-OCT images to detect glaucomatous eyes. J Glaucoma 22(9):713–718
54. Morooka S, Hangai M, Nukada M et al (2012) Wide 3-dimensional macular ganglion cell complex imaging with spectral-domain optical coherence tomography in glaucoma. Invest Ophthalmol Vis Sci 53(8):4805–4812
55. Lisboa R, Paranhos A Jr, Weinreb RN, Zangwill LM, Leite MT, Medeiros FA (2013) Comparison of different spectral domain oct scanning protocols for diagnosing preperimetric glaucoma. Invest Ophthalmol Vis Sci 54(5):3417–3425
56. Guedes V, Schuman JS, Hertzmark E et al (2003) Optical coherence tomography measurement of macular and nerve fiber layer thickness in normal and glaucomatous human eyes. Ophthalmology 110(1):177–189
57. Lederer DE, Schuman JS, Hertzmark E et al (2003) Analysis of macular volume in normal and glaucomatous eyes using optical coherence tomography. Am J Ophthalmol 135(6):838–843
58. Greenfield DS, Bagga H, Knighton RW (2003) Macular thickness changes in glaucomatous optic neuropathy detected using optical coherence tomography. Arch Ophthalmol 121(1):41–46

59. Wollstein G, Schuman JS, Price LL et al (2004) Optical coherence tomography (OCT) macular and peripapillary retinal nerve fiber layer measurements and automated visual fields. Am J Ophthalmol 138(2):218–225
60. Wollstein G, Ishikawa H, Wang J et al (2005) Comparison of three optical coherence tomography scanning areas for detection of glaucomatous damage. Am J Ophthalmol 139 (1):39–43
61. Medeiros FA, Zangwill LM, Bowd C et al (2005) Evaluation of retinal nerve fiber layer, optic nerve head, and macular thickness measurements for glaucoma detection using optical coherence tomography. Am J Ophthalmol 139(1):44–55
62. Ojima T, Tanabe T, Hangai M et al (2007) Measurement of retinal nerve fiber layer thickness and macular volume for glaucoma detection using optical coherence tomography. Jpn J Ophthalmol 51(3):197–203
63. Melo GB, Libera RD, Barbosa AS, Pereria LM, Doi LM, Melo LA Jr (2006) Comparison of optic disk and retinal nerve fiber layer thickness in nonglaucomatous and glaucomatous patients with high myopia. Am J Ophthalmol 142(5):858–860
64. Leung CK, Mohamed S, Leung KS et al (2006) Retinal nerve fiber layer measurements in myopia: an optical coherence tomography study. Invest Ophthalmol Vis Sci 47(12):5171–5176
65. Vernon SA, Rotchford AP, Negi A, Ryatt S, Tattersal C (2008) Peripapillary retinal nerve fibre layer thickness in highly myopic Caucasians as measured by Stratus optical coherence tomography. Br J Ophthalmol 92(8):1076–1080
66. Qiu KL, Zhang MZ, Leung CK et al (2011) Diagnostic classification of retinal nerve fiber layer measurement in myopic eyes: a comparison between time-domain and spectral-domain optical coherence tomography. Am J Ophthalmol 152(4):646–653
67. Kim MJ, Lee EJ, Kim TW (2010) Peripapillary retinal nerve fibre layer thickness profile in subjects with myopia measured using the Stratus optical coherence tomography. Br J Ophthalmol 94(1):115–120
68. Mohammad Salih PA (2012) Evaluation of peripapillary retinal nerve fiber layer thickness in myopic eyes by spectral-domain optical coherence tomography. J Glaucoma 21(1):41–44
69. Rauscher FM, Sekhon N, Feuer WJ et al (2009) Myopia affects retinal nerve fiber layer measurements as determined by optical coherence tomography. J Glaucoma 18(7):501–505
70. Hwang YH, Yoo C, Kim YY (2012) Myopic optic disc tilt and the characteristics of peripapillary retinal nerve fiber layer thickness measured by spectral-domain optical coherence tomography. J Glaucoma 21(4):260–265
71. Hwang YH, Yoo C, Kim YY (2012) Characteristics of peripapillary retinal nerve fiber layer thickness in eyes with myopic optic disc tilt and rotation. J Glaucoma 21(6):394–400
72. Kang SH, Hong SW, Im S, Lee S, Ahn MD (2010) Effect of myopia on the thickness of the retinal nerve fiber layer measured by Cirrus HD optical coherence tomography. Invest Ophthalmol Vis Sci 51(8):4075–4083
73. Potsaid B, Baumann B, Huang D et al (2010) Ultrahigh speed 1050 nm swept source/Fourier domain OCT retinal and anterior segment imaging at 100,000 to 400,000 axial scans per second. Opt Express 18(19):20029–20048
74. Alonzo TA, Pepe MS (2002) Distribution-free ROC analysis using binary regression techniques. Biostatistics 3(3):421–432
75. Janes H, Longton G, Pepe MS (2009) Accommodating covariates in receiver operating characteristic analysis. Stata J 9(1):17–39
76. Jeoung JW, Park KH (2010) Comparison of Cirrus OCT and Stratus OCT on the ability to detect localized retinal nerve fiber layer defects in preperimetric glaucoma. Invest Ophthalmol Vis Sci 51(2):938–945
77. Leung CK, Yu M, Weinreb RN, Lai G, Xu G, Lam DS (2012) Retinal nerve fiber layer imaging with spectral-domain optical coherence tomography: patterns of retinal nerve fiber layer progression. Ophthalmology 119(9):1858–1866. doi:10.1016/j.ophtha.2012.03.044. Epub 2012 Jun 5

78. Leung CK, Lam S, Weinreb RN, Liu S, Ye C, Liu L, He J, Lai GW, Li T, Lam DS (2010) Retinal nerve fiber layer imaging with spectral-domain optical coherence tomography: analysis of the retinal nerve fiber layer map for glaucoma detection. Ophthalmology 117(9):1684–1691
79. Leung CK, Yu M, Weinreb RN, Mak HK, Lai G, Ye C, Lam DS (2012) Retinal nerve fiber layer imaging with spectral-domain optical coherence tomography: interpreting the RNFL maps in healthy myopic eyes. Invest Ophthalmol Vis Sci 53(11):7194–7200
80. Sung KR, Kim JS, Wollstein G, Folio L, Kook MS, Schuman JS (2011) Imaging of the retinal nerve fibre layer with spectral domain optical coherence tomography for glaucoma diagnosis. Br J Ophthalmol 95(7):909–914
81. Ooto S, Hangai M, Tomidokoro A, Saito H, Araie M, Otani T, Kishi S, Matsushita K, Maeda N, Shirakashi M, Abe H, Ohkubo S, Sugiyama K, Iwase A, Yoshimura N (2011) Effects of age, sex, and axial length on the three-dimensional profile of normal macular layer structures. Invest Ophthalmol Vis Sci 52(12):8769–8779
82. Curcio CA, Allen KA (1990) Topography of ganglion cells in human retina. J Comp Neurol 300(1):5–25
83. Curtin BJ (1977) The posterior staphyloma of pathologic myopia. Trans Am Ophthalmol Soc 75:67–86
84. Kolker AE (1977) Visual prognosis in advanced glaucoma: a comparison of medical and surgical therapy for retention of vision in 101 eyes with advanced glaucoma. Trans Am Ophthalmol Soc 75:539–555
85. Coeckelbergh TR, Brouwer WH, Cornelissen FW, Van Wolffelaar P, Kooijman AC (2002) The effect of visual field defects on driving performance: a driving simulator study. Arch Ophthalmol 120:1509–1516
86. Stamper RL (1984) The effect of glaucoma on central visual function. Trans Am Ophthalmol Soc 82:792–826
87. Anctil JL, Anderson DR (1984) Early foveal involvement and generalized depression of the visual field in glaucoma. Arch Ophthalmol 102:363–370
88. Schiefer U, Papageorgiou E, Sample PA, Pascual JP, Selig B, Krapp E et al (2010) Spatial pattern of glaucomatous visual field loss obtained with regionally condensed stimulus arrangements. Invest Ophthalmol Vis Sci 51:5685–5689
89. Hitchings RA, Anderton SA (1983) A comparative study of visual field defects seen in patients with low-tension glaucoma and chronic simple glaucoma. Br J Ophthalmol 67:818–821
90. Caprioli J, Spaeth GL (1984) Comparison of visual field defects in the low-tension glaucomas with those in the high-tension glaucomas. Am J Ophthalmol 97:730–737
91. Park SC, De Moraes CG, Teng CCW et al (2011) Initial parafoveal versus peripheral scotomas in glaucoma: risk factors and visual field characteristics. Ophthalmology 118:1782–1789
92. Chihara E, Tanihara H (1992) Parameters associated with papillomacular bundle defects in glaucoma. Graefes Arch Clin Exp Ophthalmol 230:511–517
93. Chihara E, Sawada A (1990) Atypical nerve fiber layer defects in high myopes with high-tension glaucoma. Arch Ophthalmol 108:228–232
94. Kimura Y, Hangai M, Matsumoto A, Akagi T, Ikeda HO, Ohkubo S, Sugiyama K, Iwase A, Araie M, Yoshimura N (2013) Macular structure parameters as an automated indicator of paracentral scotoma in early glaucoma. Am J Ophthalmol 156(5):907–917
95. Lee J, Hangai M, Kimura Y, Takayama K, Kee C, Yoshimura N (2013) Measurement of macular ganglion cell layer and circumpapillary retinal nerve fiber layer to detect paracentral scotoma in early glaucoma. Graefes Arch Clin Exp Ophthalmol 251(8):2003–2012
96. Yamada H, Hangai M, Nakano N, Takayama K, Kimura Y, Miyake M, Akagi T, Ikeda HO, Noma H, Yoshimura N (2014) Asymmetry analysis of macular inner retinal layers for glaucoma diagnosis. Am J Ophthalmol 158(6):1318–1329

Chapter 4
High Myopia and Myopic Glaucoma: Findings in the Peripapillary Retina and Choroid in Highly Myopic Eyes

Yasushi Ikuno

Abstract Because increasing evidence indicates that there is a close relationship between glaucoma and myopia, we hypothesized that conformational changes around the optic disc and axial elongation may biomechanically stress the optic nerve and increase the susceptibility of the lamina cribrosa to intraocular pressure. The area has a unique appearance, including the shape of the disc, an enlarged area of peripapillary atrophy, and nasal elevation with temporal flattening of the disc. These signs potentiality result from stretching of the posterior ocular wall and oblique insertion of the optic nerve, and investigators are expecting to find the key to the pathogenesis of glaucoma. Moreover, recent advances in imaging technologies are enabling visualization of the deep structural characteristics. This chapter reviews the morphologic and histologic changes in the peripapillary area in highly myopic eyes and addresses the underlying mechanism of glaucoma.

Keywords Myopia • Optic nerve head • Optic disc tilting • Optical coherence tomography • Choroid • Peripapillary atrophy

4.1 Introduction

Recent investigations have shed light on a relationship between myopia and glaucoma. The detailed mechanism is not fully understood; however, it is believed to result from increased susceptibility to intraocular pressure (IOP) in highly myopic eyes due to deformation of the eye wall at or around the optic disc area resulting from axial length elongation. The details of this relationship remain unclear because of difficulties observing the deep structures around the myopic disc *in vivo*. Recent advances in imaging modalities have enabled visualization of these tissues and fostered an understanding of the underlying pathologies stemming from deformity of the posterior wall. This chapter reviews the currently recognized

Y. Ikuno, M.D. (✉)
Ikuno Eye Center, 2-9-10-3F Juso-Higashi, Yodogawa-Ku, Osaka 532-0023, Japan
e-mail: yasushi.ikuno@gmail.com

K. Sugiyama, N. Yoshimura (eds.), *Myopia and Glaucoma*,
DOI 10.1007/978-4-431-55672-5_4

optic nerve and peripapillary tissue changes in high myopia and discusses a possible relationship with glaucoma.

4.2 General Morphology of the Myopic Optic Disc

4.2.1 Ophthalmoscopic Appearance

The myopic nerve head is often vertically ovoid along the long axis and appears oblique, i.e., the so-called tilted disc (Fig. 4.1). In non-myopic eyes, the nerve running into the eye usually courses at almost a right angle to the ocular surface. However, in myopic eyes, the course of the nerve axis is more oblique toward the temporal side as a result of posterior ocular wall protrusion (Fig. 4.2). This causes conformational changes in the disc surface that flatten the temporal side and elevate the nasal side [1]. Other characteristics are a secondary enlarged macrodisc, shallow disc cupping, and decreased contrast between the color of the neuroretinal rim and the color of the optic cup (Fig. 4.3). These features result from stretching of the posterior ocular structures because of the myopic shift.

A histomorphometric study reported that high myopic disc is about 1.5 times larger than non-myopic in absolute glaucoma [2], and fundus photographs show a substantially larger, and shallower disc in primary open-angle glaucoma with high myopia [3]. A large population study of Asian individuals reported that the disc area in myopic eyes is about 2–3 times larger than in emmetropic eyes and that the disc area is associated significantly with the degree of myopia. Interestingly, a graph of disc sizes showed a steep curve in high myopia, but the curve was relatively

Fig. 4.1 Typical myopic disc with tilting on fundus photograph. The disc appears oval with the maximal diameter along the vertical axis

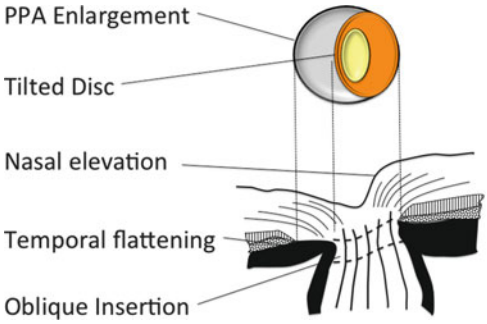

Fig. 4.2 The schema of oblique insertion and disc tilting in high myopia. The optic nerve runs oblique to the eye wall, resulting in flattening of the temporal side and elevating of the nasal side

Fig. 4.3 A typical myopic macrodisc. The disc is not tilted, and unlike that in Fig. 4.1, this disc is flat with shallow cupping

horizontal in moderate myopia, suggesting that the highly myopic disc has specific features among the different degrees of myopia [4].

4.3 Peripapillary Atrophy

4.3.1 Definition

The myopic temporal crescent, sometimes referred to as beta-zone peripapillary atrophy (PPA) and conus myopicus (myopic conus), is a white, sharply defined area on the temporal side of the optic disc where the inner scleral surface is directly observable (Fig. 4.4). The myopic temporal crescent results from displacement of the choroid and retinal pigment epithelium (RPE) because of protrusion of the posterior pole [1]. A larger area of PPA and a higher refractive error are highly

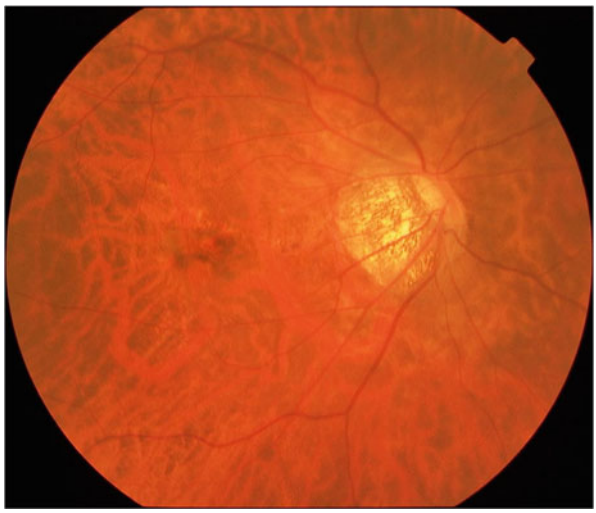

Fig. 4.4 The typical appearance of beta-peripapillary atrophy in high myopia. A whitish lesion with a well-defined border is seen that normally develops inferotemporal or temporal to the optic disc

correlated, and steep myopic increases exceeding −7 to −8 diopters have been reported [5], indicating that a large area of PPA is a hallmark of high myopia. There are two types of PPA. The first is a peripheral zone (alpha zone) characterized by irregular hypopigmentation and hyperpigmentation by fundus observation that is adjacent to the retina on the outer side; the second is the beta zone on the inner side, which is characterized by visible sclera and large choroidal vessels [6]. The myopic crescent normally presents temporal or inferotemporal to the disc and must be differentiated from the congenital tilted disc, which normally occurs inferiorly [7].

4.3.2 Histological Observation

Histologically, the alpha zone corresponds to irregularities in the RPE, while the beta zones is characterized by complete loss of RPE cells and almost complete loss of photoreceptors and closure of the choriocapillaris [8].

Recently, gamma and delta zones also have been proposed based on the results of a histologic study of myopic eyes [9]. The gamma zone is between the end of Bruch's membrane and the edge of the optic nerve head and was found predominantly in eyes with an axial length exceeding 26.5 mm, suggesting that the zone is specific to high myopia. The delta zone is part of the gamma zone in which blood vessels were not present. Interestingly, the length of the beta zone was not associated with high myopia but with glaucoma, while the lengths of the gamma and delta zones were associated with high myopia but not with glaucoma. We hypothesized that these proportional changes in the PPA zone may be associated with the susceptibility of the IOP in highly myopic eyes and may be why glaucoma develops in certain highly myopic eyes.

4.3.3 Optical Coherence Tomographic Findings

Some unique features within the area of PPA are specific to myopia or glaucoma. Spectral-domain optic coherence tomography (OCT) has shown that Bruch's membrane is often absent within the beta-PPA area in highly myopic eyes. The scleral bed configurations within the PPA can be classified into three types based on OCT findings: straight, a downward curving Bruch's membrane, or a downward bending slope without Bruch's membrane. Only the last is associated significantly with the myopic refractive error, and interestingly, the second is associated significantly with glaucoma [10]. This fact suggests that the configuration of the scleral bed within the PPA is related closely to myopic glaucoma, which partly agrees with histologic observations [9].

New imaging modalities including SD-OCT provide detailed information about the anatomic relationships among the disc edge, Bruch's membrane, and RPE. Observation using these new modalities has resulted in an argument that the beta-PPA should be redefined based on the findings using the latest generation of imaging tools. SD-OCT studies have found that the RPE was within the beta-PPA area in many cases, which is contrary to the initial definition based on histologic studies without RPE cells [11, 12].

4.3.4 Progression

The area of PPA enlarges over time with myopic progression (Fig. 4.5). The congenital crescent that normally does not enlarge must be ruled out. The myopic disc shifts nasally with axial length elongation, which induces myopic crescent development temporally. A follow-up study found a significant correlation between optic disc deviation and myopic progression [13].

Serial disc photographs also showed progressive tilting of the optic nerve head with development or enlargement of the area of PPA in myopic children. In the group with changes in the optic nerve head and area of PPA, the mean horizontal-to-vertical disc diameter ratio decreased from 0.92 to 0.86, and the mean maximal PPA width-to-vertical disc diameter ratio increased from 0.08 to 0.20 during a mean follow-up period of 38.1 months. These changes were most marked in children between 7 and 9 years of age and were associated with a greater myopic shift [14]. Thus, a myopic shift induces disc tilting and consequent PPA enlargement in myopic eyes.

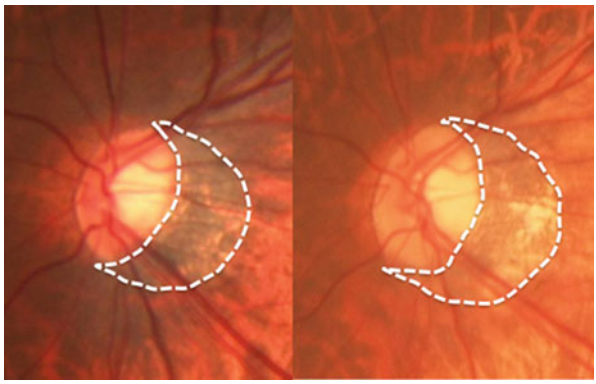

Fig. 4.5 Enlargement of peripapillary atrophy (PPA) over years. The same patient at baseline (*left*) and 10 years later (*right*); enlargement of PPA and increased disc tilting are seen (*white dashed lines*). The axial length has elongated from 28.67 mm to 29.03 mm

4.4 Tilted Disc

4.4.1 Ophthalmoscopic Appearance

Tilting is one of the most common features of a myopic disc; the nasal margin typically becomes elevated relative to the temporal margin. Angulation of the optic cup axis inferonasally is also common. Myopic discs with acquired crescents and congenital tilted discs can be difficult to distinguish because both have a severely attenuated RPE, Bruch's membrane, and choroid close to the disc.

4.4.2 Relation to Myopia

Several studies have reported a positive association between tilted discs and long axial lengths. One study found that 55 of 150 myopic eyes had markedly tilted optic discs, with a cut-off value of the disc index less than 0.8. In addition, smaller disc ovality was observed in more highly myopic eyes with a longer axial length [15]. The relationship between optic disc tilt and myopia also has been reported in pediatric patients. Schoolchildren with tilted discs have significantly longer axial lengths and greater myopic refractive errors [16].

4.4.3 Conventional Indices for Tilted Discs

Because the maximal angle of the disc tilting cannot be measured directly, it is estimated by the degree of disc ovality (Fig. 4.6). When viewed along the visual axis, the less perpendicular the optic nerve is when it enters the globe, the greater the elliptical appearance is. The papillary index, defined by the shortest axis/longest

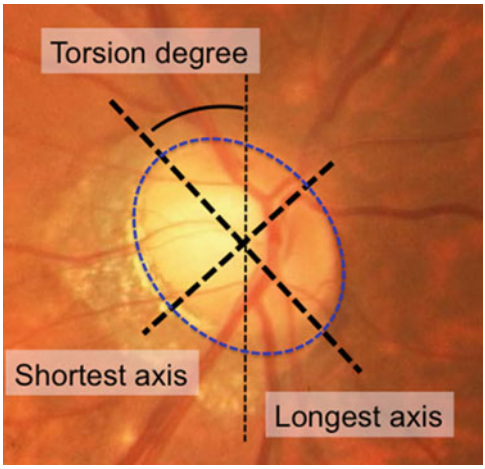

Fig. 4.6 Measurement of disc tilting. The disc is regarded as an ellipsoid and the maximal and minimal diameters crossing perpendicularly at the center of the optic nerve head are obtained. The index is the ratio of the minimal/maximal diameters. The angle between the maximal diameter and the vertical line is expressed as the degree of torsion

axis on fundus photographs, has been used as the gold standard to represent the degree of disc tilting [17]. The threshold to define the tilted disc often is lower than 0.8–0.75. Non-myopic discs are minimally oval with the vertical diameter slightly longer than the horizontal, and the index is close to 1.0.

The second geometric variable in tilted discs is rotation around the sagittal axis of the optic nerve (Fig. 4.6), which is referred to optic disc torsion. The longest diameter usually falls within 15° of the vertical meridian; axes beyond 15° are commonly defined as "torted."

4.4.4 Peripapillary Tilting Index

Because tilted discs associated with myopia occur as a result of posterior conformational changes from axial elongation, the morphologic changes at the peripapillary area are supposed to be related closely to the direction and degree of disc tilting. Measuring the disparity between the maximal and minimal surface elevations of the disc is an indirect way to measure the angle of the optic nerve as it enters the eye. The greater the elevation is in surface levels against the opposite side, the greater the tilting is assumed to be.

We developed a new system to measure this disparity in the 360° of the disc. We use a circular peripapillary scan with the average RPE height as the reference plane. The RPE line is divided into 24 sectors and the heights in all sectors is averaged. The difference in height from the average value is referred to as the peripapillary tilting index (PTI) (Fig. 4.7). This value does not exactly represent the degree of disc oblique insertion, but the degree of tilting in each direction around the disc. Another advantage of this system is that it identifies the direction in which the disc is most tilted. The minimal PTI value agreed well with the disc ovality index. We

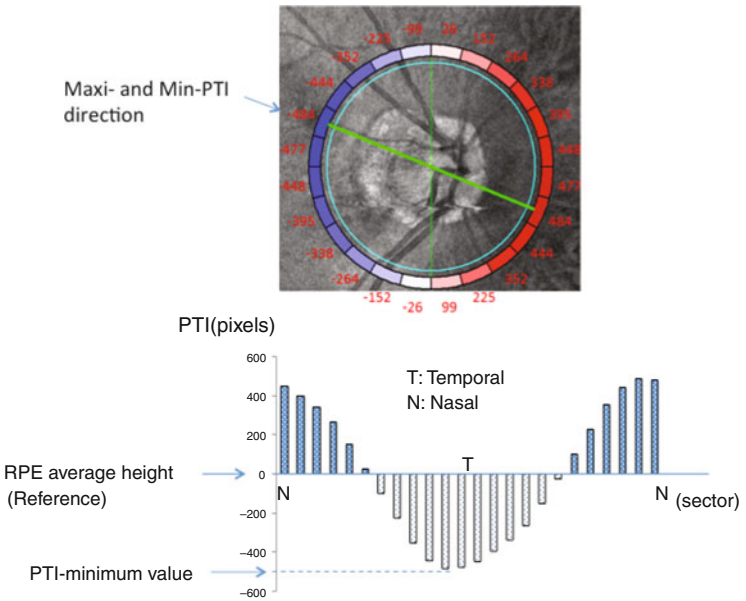

Fig. 4.7 Measurement of the peripapillary tilting index. The average position of the retinal pigment epithelium in 24 sectors in a peripapillary circular scan is obtained, and the difference from the average value is measured in each sector. This shows the degree of tilting in a particular direction

found that the minimal PTI was in the inferotemporal direction in myopic discs, indicating that myopic discs predominantly tilt in that direction. We currently are investigating the relationship with myopic normal tension glaucoma (NTG).

4.5 Peripapillary Choroidal Thickness

4.5.1 Choroidal Thickness in Normal Eyes

There is wide interindividual variability in choroidal thickness with age, refractive error, and axial length. The choroid in myopic eyes is thinner because of stretching of the posterior eye. For example, the mean subfoveal choroidal thickness ranges from 250 to 350 μm in emmetropic eyes, while in high myopia it is about 100 μm, depending on the degree of myopia [18, 19]. A histologic study reported that the loss of capillaries and fibrous tissue replacement are evident in highly myopic eyes [20].

Choroidal thinning is disproportional at the macula [18, 19]. In highly myopic eyes, the inferior and nasal sectors are thinner, and the temporal and superior sectors are relatively thicker. The subfovea is the thickest in non-myopic eyes.

Thus, the stretching affects each locations differently in highly myopic eyes. In the peripapillary area, the inferior sector is significantly thinner than other sectors in the peripapillary lesions of non-myopic normal eyes [21].

4.5.2 Glaucoma and Choroidal Thickness

The mechanism of NTG in myopic eyes is puzzling. We hypothesized that this might depend on the posterior eye wall configuration and conducted a study to measure the choroidal thickness in eyes with myopic glaucoma. The study included 12 eyes of eight patients under 45 years of age who had NTG with refractive errors between −6 and −12 diopters and axial lengths exceeding 26.5 mm and 12 eyes of matched healthy volunteers with a similar degree of myopia. The mean choroidal thickness in the NTG group was significantly thinner at the fovea and superior, superotemporal, temporal, and inferotemporal to the optic nerve head (Fig. 4.8).

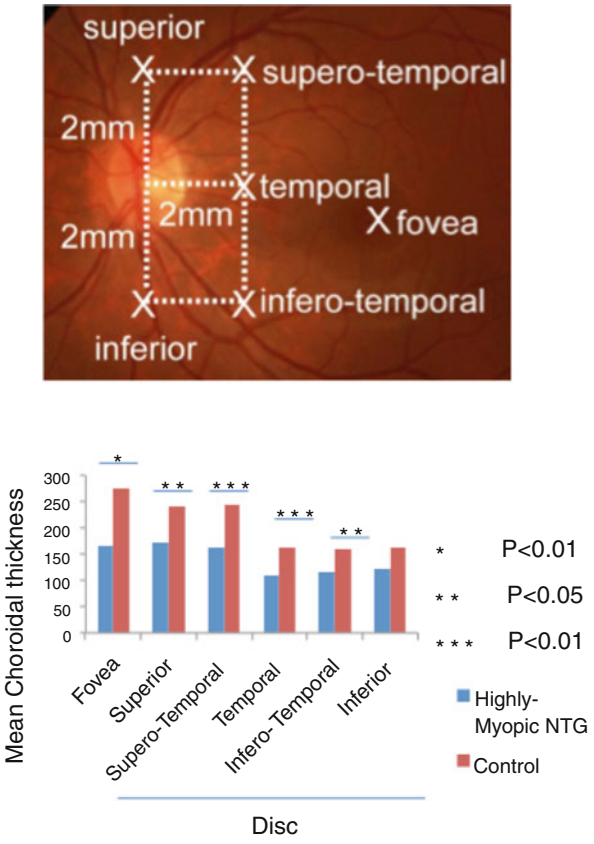

Fig. 4.8 The mean choroidal thickness in highly myopic eyes with or without normal tension glaucoma (NTG). The thickness is significantly smaller around the disc and at the macula in NTG

This suggested that choroidal thinning is related to highly myopic NTG and the indices may be a useful diagnostic parameter for myopic NTG.

4.5.3 Controversies in Glaucoma and Choroidal Thicknesses

However, a controversy remains. Many studies have reported that there is no significant difference in the choroidal thickness between normal and glaucomatous eyes, such as those with primary open angle glaucoma [22]. However, others have reported that NTG is associated with significant thinning inferonasal, inferior, and inferotemporal to the optic nerve head [23]. Interestingly, the choroidal thickness varies based on the damage to the optic nerve, and the sclerotic type was associated with a significantly thinner choroid than compared with the diffuse and focal types and even healthy controls [24]. Thus, the choroidal thickness may not differ in most types of glaucoma but may differ in some specific conditions such as high myopia or in eyes with peripapillary thinning.

4.6 Summary

High myopia is a disease of morphologic changes of the posterior ocular wall that causes mechanical stress on the deep structures, such as the optic nerve, peripapillary choroid or sclera, and the lamina cribrosa. The peripapillary region in highly myopic eyes is markedly deformed due to axial length elongation and seems to contribute greatly to the high glaucoma risk. However, its relationship is not totally understood. Modern imaging technologies such as OCT may reveal the underlying mechanism of the stress around the disc area. This field has come under intense scrutiny in the last 10 years, and hopefully the predictive factors and risks will be determined in the near future.

References

1. Apple DJ et al (1982) Congenital anomalies of the optic disc. Surv Ophthalmol 27(1):3–41
2. Dichtl A et al (1998) Histomorphometry of the optic disc in highly myopic eyes with absolute secondary angle closure glaucoma. Br J Ophthalmol 82(3):286–289
3. Jonas J, Dichtl A (1997) Optic disc morphology in myopic primary open-angle glaucoma. Graefes Arch Clin Exp Ophthalmol 235(10):627–633
4. Wu R-Y et al (2011) Relationship of central corneal thickness with optic disc parameters: the Singapore Malay Eye Study. Invest Ophthalmol Vis Sci 52(3):1320–1324
5. Xu L et al (2010) Definition of high myopia by parapapillary atrophy. The Beijing Eye Study. Acta Ophthalmol 88(8):e350–e351

6. Jonas J (2005) Clinical implications of peripapillary atrophy in glaucoma. Curr Opin Ophthalmol 16(2):84–88
7. Vongphanit J et al (2002) Population prevalence of tilted optic disks and the relationship of this sign to refractive error. Am J Ophthalmol 133(5):679–685
8. Jonas J, Nguyen X (1989) Parapapillary chorioretinal atrophy in normal and glaucoma eyes. I. Morphometric data. Invest Ophthalmol Vis Sci 30(5):908–918
9. Jonas J et al (2012) Parapapillary atrophy: histological gamma zone and delta zone. PLoS One 7(10):e47237
10. Hayashi K et al (2012) Spectral-domain optical coherence tomography of β-zone peripapillary atrophy: influence of myopia and glaucoma. Invest Ophthalmol Vis Sci 53(3):1499–1505
11. Park SC et al (2010) In-vivo microstructural anatomy of beta-zone parapapillary atrophy in glaucoma. Invest Ophthalmol Vis Sci 51(12):6408–6413
12. Lee K et al (2010) Cross-sectional anatomic configurations of peripapillary atrophy evaluated with spectral domain-optical coherence tomography. Invest Ophthalmol Vis Sci 51 (2):666–671
13. Nakazawa M et al (2008) Longterm findings in peripapillary crescent formation in eyes with mild or moderate myopia. Acta Ophthalmol 86(6):626–629
14. Kim T-W et al (2012) Optic disc change with incipient myopia of childhood. Ophthalmology 119(1):21–26
15. Tay E et al (2005) Optic disk ovality as an index of tilt and its relationship to myopia and perimetry. Am J Ophthalmol 139(2):247–252
16. Samarawickrama C et al (2011) Myopia-related optic disc and retinal changes in adolescent children from Singapore. Ophthalmology 118(10):2050–2057
17. Giuffrè G (1991) Chorioretinal degenerative changes in the tilted disc syndrome. Int Ophthalmol 15(1):1–7
18. Ikuno Y et al (2010) Choroidal thickness in healthy Japanese subjects. Invest Ophthalmol Vis Sci 51(4):2173–2176
19. Ikuno Y, Tano Y (2009) Retinal and choroidal biometry in highly myopic eyes with spectral-domain optical coherence tomography. Invest Ophthalmol Vis Sci 50(8):3876–3880
20. Ohno H (1983) Electron microscopic studies of myopic retinochoroidal atrophies 1. Choroidal changes (in Japanese). Folia Ophthalmol Jpn 43:1244–1253
21. Ho J et al (2011) Analysis of normal peripapillary choroidal thickness via spectral domain optical coherence tomography. Ophthalmology 118(10):2001–2007
22. Banitt M (2013) The choroid in glaucoma. Curr Opin Ophthalmol 24(2):125–129
23. Hirooka K et al (2012) Evaluation of peripapillary choroidal thickness in patients with normal-tension glaucoma. BMC Ophthalmol 12(1):29
24. Roberts KF et al (2012) Peripapillary choroidal thickness in healthy controls and patients with focal, diffuse, and sclerotic glaucomatous optic disc damage peripapillary choroidal thickness in glaucoma. Arch Ophthalmol 130(8):980–986

Chapter 5
Visual Field Damage in Myopic Glaucoma

Makoto Araie

Abstract This chapter summarizes findings on visual field damage in myopic glaucoma. Population-based studies have demonstrated that irrespective of myopic power, myopia is a risk factor for primary open angle glaucoma (POAG). Although it is relatively rare, otherwise normal myopic eyes, especially highly myopic eyes, may have a higher risk of glaucoma-like visual field (VF) damage in the superior temporal subfield. High myopia in otherwise normal eyes is also associated with a generalized diffuse reduction in VF sensitivity. In POAG, the strength of myopia is significantly and positively correlated with the extent of VF damage in the lower cecocentral subfield, although there is no such correlation in late-stage POAG with normal intraocular pressure (IOP). Although the exact mechanism of this phenomenon remains unknown, stronger myopia is correlated with less damage in the superior paracentral subfield in both normal- and elevated-IOP POAG with mild to moderate VF damage. Additionally, any degree of myopia is a risk factor for further progression of VF damage in eyes without ocular hypotensive treatment, and high myopia is a risk factor for further progression in both treated and untreated POAG eyes. On the other hand, stronger myopia is associated with a slower rate of progression in non-high-myopic eyes with ocular hypotensive therapy.

Keywords Myopia • Open angle glaucoma • Visual field damage • Progression

5.1 Introduction

Population-based studies, including studies carried out in Japan, have consistently demonstrated that myopia is a risk factor for primary open angle glaucoma (POAG), with an odds ratio of about 2.0 for all types of myopia [1, 2]. According to Grødum et al., who screened approximately 33,000 individuals aged between 57 and 79 years, the correlation between the prevalence of glaucoma and myopic power was more evident at lower intraocular pressure (IOP) levels and weakened gradually with increasing IOP level [3]. This suggests that the importance of

M. Araie, M.D., Ph.D. (✉)
Kanto Central Hospital of the Mutual Aid Association of Public School Teachers, 6-25-1, Kamiyoga, Setagaya-ku, Tokyo 158-8531, Japan
e-mail: araie-tky@umin.net

K. Sugiyama, N. Yoshimura (eds.), *Myopia and Glaucoma*,
DOI 10.1007/978-4-431-55672-5_5

myopia as a risk factor for POAG is especially clinically relevant in POAG patients with normal IOP (i.e., those with normal tension glaucoma; NTG). In Japan, the prevalence of myopia is among the highest in the world [4, 5], a section of the population that also has an especially high prevalence of NTG [6]. Therefore, the relationship between myopia and the clinical features of glaucoma-induced visual field (VF) damage is of special clinical concern in Japan.

Myopic eyes frequently present a characteristic appearance: the optic nerve head (ONH) is tilted and oval-shaped, with a temporal crescent-shaped area of peripapillary chorioretinal atrophy (PPA), to which the structural vulnerability of the myopic ONH has been attributed [7–10]. Such structural vulnerability is compatible with the above-mentioned clinical findings that the correlation between myopic refraction and the prevalence of glaucoma is stronger in NTG patients [3]. The appearance of the glaucomatous optic disc has been shown to have several distinct types: generalized enlargement (GE) of cupping, focal glaucomatous (FG), myopic glaucomatous (MG), and senile sclerotic (SS), each having a different clinical association and/or prognosis [11–17]. In this chapter, however, myopic glaucoma will refer to POAG with myopic refraction of <-1.0 or 0.5 diopters, rather than POAG with an MG optic disc.

5.2 Pattern of Visual Field Damage in Otherwise Normal Myopic Eyes

Otherwise normal myopic eyes, especially those with high myopia, may show VF damage that occurs mainly in the superior temporal subfield [18–21], as well as apparent cleavage of the retinal nerve fiber layer [22] and a relative loss of sensitivity in the short wavelength-sensitive cones (S-cones). These conditions are associated with increased axial length [23]. One study reported that a significant proportion of subjects with high myopia (spherical equivalent of <-6.0 diopters) and VF and ONH findings suggestive of glaucoma did not show any functional and structural progression over a 7 year period, suggesting that in at least some cases, high myopia is associated with non-progressive glaucoma-like VF damage [24]. On the other hand, later studies reported that otherwise normal myopic eyes were only rarely associated with VF damage as detected by standard white-on-white automated perimetry, although a diffuse loss of sensitivity of about 0.2 dB/diopter was seen in myopic eyes with a spherical equivalent refraction of -4.0 diopters or worse [25, 26]. According to Aung et al. [26], 4 % of otherwise normal myopic eyes with spherical equivalent refraction of -4.0 diopters or worse showed VF damage when tested with trial frame lenses for optical correction, but not with contact lenses. An additional 2 % of the eyes showed VF damage when tested with contact lenses, but not when tested with trial frame lenses. Only 1 % of the eyes showed reproducible VF damage when tested with both methods of optical correction.

5.3 Pattern of Visual Field Damage in Myopic Glaucoma

Previously, VF damage in myopic POAG eyes has been studied with kinetic perimetry, revealing that such eyes are more likely to have cecocentral VF damage, especially in the lower cecocentral subfield, or sectoral damage in the temporal VF [27–29]. Current VF testing is performed with static automated perimetry (SAP), which examines the central 30° of the VF with a grid of test points that is centered on the fixation (fovea) and has an inter-test point distance of 6° (a common example is the central 30-2 test program of the Humphrey Visual Field Analyzer, Carl Zeiss Meditec, Dublin, CA, USA). In studies of the influence of myopic refraction on the SAP-measured VF, some subjects with high myopia must use high-power trial frame lenses for optical correction during testing and cannot readily use contact lenses instead because they do not normally use them. Thus, prismatic deviation in extra-axial test points must be taken into consideration, particularly in VF testing of peripheral test points in patients wearing high-power glass lenses, because the ray from an off-axis object entering a minus power lens is bent closer to the optic axis of the lens. Computer calculations using ray tracing and Gullstrand's model eye indicate that the angle of the discharging ray to a test point 30° outward from the optic axis is 23°, instead of 30°, when a −10 diopter lens is placed 12 mm in front of the corneal apex [30]. Thus, it is difficult to directly compare VF test results for peripheral test points between eyes with strongly differing refractive statuses. On the other hand, test points 10° outward from the optic axis suffer a prismatic deviation of 2° with the use of a −10 diopter lens, a relatively small deviation, especially in comparison with the 6° inter-test point distance. Thus, it must be noted that the effects of highly myopic refraction on the VF in POAG can be more accurately studied in the central 10° of the VF than in the mid-peripheral VF.

Previously, we studied the effects of myopic refraction by examining total deviation (TD) values at each test point of the central 30-2 test program of the Humphrey visual field analyzer. Our study compared POAG eyes with elevated IOP and those with normal IOP (i.e., those with normal tension glaucoma; NTG) that had an average mean deviation (MD) value of about −12 dB, using the following formula [31]:

$$TD_i = A \times (\text{myopic power in diopters}) + B \times MD + C \tag{5.1}$$

Where TD_i is the TD value at the i-th test point, A and B are regression coefficients, and C is a regression constant. The extent of age-corrected damage at a questioned i-th test point, TD_i, was thought to be significantly influenced by myopic refraction when the regression coefficient, A, was significantly different from zero ($P < 0.05$) after correcting for the influence of overall glaucomatous damage (i.e., the stage of the disease), that is, B × MD. The background of the subjects and our results are summarized in Table 5.1 and Fig. 5.1. We obtained similar results in both types of POAG: the extent of VF damage in the lower cecocentral subfield was positively correlated with myopic power (i.e., higher myopia was associated with more VF

Table 5.1 Background data of patients with mild to moderate glaucomatous damage

	POAG with elevated IOP	POAG with normal IOP
Number of cases (eyes)	138 (197)	86 (120)
Age (years)	49.9 ± 11.7	48.2 ± 9.4
Refraction (diopters)	−4.1 ± 3.6	−3.8 ± 326
Mean deviation (dB)	−12.4 ± 9.0	−11.8 ± 7.2

Figures are mean ± SD
POAG primary open angle glaucoma, *IOP* intraocular pressure

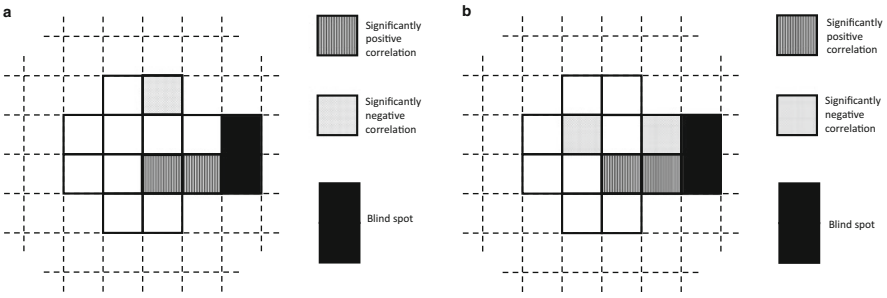

Fig. 5.1 (**a**) Correlation of total deviation values and myopic power in POAG eyes with elevated IOP and mild to moderate damage. POAG: primary open angle glaucoma, IOP: intraocular pressure. (**b**) Correlation of total deviation values and myopic power in POAG eyes with normal IOP and mild to moderate damage. *POAG* primary open angle glaucoma, *IOP* intraocular pressure

damage), while damage in the upper paracentral subfield was negatively correlated with myopic power (i.e., higher myopia was associated with less VF damage). The influence of myopic refraction on VF is apparently different in POAG eyes than in otherwise normal highly myopic eyes, in which it has been reported that the superior temporal subfield is mainly affected [18–21]. This indicates that the interaction between co-existing myopic changes and glaucoma exacerbates damage in the area of the ONH corresponding to the lower cecocentral visual subfield. In the superior paracentral subfield, higher myopia was found to be associated with less damage. Although this finding is rather unexpected, it is possible that anatomical changes induced in and around the ONH as myopia progresses can lessen its susceptibility resistance to some of the pathogenic factors of POAG. The degree of optic disc torsion induced by myopia may be at least partly related to this characteristic pattern of VF damage in myopic POAG [32].

The influence of myopia on VF damage in POAG may be glaucoma stage-dependent, although most existing studies have included only eyes with mild to moderate glaucomatous damage, and few of the study participants listed in Table 5.1 were in the late stage of the disease (MD ≤ −15 dB). Thus, we carried out a second study including only late-stage POAG patients (MD ≤ −15 dB) [30] (Table 5.2). We found that the lower cecocentral subfield was as likely to be damaged in late-stage POAG with elevated IOP as it was in the earlier stage of the disease [30, 31] (Fig. 5.2). Interestingly, this was not the case in late-stage NTG

Table 5.2 Background data of patients with advanced glaucomatous damage

	POAG with elevated IOP	POAG with normal IOP
Number of cases (eyes)	176 (176)	137 (137)
Age (years)	56.9 ± 12.1	57.9 ± 12.3
Refraction (diopters)	−2.4 ± 3.6	−2.4 ± 3.5
Mean deviation (dB)	−21.9 ± 4.4	20.7 ± 3.6

POAG primary open angle glaucoma, *IOP* intraocular pressure
Figures are mean ± SD

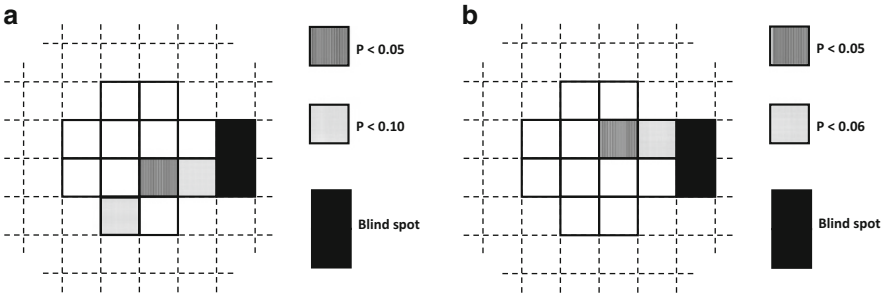

Fig. 5.2 (**a**) Test points in which total deviation values were positively correlated with myopic power in POAG eyes with elevated IOP. *POAG* primary open angle glaucoma, *IOP* intraocular pressure. (**b**) Test points in which total deviation values were negatively correlated with myopic power in POAG eyes with normal IOP. *POAG* primary open angle glaucoma, *IOP* intraocular pressure

eyes. The superior paracentral subfield was more likely to be relatively preserved in late-stage NTG eyes with higher myopic power (Fig. 5.2). This disease stage-dependent difference in the pattern of myopia-related influence on glaucomatous VF damage in POAG eyes with elevated IOP and those with normal IOP, i.e., NTG, suggests that IOP-dependent pathomechanisms may interact with myopia-induced changes in and around the ONH as glaucomatous damage progresses. The lower cecocentral subfield is usually preserved until the late stages of glaucoma [33, 34] and has the greatest functional importance in vision-related quality of life [35]. These results suggest that myopic patients with POAG and elevated IOP, especially those with high myopia, may be more likely to lose their central vision in the late stages of glaucoma (Fig. 5.3), and therefore need more careful clinical follow-up and IOP control.

In addition to the above results, we also found that a higher myopic power also had a deleterious effect on central visual acuity in POAG eyes with advanced damage. In a separate group of late-stage POAG eyes, we used a multiple linear regression analysis to study the effects of myopic power on central visual acuity (Table 5.3), with best-corrected visual acuity (log MAR) as the response variable, and age, overall VF damage (in MD), myopic power (in diopters), IOP (POAG with normal IOP vs. POAG with elevated IOP), and the more damaged hemifield (upper

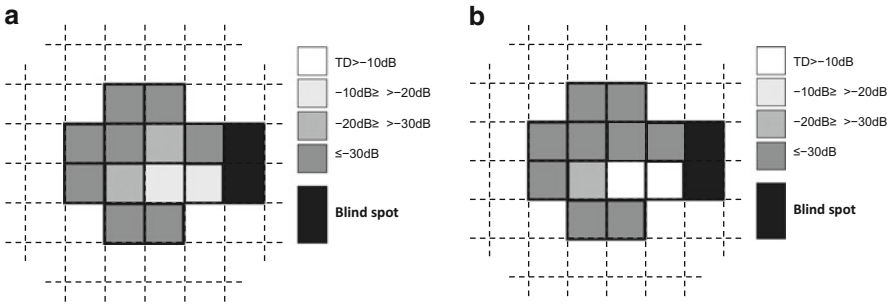

Fig. 5.3 (**a**) Visual field simulation of highly myopic (−10.0 diopters) POAG eyes with elevated IOP and mean deviation values of −30 dB, based on the results of multiple regression analysis. (**b**) Visual field simulation of emmetropic POAG eyes with normal IOP and mean deviation values of −30 dB, based on the results of multiple regression analysis

Table 5.3 Background data of patients in analysis of relationship between best-corrected visual acuity and myopic refraction

Number of cases (eyes)	83 (104)
POAG with elevated IOP	57 (71)
POAG with normal IOP	26 (33)
Age (years)	55.6 ± 12.7
Refraction (diopters)	−4.0 ± 4.5
Mean deviation (dB)	−23.6 ± 3.0
Best corrected visual acuity[a]	0.02 ~ 1.2

Figures are mean ± SD
POAG primary open angle glaucoma, *IOP* intraocular pressure
[a]Decimal visual acuity

vs. lower hemifield) as the explanatory variables. We found that best-corrected visual acuity was associated with higher myopic power ($P < 0.001$) and higher IOP (POAG with elevated IOP) ($P = 0.035$), a finding that agreed with those we obtained for the central VF.

Our findings on increasing myopia in POAG are compatible with the structural finding that highly myopic eyes are more susceptible to papillo-macular nerve fiber layer defects [36, 37]. In addition, many previous histological studies have suggested that myopia-associated structural changes in the ONH make the optic nerve fibers more vulnerable to various insults [7–10].

5.4 Visual Field Damage Progression in Myopic Glaucoma

Since myopia is a definite risk factor for POAG [1, 2], it is easy to speculate that VF damage is more likely to progress in eyes with myopic glaucoma than in those with non-myopic glaucoma. Indeed, previous studies have observed VF damage more frequently in myopic patients with untreated ocular hypertension [38, 39],

supporting the view that myopia is a risk factor for more rapid progression of the disease, and have also found that myopia is a significant risk factor for the initial development of POAG [40, 41]. Further, several studies agreed that high myopia was a risk factor for the progression of VF damage even with medical treatment [42–45]. On the other hand, as far as medically treated POAG eyes with mild to moderate myopia are concerned, there is evidence that mild to moderate myopia is not a significant risk factor for further progression of VF damage [44, 46–49]. For example, Sohn et al. carried out a retrospective observational study in which they observed the progression of VF damage over 5 or more years in 4 subgroups of NTG patients, all receiving treatment: non-myopic, mild myopic, moderate myopic, and high myopic. They found that the rate of progression was around −1.0 dB of MD change/year in all 4 subgroups, with no significant inter-group differences [49]. We also carried out a retrospective observational study, in which we analyzed, over an 8 year period, the VF test results of non-high-myopic NTG patients undergoing medical treatment. We found that the progress of VF damage was slow but statistically significant, with an average MD change/year of −0.16 dB [50]. Additionally, a subfield-based analysis of the time-course change in VF damage showed that stronger myopia was a significant positive prognostic factor for VF damage progression in the superior paracentral subfield, i.e., progression was more likely in the less myopic eyes. These findings were compatible with the results of our previous cross-sectional studies, in which we found that in POAG eyes with normal IOP, TD values in the superior paracentral subfield were negatively, significantly correlated with myopic power, and that higher myopia was associated with less damage in the superior paracentral subfield [30, 31]. Further, this result was reproduced in a prospective cohort study. We prospectively followed, for 3 years, 146 eyes of patients with POAG and normal IOP. The patients had a mean untreated IOP of 14 mmHg, mild to moderate visual field damage and mean spherical equivalent refraction of −3.5 diopters under topical nipradilol or timolol [51]. The IOP after treatment averaged 13.2 mmHg, and an analysis using the Cox proportional hazards model revealed that optic disc hemorrhage (hazard ratio [HR] 4.00, $p < 0.001$) and weaker myopia (per diopter, HR 1.15, $p = 0.013$) were significant risk factors, when progression was defined by VF damage progression and/or deterioration of disc appearance. When progression was solely defined by VF damage progression, weaker myopia was again a significant risk factor, and stronger myopia was associated with slower progression (HR 1.17, $p = 0.038$).

As regards VF damage progression in myopic glaucoma, it may be assumed that in eyes without ocular hypotensive treatment, any degree of myopia is a risk factor for further VF damage progression, that high myopia is a risk factor for further VF damage progression irrespective of ocular hypotensive treatment, and that stronger myopia is associated with slower progression in non-high-myopic eyes under ocular hypotensive therapy. It is not clear whether the difference between high myopia and non-high myopia in their effect on progression is related to interactions between the extent of myopic changes in and around the ONH and the partial relief of IOP-dependent insults by ocular hypotensive therapy.

References

1. Marcus MW, De Vries MM, Junoy Montolio FG et al (2011) Myopia as a risk factor for open-angle glaucoma: a systematic review and meta-analysis. Ophthalmology 118:1989–1994
2. Suzuki Y, Iwase A, Araie M, Tajimi Study Group et al (2006) Risk factors for open-angle glaucoma in a Japanese population: the Tajimi Study. Ophthalmology 113:1613–1617
3. Grødou K, Heijl A, Bengtsson B (2001) Refractive error and glaucoma. Acta Ophthalmol Scand 79:560–566
4. Sawada A, Tomidokoro A, Araie M et al (2008) Refractive errors in an elderly Japanese population: the Tajimi study. Ophthalmology 115:363–370
5. Tokoro T (1991) Refractive error and its correction, 2nd edn. Kanehara, Tokyo
6. Iwase A, Suzuki Y, Araie M et al (2004) The prevalence of primary open-angle glaucoma in Japanese: the Tajimi Study. Ophthalmology 111:1641–1648
7. Chihara E (2013) Myopia and diabetes mellitus as modificatory factors of glaucomatous optic neuropathy. Jpn J Ophthalmol 58:16–25
8. Ditchl A, Jonas JB, Naumann GOH (1998) Histomorphometry of the optic disc in highly myopic eyes with absolute secondary angle closure glaucoma. Br J Ophthalmol 82:286–289
9. Cahane M, Bartov E (1992) Axial length and scleral thickness effect on susceptibility to glaucomatous damage: a theoretical model implementing Laplace's law. Ophthalmic Res 24:280–284
10. Burgoyne C (2004) Myopic eyes and glaucoma. J Glaucoma 13:85–86
11. Nicolela MT, Drance SM (1996) Various glaucomatous optic nerve appearances. Clinical Correlations. Ophthalmology 103:640–649
12. Broadway DC, Drance SM (1998) Glaucoma and vasospasm. Br J Ophthalmol 82:862–870
13. Geijssen HC, Greve EL (1990) Focal ischaemic normal pressure glaucoma versus high pressure glaucoma. Doc Ophthalmol 75:291–302
14. Spaeth GL (1994) A new classification of glaucoma including focal glaucoma. Surv Ophthalmol 38:S9–S17
15. Reis AS, Artes PH, Belliveau AC et al (2012) Rates of change in the visual field and optic disc in patients with distinct patterns of glaucomatous optic disc damage. Ophthalmology 119:294–303
16. Nicolela MT, McCormick TA, Drance SM et al (2003) Visual field and optic disc progression in patients with different types of optic disc damage. Ophthalmology 110:2178–2184
17. Roberts KF, Artes PH, O'Leary N et al (2012) Peripapillary choroidal thickness in healthy controls and patients with focal, diffuse, and sclerotic glaucomatous optic disc damage. Arch Ophthalmol 130:980–986
18. Kurozumi I, Matsuno C, Kani K et al (1966) Report of myopia accompanied with visual field defect. Nippon Ganka Gakkai Zasshi (Jpn J Ophtnalmol Soc) 70:2238–2245
19. Huang S-J (1993) Early change of visual function in high myopia -measured and analyzed by octopus automated perimeter. Nippon Ganka Gakkai Zasshi (Jpn J Ophtnalmol Soc) 97:881–887
20. Rudnicka AR, Edgar DF (1995) Automated static perimetry in myopes with peripapillary crescents-part I. Ophthalmic Physiol Opt 15:409–412
21. Rudnicka AR, Edgar DF (1996) Automated static perimetry in myopes with peripapillary crescents-part II. Ophthalmic Physiol Opt 16:416–429
22. Chihara E, Chihara K (1992) Apparent cleabage of the retinal nerve fiber layer in asymptomatic eyes with high myopia. Graefes Arch Clin Exp Ophthalmol 230:416–420
23. Kawabata H, Murayama K, Adachi-Usami E (1996) Sensitivity loss in short wavelength sensitive cones in myopic eyes. Nippon Ganka Gakkai Zasshi (Jpn J Ophtnalmol Soc) 100:868–876
24. Doshi A, Kreidl KO, Lombardi L et al (2007) Nonprogressive glaucomatous cupping and visual field abnormalities in young Chinese males. Ophthalmology 114:472–479
25. Collins JW, Carney LG (1990) Visual performance in high myopia. Curr Eye Res 9:217–223
26. Aung T, Foster PJ, Seah SK et al (2001) Automated static perimetry: the influence of myopia and its method of correction. Ophthalmology 108:290–295

27. Carroll EL, Forbes M (1968) Centrocaecal scotoma due to glaucoma. Trans Am Acad Ophthalmol Otolaryngol 72:643–648
28. Greve EL, Furuno F (1980) Myopia and glaucoma. Graefes Arch Clin Exp Ophthalmol 213:33–41
29. Brais P, Drance SM (1972) The temporal field in chronic simple glaucoma. Arch Ophthalmol 88:518–522
30. Mayama C, Suzuki Y, Araie M et al (2002) Myopia and advanced -stage open-angle glaucoma. Ophthalmology 109:2072–2077
31. Araie M, Arai M, Koseki N et al (1995) Influence of myopic refraction on visual field defects in normal tension and primary open angle glaucoma. Jpn J Ophthalmol 39:60–64
32. Park HY, Lee K, Park CK (2012) Optic disc torsion direction predicts the location of glaucomatous damage in normal-tension glaucoma patients with myopia. Ophthalmology 119:1844–1851
33. Shields MB (1998) Textbook of glaucoma, 4th edn. Williams & Wilkins, Baltimore. Chap. 5–6
34. Weber J, Schultze T, Ulrich H (1989) The visual field in advanced glaucoma. Int Ophthalmol 13:47–50
35. Sumi I, Shirato S, Matsumoto S, Araie M (2003) The relationship between visual disability and visual field in patients with glaucoma. Ophthalmology 110:332–339
36. Chihara E, Tanihara H (1992) Parameters associated with papillomacular bundle defects in glaucoma. Graefes Arch Clin Exp Ophthalmol 230:511–517
37. Kimura Y, Hangai M, Morooka S et al (2012) Retinal nerve fiber layer defects in highly myopic eyes with early glaucoma. Invest Ophthalmol Vis Sci 53:6472–6478
38. Quigley HA, Enger C, Katz J et al (1994) Risk factors for the development of glaucomatous visual field loss in ocular hypertension. Arch Ophthalmol 112:644–649
39. Perkins ES, Phelps CD (1982) Open angle glaucoma, ocular hypertension, low-tension glaucoma, and refraction. Arch Ophthalmol 100:1464–1467
40. Czudowska MA, Ramdas WD, Wolf RC et al (2010) Incidence of glaucomatous visual field loss: A ten-year follow up from the Rotterdam study. Ophthalmology 117:1705–1712
41. Jiang X, Varma R, Wu S et al (2012) Baseline risk factors that predict the development of open-angle glaucoma in a population: the Los Angeles Latino Eye Study. Ophthalmology 119:2245–2253
42. Nakase Y (1987) Primary open angle glaucoma in high myopia. Report 1 effect of high myopia on visual field defects. Nippon Ganka Gakkai Zasshi (Jpn J Ophtnalmol Soc) 91:376–382
43. Chihara E, Liu X, Dong J et al (1997) Severe myopia as a risk factor for progressive visual field loss in primary open-angle glaucoma. Ophthalmology 211:66–71
44. Perdicchi A, Iester M, Scuderi G et al (2007) Visual field damage and progression in glaucomatous myopic eyes. Eur J Ophthalmol 17:534–537
45. Lee YA, Shih YF, Lin LL et al (2008) Association between high myopia and progression of visual field loss in primary open-angle glaucoma. J Formos Med Assoc 107:952–957
46. Phelps CD (1982) Effect of myopia prognosis in treated primary open-angle glaucoma. Am J Ophthalmol 93:622–628
47. Nouri-Mahdavi K, Hoffman D, Coleman AL et al (2004) Predictive factors for glaucomatous visual field progression in the advanced glaucoma intervention study. Ophthalmology 111:1627–1635
48. Jonas JB, Martus P, Budde WM (2002) Anisometropia and degree of optic nerve damage in chronic open-angle glaucoma. Am J Ophthalmol 134:547–551
49. Sohn SW, Song JS, Kee C (2010) Influence of the extent of myopia on the progression of normal-tension glaucoma. Am J Ophthalmol 149:831–838
50. Sakata R, Aihara M, Murata H et al (2013) Contributing factors for progression of visual field loss in normal-tension glaucoma patients with medical treatment. J Glaucoma 22:250–254
51. Araie M, Shirato S, Yamazaki Y, Nipradilol-Timolol Study Group et al (2012) Risk factors for progression of normal-tension glaucoma under β-blocker monotherapy. Acta Ophthalmol 90:37–43

Chapter 6
Myopic Optic Neuropathy

Kyoko Ohno-Matsui

Abstract It is well known that the visual field (VF) defects are not uncommon in eyes with pathologic myopia. It has not been clear if such VF defects which are not explained by myopic chorioretinal lesions are due to glaucoma or some other causes especially in extremely myopic eyes, because it is difficult to properly diagnose glaucoma due to the deformity of the optic disc. The recent advance in ocular imaging, especially optical coherence tomography (OCT), has enabled us to visualize the deep structures on and around the optic nerve. By using swept-source OCT and 3D MRI, various findings which are considered to be caused by mechanical stretching around the optic nerve in eyes with pathologic myopia have been identified. This chapter describes how the papillary and peripapillary regions are mechanically altered in eyes with pathologic myopia and how such abnormalities could possibly relate to the VF defects.

Keywords Pathologic myopia • Myopic optic neuropathy • Acquired pit • Subarachnoid space • Intrachoroidal cavitation

6.1 Introduction

It is well known that the visual field (VF) defects are not uncommon in eyes with pathologic myopia. These VF defects can be divided into two types: those that are the result of the chorioretinal lesions commonly found in highly myopic eyes, and those that are not associated with these lesions and have no identifiable causes. VF defects that could not be explained by the observed fundus lesions were detected in as much as 13 % of highly myopic eyes and were progressive [1].

It has not been clear if such VF defects which are not explained by myopic chorioretinal lesions are due to glaucoma or some other causes especially in extremely myopic eyes, because it is difficult to properly diagnose glaucoma due to the deformity of the optic disc. The optic discs in highly myopic eyes are tilted and deformed, and they show various appearances (Fig. 6.1). In eyes with extreme

K. Ohno-Matsui, M.D. (✉)
Department of Ophthalmology and Visual Science, Tokyo Medical and Dental University, 1-5-45 Yushima, Bunkyo-ku, Tokyo 113-8519, Japan
e-mail: k.ohno.oph@tmd.ac.jp

K. Sugiyama, N. Yoshimura (eds.), *Myopia and Glaucoma*,
DOI 10.1007/978-4-431-55672-5_6

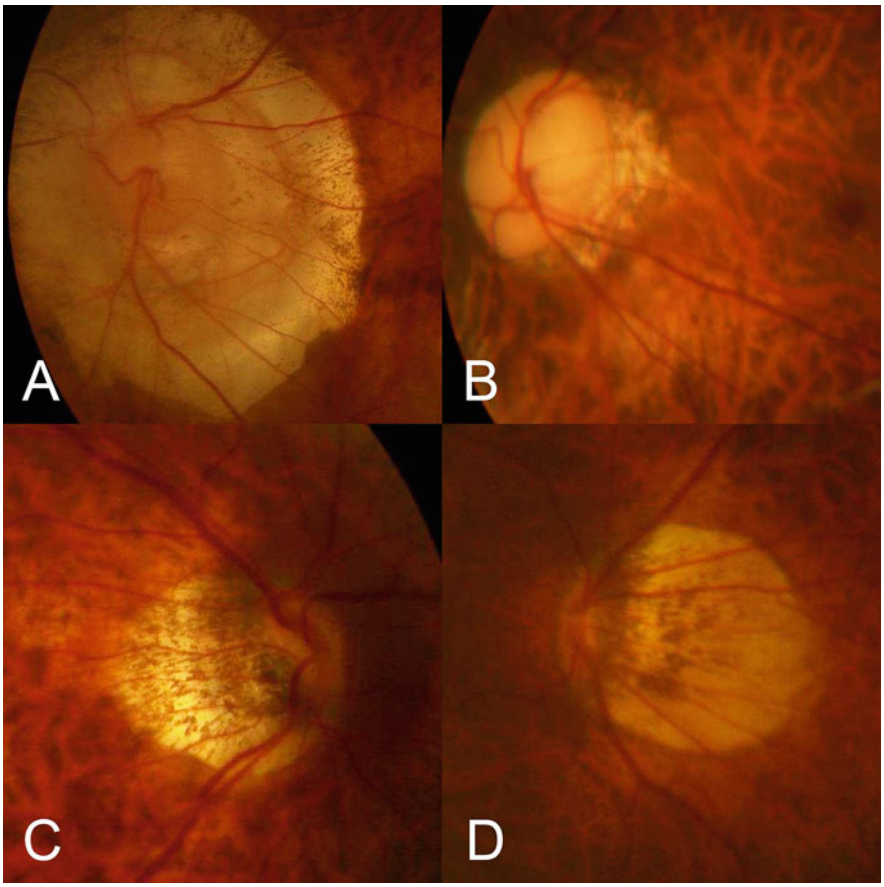

Fig. 6.1 Various appearance of optic disc in eyes with pathologic myopia. (**a** and **b**) Optic disc area is enlarged and shows 'megalodisc' appearance. (**c** and **d**) Optic disc is small and tilted

tilting of the optic disc, it is even impossible to observe most parts of the optic disc by funduscopic evaluation. Also, a presence of large conus and chorioretinal atrophy makes the interpretation of VF results rather difficult.

The recent advance in ocular imaging, especially optical coherence tomography (OCT), has enabled us to visualize the deep structures on and around the optic nerve. By using swept-source OCT and 3D MRI, we identified various findings which are considered to be caused by mechanical stretching around the optic nerve in eyes with pathologic myopia. These results prompted us to consider that at least in some patients, a mechanical damage on and around the papillary region might play an important role in developing the VF damage in highly myopic eyes. Thus, there might be a condition which should be called as "myopic optic neuropathy" [1]. This chapter describes how the papillary and peripapillary regions are

mechanically altered in eyes with pathologic myopia and how such abnormalities could possibly relate to the VF defects.

6.2 Optical Coherence Tomography (OCT) Findings of Papillary and Peripapillary Region of Eyes with Pathologic Myopia

6.2.1 Dilation of Perioptic Subarachnoid Space (SAS) and Thinning of Peripapillary Sclera

Recently, due to an advancement of OCT, like enhanced depth imagin (EDI)-OCT and swept-source OCT, it has been possible to visualize the deep structure in the optic nerve.

Park et al. [2] used EDI-OCT and observed the SAS around the optic nerve in 25 of the 139 glaucomatous eyes (18 %). Most of the 25 eyes had high myopia and extensive parapapillary atrophy. We [3] used swept-source OCT and found that SAS was found in 124 of 133 highly myopic eyes (93.2 %) but not in the emmetropic eyes. The SAS appeared to be dilated in highly myopic eyes. In the B-scan images, the SAS was triangular, with the base toward the eye surrounding the optic nerve in the region of the scleral flange (Fig. 6.2). There was a change in the scleral curvature at the attachment of the dura mater of the SAS to the peripapillary sclera. This shows that the distance between the point which the sclera was divided into the dura mater and the optic nerve increased in highly myopic eyes, as suggested by Okisaka [4] based on his histological evaluations. Only the nerve fiber layer and the scleral flange were observed on the SAS, consistent with a histological study by Jonas et al. [5]. The width of the SAS ranged from 263 to 1850 μm in our study. Jonas et al. [5] reported that the mean length of the scleral flange was 1.67 ± 0.74 mm in histological evaluation of 36 human globes with an axial length longer than 26.5 mm. In our study using swept-source OCT, the shortest distance between the inner surface of lamina cribrosa and SAS was 252.4 ± 110.9 μm, and the thinnest region of peripapillary sclera above SAS (scleral flange thickness) was 190.6 ± 51.2 μm [3]. Jonas [6] reported that the shortest distance between inner lamina cribrosa surface and SAS in non-highly myopic eyes without glaucoma was 557.9 ± 172.1 μm in histological evaluation.

The expanded area of exposure to CSF pressure along with thinning of the posterior eye wall may influence staphyloma formation and the way in which certain diseases, such as glaucoma, are manifested. In one of our myopic patients, there appeared to be a direct communication between the intraocular cavity and SAS through pit-like pores (Fig. 6.3). The clinical significance of a direct communication between intraocular space and SAS is not clear. This communication could cause a disrupted integrity of peripapillary sclera and changes of concentrations of materials in intraocular space and SAS. However, the translaminar pressure

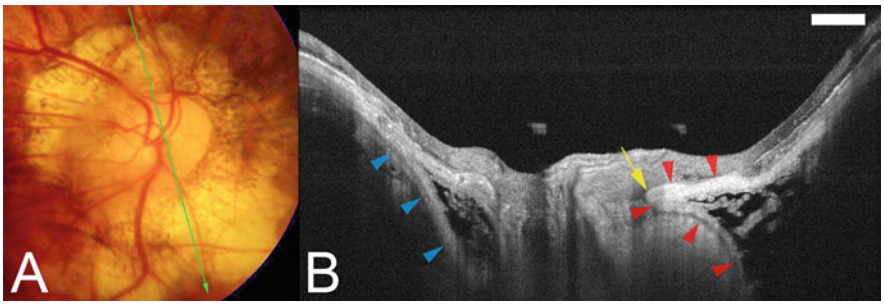

Fig. 6.2 Swept-source OCT images of subarachnoid space (SAS) around the retrobulbar optic nerve. (**a**) Large conus is found around the myopic optic disc. (**b**). Swept-source OCT slice scanned along the *green line* in (**a**) shows the SAS as a hyporeflective space along both the upper and lower borders of the ON. The SAS is triangular, with the base toward the eye. The peripapillary sclera is continuous with the pia mater along the inner boundary of the SAS (*red arrowheads*). The SAS protrudes toward the ON at the transition point of the peripapillary sclera and the pia mater (*arrow*). The peripapillary sclera is also continuous with the dura mater along the outer boundary of the SAS (*blue arrowheads*). The arachnoid trabeculae are seen as wide, linear streaks within the SAS (Reproduced from reference number [3] with permission)

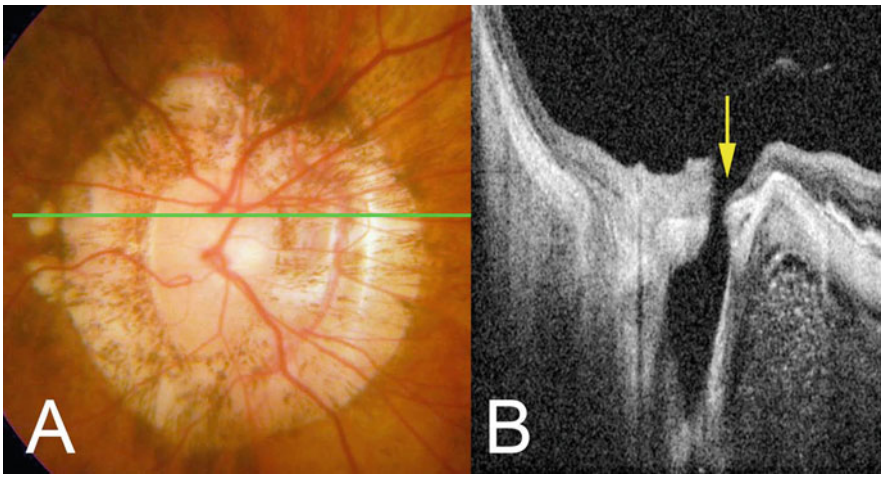

Fig. 6.3 Fundus photograph and swept-source OCT images showing direct communication between the intraocular space and the SAS. (**a**) Color fundus photograph of the optic disc showing a large annular conus. (**b**).On OCT section across *green line* in (**a**) shows that vitreous cavity is continuous with SAS through pitlike pores (*arrow*) (Reproduced from reference number [3] with permission)

becomes theoretically zero, which might act favorably for the progression of VF defects.

These OCT findings are compatible with earlier histological observations. Curtin [7] described that a dilation of perioptic subarachnoid space (SAS), eversion of the inner aspect of the scleral canal, anterior displacement of the lamina cribrosa, and

marked degrees of supertraction are especially specific to the highly myopic globe. Compared with the normal disc anatomy, staphyloma development has produced a marked thinning of the posterior sclera. The involvement of the innermost scleral fibers of the posterior foramen in the distention process causes the lamina cribrosa to advance toward the retinal surface. Okisaka [8] reported that in emmetropic eyes the perioptic SAS was narrow and the SAS blindly ended at the level of lamina cribrosa. The dura of the SAS was attached to the peripapillary sclera just around the lamina cribrosa. In contrary, in highly myopic eyes, the perioptic SAS was enlarged together with an increase of the axial length. In a cross section of the optic nerve, the SAS showed an inversely triangular shape whose base was toward the eye. In parallel to the dilation of SAS, the dura attachment site was markedly away from the optic nerve margin.

6.2.2 *Formation of Acquired Pits in the Optic Disc Area and in the Conus Area*

By using swept-source OCT, Ohno-Matsui et al. found that the optic nerve pits were not uncommon in highly myopic eyes [9]. Pit-like clefts were found at the outer border of the optic nerve or within the adjacent scleral crescent in 32 of 198 highly myopic eyes (16.2 %) but in none of the emmetropic eyes. The pits were located in the optic disc area (optic disc pits) in 11 of 32 eyes and in the area of the conus outside the optic disc (conus pits) in 22 of 32 eyes. The optic disc pits existed at the inferior or superior edge of the optic disc (Fig. 6.4). Conus pits were observed in eyes with type IX staphyloma and were present nasal to the scleral ridge or outside

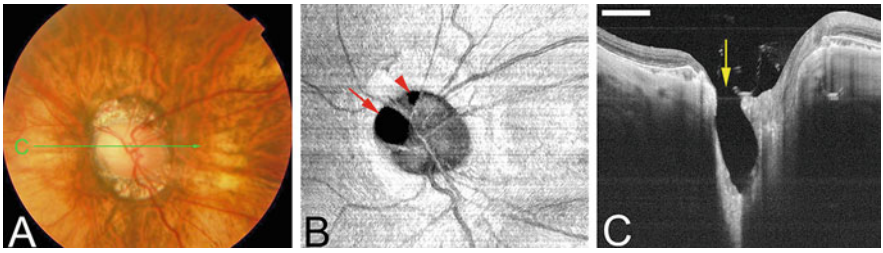

Fig. 6.4 Deeply excavated pit-like structures in the optic disc area. Bar; 1 mm. (**a**) Photograph of the left fundus shows horizontally oval optic disc and surrounding conus. The *green line* shows the area scanned by swept source OCT for the images shown in **c**. (**b**) En face view of the optic disc reconstructed from three-dimensional swept source OCT images shows one large pit at the superonasal edge of the optic disc (*arrow*) and one small pit at the superior edge of the optic disc (*arrowhead*). (**c**) B-scan image of OCT across the scanned line in Fig.6.4a shows an oval-shaped, deeply excavated pit (arrow) at the superonasal part of the optic disc with a wide opening. The depth of the pit from its opening was 1,071 μm. The nerve fibers overlying the pit are discontinuous and the lamina is torn off from the peripapillary sclera at the site of the pit (Reproduced from reference number [9] with permission)

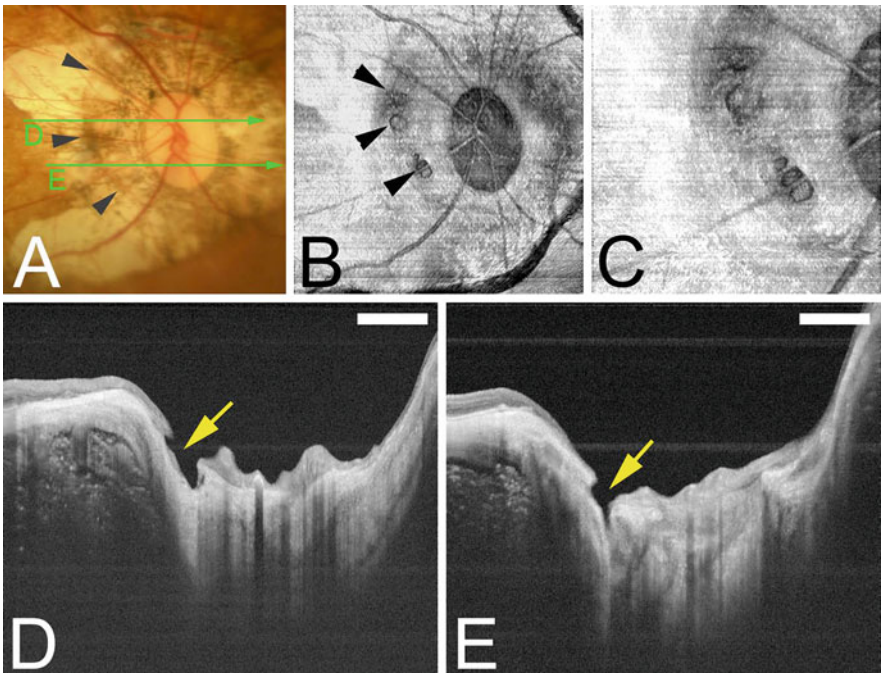

Fig. 6.5 Conus pits present on the temporal side of the scleral ridge in an eye with type IX staphyloma (Curtin's classification). Bar, 1 mm. (**a**) Photograph of right fundus of 64-year-old woman shows an oval disc with a large annular conus. A scleral ridge is shown by *arrowheads*. The *green lines* show the area scanned by swept-source optical coherence tomography (swept-source OCT) for the images shown in Figures **d** and **e**. (**b**) En face image of the optic disc area reconstructed from three-dimensional swept-source OCT images shows multiple pits on the slope inside the ridge at approximately same distance from the optic disc margin (*arrowheads*). (**c**) Magnified view of Figure **b** shows a collection of pits just temporal to the scleral ridge. (**d**) B-scan swept-source OCT image shows that the pit is present on the inner slope of the ridge (*arrow*). The peripapillary sclera and overlying nerve fiber tissue is discontinuous at the pit site. (**e**) Another pit can be seen inferotemporal to the optic disc (Reproduced with permission from reference number [9])

the ridge temporal to the nerve (Fig. 6.5). The optic disc pits were associated with discontinuities of the lamina cribrosa, whereas the conus pits appeared to develop from a scleral stretch-associated schisis or to emissary openings for the short posterior ciliary arteries in the sclera. The nerve fiber tissue overlying the pits was discontinuous at the site of the pits, and this discontinuity might be related to VF loss of highly myopic patients.

6.2.3 ICC (Intrachoroidal Cavitation)

Peripapillary ICC is observed as yellowish-orange lesion inferior to the optic disc along the inferior margin of the myopic conus funduscopically (Fig. 6.6). By using

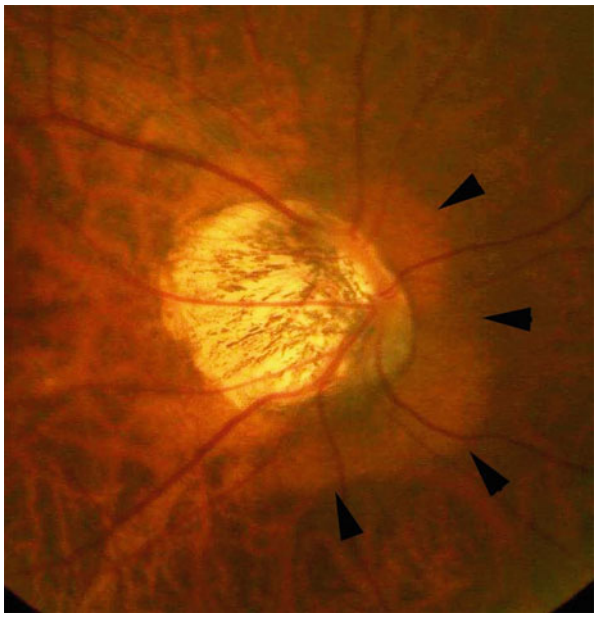

Fig. 6.6 Fundus images of peripapillary intrachoroidal cavitation (peripapillary ICC). ICC is observed as yellowish orange lesion around the myopic conus (*arrowheads*)

OCT, Freund et al. reported that this lesion was a localized detachment of the retinal pigment epithelium, however, the observation using more recent OCT showed that this lesion was located within the choroid and called as 'ICC'. Shimada et al. reported that ICC was found in 4.9 % of highly myopic eyes, and interestingly, 70 % of the patients with ICC had glaucomatous visual field defects. By using EDI-OCT and swept-source OCT, Spaide et al. showed that ICC developed following the disrupted integrity of border tissue of Jacoby around the optic nerve, and the scleral curvature was bowed posteriorly at the area of ICC. Spaide also reported that the inner retina was herniated into the ICC space and in some cases, the defect of full-thickness of neural retina was observed along the border of ICC. Subsequent to the full thickness retinal defect, it is expected that the visual field defects develop in the area of the entire course of retinal nerve fiber layer which traverse the site of retinal defect. Spade also showed that the tissue separation was seen in the suprachoroid at least in some cases. The development of ICC (or suprachoroidal separation?) and subsequent defect of herniated inner retina is considered an important cause of visual field defects in eyes with pathologic myopia.

Recently, Yeh et al. reported that ICC was found not only in highly myopic eyes but also in mildly myopic eyes, emmetropic eyes, and even in hyperopic eyes as well. This is considered to be because the degree of optic disc tilting is not always parallel to the axial length. These suggest that ICC might be related to the glaucomatous visual field defects in non-myopic eyes as well.

6.3 Separation of Circle of Zinn-Haller from the Optic Nerve

Medial and lateral paraoptic short PCAs converge towards the optic disc and form an elliptical anastomotic circle, the so-called circle of Haller and Zinn, through the formation of superior and inferior perioptic optic nerve arteriolar anastomoses [10]. The Zinn-Haller arterial ring is the main vascular supply of the lamina cribrosa which is the major insult site of optic nerve damage in eyes with glaucoma. Because of its intrascleral location, it had been difficult to observe the circle of Zinn-Haller *in situ*. Thus, most of the studies of the circle of Zinn-Haller have been done using histological sections [11, 12] or vascular castings with methyl methacrylate [10, 13, 14] of human cadaver eyes. In earlier *in situ* studies, the Zinn-Haller arterial ring of human eyes was observed by fluorescein fundus angiography and indocyanine green (ICG) angiography in eyes with pathologic myopia with a large peripapillary atrophy [15–20]. We performed ICG angiography on 382 highly myopic eyes and found that the circle of Zinn-Haller was visible in 206 of 382 eyes (53.9 %) [18]. Zinn-Haller was seen to almost completely surround the optic nerve head.

EDI-OCT showed cross sections of the vessels that were identified in the ICG angiography images to make up the circle of Zinn-Haller (Fig. 6.7). An intrascleral course of the Zinn-Haller ring was clearly observed in serial adjacent OCT sections. In the ICG angiographic images, the filling of the Zinn-Haller ring was seen to be continuous from the filling of the short posterior ciliary arteries, and OCT also showed the continuous course from the retrobulbar short posterior ciliary arteries to the circle of Zinn-Haller. Centripetal branches that ran toward the optic nerve from

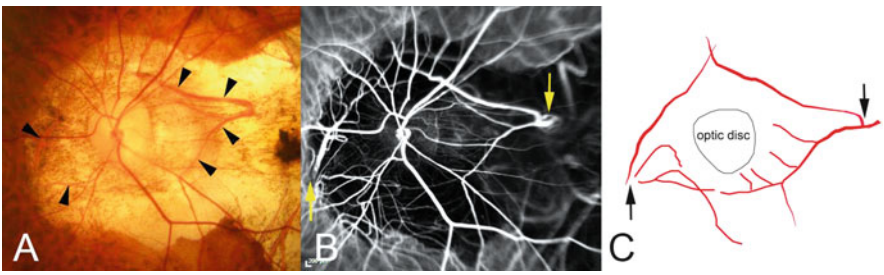

Fig. 6.7 Rhomboid shaped-Zinn Haller arterial ring in eyes with pathologic myopia. (**a**) Fundus photograph of *left* eye shows a large annular conus. Blood vessels suggesting the Zinn-Haller ring are seen within the conus (*arrowheads*). (**b**) ICG angiographic finding at 1 min after the dye injection showing a rhomboid-shaped Zinn-Haller ring surrounding the optic disc. Medial and lateral short posterior ciliary arteries enter the Zinn-Haller ring at the points shown by *arrows*. (**c**) Schematic drawing of ICG angiographic finding. The Zinn-Haller arterial ring is drawn in *red* and has a horizontally long rhomboid shape. The medial and lateral short posterior ciliary arteries enter the Zinn-Haller ring at the most horizontally protruded point (*arrows*). Centripetal branches running toward the optic nerve from Zinn-Haller ring are shown (Reproduced with permission from reference number [18])

the Zinn-Haller ring were observed in 20 eyes by ICG angiography and were confirmed by OCT. In highly myopic eyes with large conus, the circle of Zinn-Haller had a horizontally long rhomboid shape (Fig. 6.6), and the entry point of the lateral and/or medial short posterior ciliary arteries was at the most distant point from the optic disc margin.

Jonas [21] found that the arterial circle of Zinn-Haller was found to exist peripheral to the outer margin of the scleral flange (show Fig. 6.4 of Jonas article) in his histological study. Jonas [21] suggested that in addition to the thinning of the peripapillary scleral flange, the increased distance between the peripapillary arterial circle of Zinn-Haller and the optic disc border in highly myopic eyes may be an additional factor for the increased glaucoma susceptibility in highly myopic eyes.

6.4 Others

Park and colleagues [22] reported an interesting case with 'tight orbit syndrome' due to a large globe due to progressive high axial myopia. Different from thyroid ophthalmopathy, the proptosis was not prominent in their patient because the tight eye lid made the eyeball to be stuck in the bony orbit. Large globe with tight lid may cause the eyeball to be compressed with elevation of episcleral venous pressure [23]. Tight orbit syndrome has been reported to be an unrecognized cause of open-angle glaucoma [24]. In their patient, the orbital decompression may be effective in relieving the compression pressure on the globe, decreasing the episcleral venous pressure, and normalization of IOP. They concluded that the orbital decompression may be the surgical choice in patients with tight orbit syndrome because of high myopia who presents progressive intractable glaucoma.

At this point, it is not certain if VF defects in some highly myopic eyes are due to 'tight orbit syndrome'. However, in the cases with very big globe, this syndrome may also explain the mechanism of optic nerve damage in some patients.

6.5 Pattern of Visual Field Defects in Eyes with Pathologic Myopia

Considering the above changes, two major factors are suggested as causes of developing VF defects in pathologic myopia. One is a disrupted continuity of retinal nerve fibers caused by acquired pit formation and a formation of inner retinal defect along the peripapillary ICC. This kind of mechanical disruption of retinal nerve fiber might be specific to highly myopic eyes. In this case, the VF examination shows a scotoma which corresponds to the entire course of retinal nerve fiber layer which disrupted at the pit or along the edge of ICC. This part is considered to be specific to pathologic myopia.

The second factor is an increased susceptibility of developing glaucoma, and this factor makes the differential diagnosis between glaucoma and myopic optic neuropathy a little complicated. As Jonas [6] reported, the lamina cribrosa as well as peripapillary sclera is thinned in highly myopic eyes. When the perioptic SAS is enlarged, the area of peripapillary sclera directly on the SAS is also enlarged. However, the pit formation also disrupts the integrity of peripapillary sclera and also causes a dissociation of lamina cribrosa from peripapillary sclera at their junction. Thus, a pit formation also causes an increased susceptibility of developing glaucoma in highly myopic eyes. Thus, simply mechanical disruption of retinal nerve fibers and an increased susceptibility of developing glaucoma are mixed in a complicated fashion in eyes with pathologic myopia.

6.6 Underlying Pathologies Related to the Optic Nerve Damage

6.6.1 Staphyloma Type

In highly myopic patients who showed VF defects which are not explained by myopic fundus lesions, we performed multiple regression analyses to determine the correlations between the visual field score and 6 possible factors; age at the initial examination, age at the last examination, axial length, initial IOP, mean IOP during the follow-up, Mx/Mn ratio of the optic disc, and the presence of an abrupt change of scleral curvature temporal to the optic disc [1]. The presence of an abrupt change of scleral curvature temporal to the optic disc was defined as having type VII or type IX staphyloma. The results showed that the presence of an abrupt change of scleral curvature temporal to the optic disc was the only factor which correlated with a progression of visual field defects in highly myopic patients. Conus pits in highly myopic eyes almost always occur in eyes with type IX staphyloma [9], suggesting that conus pits partly explain why eyes with type IX staphyloma have VF defects significantly more frequently. Also, the retinal nerve fiber is bent and thinned at the ridge of type IX staphyloma. The bending of retinal nerve fiber layer could impair the axonal flow, and such bending and thinning of the retinal nerve fiber might be one of the causes of VF defects.

6.6.2 Eye Deformity

We recently analyzed the shape of the human eye by using 3D MRI [25]. The ocular shape viewed from the inferior was divided into four distinct types; nasally distorted type, temporally distorted type, cylindric type, and barrel type. Statistical comparisons between the eyes with different ocular shapes showed that the eyes

with significant VF defects were found significantly more frequently in eyes with a temporally distorted shape. When we identified the area where the optic nerve was attached to the globe, the optic nerve was found to attach at the nasal edge of a temporal protrusion. This showed the presence of a change of the ocular shape just temporal to the optic disc. This corresponds to the stereoscopic fundus observation that eyes with a ridge-like protrusion just temporal to the optic disc tend to have VF defects significantly more frequently than eyes without the temporal ridge [1]. The 3D MRI results support our earlier observations, and all of the data suggest that an asymmetric stretching of the eye around the optic disc and the retinal nerve fiber layer might cause a deformation of lamina cribrosa that could then disturb axonal flow.

6.6.3 Irregular Scleral Shape

We also analyzed the shape of sclera by using swept-source OCT [26]. The entire thickness of the sclera was observed in highly myopic eyes by using swept-source OCT. The curvatures of the inner scleral surface of highly myopic eyes could be divided into curvatures that sloped toward the optic nerve, those that were symmetrical and centered on the fovea, those that were asymmetrical, and those that were irregular. Patients with irregular curvature were significantly older and had significantly longer axial lengths than those with other curvatures. Also, the subfoveal scleral thickness was significantly thinner in eyes with irregular curvature (average; 189.1 ± 60.9 μm) than the eyes with other curvatures. Myopic fundus lesions as well as VF defects were present significantly more frequently in the eyes with irregular curvature. By comparison between OCT images and 3D MRI images, all of the eyes with temporally dislocated shape by 3D MRI had irregular curvature by swept-source OCT.

Combining these studies, the eye shape shown as temporally dislocated type by 3D MRI, irregular curvature by swept-source OCT, and type IX by stereoscopic fundus observation may be the same. Irregular stretching around the optic nerve (especially temporal to the optic nerve) is a common feature and these suggest that these eye shape might be a terminal eye deformity in highly myopic eyes and irregular stretching temporal to the optic nerve might be a key contributing factor causing myopic optic neuropathy.

6.7 Closing Remarks

Although it has not been fully clarified about why VF defects occur in highly myopic eyes, the advance in OCT technologies showed that structural alterations on and around the optic nerve might be a cause of VF defects in the patients with pathologic myopia at least to some extent. These suggest that there is a condition

which is different from glaucoma and should be called as ‘myopic optic neuropathy’. Because of the high incidence of VF defects and the progression of the VF defects, we suggest that high myopia be considered a high risk group of VF defects and should be monitored carefully. Careful observation on and around the optic nerve by using OCT as well as periodic VF examinations are considered helpful to diagnose the presence of myopic optic neuropathy. Also, these alterations which were found in eyes with pathologic myopia might also relate to glaucomatous optic nerve damage seen in eyes with mild to moderate myopia. Based on these new findings, new treatment modalities are expected to be established.

References

1. Ohno-Matsui K, Shimada N, Yasuzumi K et al (2011) Long-term development of significant visual field defects in highly myopic eyes. Am J Ophthalmol 152(2):256–265.e1
2. Park SC, De Moraes CG, Teng CC et al (2012) Enhanced depth imaging optical coherence tomography of deep optic nerve complex structures in glaucoma. Ophthalmology 119:3–9
3. Ohno-Matsui K, Akiba M, Moriyama M et al (2011) Imaging the retrobulbar subarachnoid space around the optic nerve by swept source optical coherence tomography in eyes with pathologic myopia. Invest Ophthalmol Vis Sci 52:9644–9650
4. Okisaka S (1987) Myopia. Kanehara Shuppan, Tokyo, pp 110–121
5. Jonas JB, Jonas SB, Jonas RA et al (2011) Histology of the parapapillary region in high myopia. Am J Ophthalmol 152(6):1021–1029
6. Jonas JB, Berenshtein E, Holbach L (2004) Lamina cribrosa thickness and spatial relationships between intraocular space and cerebrospinal fluid space in highly myopic eyes. Invest Ophthalmol Vis Sci 45(8):2660–2665
7. Curtin BJ (1985) Basic science and clinical management. In: Curtin BJ (ed) The myopias. Harper and Row, New York
8. The Branch Vein Occlusion Study Group (1984) Argon laser photocoagulation for macular edema in branch vein occlusion. Am J Ophthalmol 98(3):271–282
9. Ohno-Matsui K, Akiba M, Moriyama M et al (2012) Acquired optic nerve and peripapillary pits in pathologic myopia. Ophthalmology 119(8):1685–1692
10. Olver JM, Spalton DJ, McCartney AC (1994) Quantitative morphology of human retrolaminar optic nerve vasculature. Invest Ophthalmol Vis Sci 35(11):3858–3866
11. Jonas JB, Jonas SB (2010) Histomorphometry of the circular peripapillary arterial ring of Zinn-Haller in normal eyes and eyes with secondary angle-closure glaucoma. Acta Ophthalmol 88(8):1755–3768
12. Ko MK, Kim DS, Ahn YK (1999) Morphological variations of the peripapillary circle of Zinn-Haller by flat section. Br J Ophthalmol 83(7):862–866
13. Olver JM, Spalton DJ, McCartney AC (1990) Microvascular study of the retrolaminar optic nerve in man: the possible significance in anterior ischaemic optic neuropathy. Eye (Lond) 4 (Pt 1):7–24
14. Morrison JC, Johnson EC, Cepurna WO, Funk RH (1999) Microvasculature of the rat optic nerve head. Invest Ophthalmol Vis Sci 40(8):1702–1709
15. Ohno-Matsui K, Morishima N, Ito M et al (1997) Indocyanine green angiography of retrobulbar vascular structures in severe myopia. Am J Ophthalmol 123(4):494–505
16. Hollo G (1998) Peripapillary circle of Zinn-Haller revealed by fundus fluorescein angiography. Br J Ophthalmol 82(3):332–333
17. Ko MK, Kim DS, Ahn YK (1997) Peripapillary circle of Zinn-Haller revealed by fundus fluorescein angiography. Br J Ophthalmol 81(8):663–667

18. Ohno-Matsui K, Futagami S, Yamashita S, Tokoro T (1998) Zinn-Haller arterial ring observed by ICG angiography in high myopia. Br J Ophthalmol 82(12):1357–1362
19. Yasuzumi K, Ohno-Matsui K, Yoshida T et al (2003) Peripapillary crescent enlargement in highly myopic eyes evaluated by fluorescein and indocyanine green angiography. Br J Ophthalmol 87(9):1088–1090
20. Park KH, Tomita G, Onda E et al (1996) In vivo detection of perineural circular arterial anastomosis (circle of Zinn-Haller) in a patient with large peripapillary chorioretinal atrophy. Am J Ophthalmol 122(6):905–907
21. Jonas JB, Jonas SB, Jonas RA et al (2012) Parapapillary atrophy: histological gamma zone and delta zone. PLoS One 7(10):18
22. Park HY, Paik JS, Cho WK et al (2012) Tight orbit syndrome resulting from large globe with high myopia: intractable glaucoma treated by orbital decompression. Clin Exp Ophthalmol 40 (2):214–216. doi:10.1111/j.1442-9071.2011.02673.x. Epub 2011 Oct 20
23. Robert PY, Rivas M, Camezind P et al (2006) Decrease of intraocular pressure after fat-removal orbital decompression in Graves disease. Ophthal Plast Reconstr Surg 22 (2):92–95
24. Lee GA, Ritch R, Liang SY et al (2010) Tight orbit syndrome: a previously unrecognized cause of open-angle glaucoma. Acta Ophthalmol 88(1):120–124
25. Moriyama M, Ohno-Matsui K, Hayashi K et al (2011) Topographical analyses of shape of eyes with pathologic myopia by high-resolution three dimensional magnetic resonance imaging. Ophthalmology 118(8):1626–1637
26. Ohno-Matsui K, Akiba M, Modegi T et al (2012) Association between shape of sclera and myopic retinochoroidal lesions in patients with pathologic myopia. Invest Ophthalmol Vis Sci 9:9

Chapter 7
High Myopia and Myopic Glaucoma: Anterior Segment Features

Takanori Kameda and Yasuo Kurimoto

Abstract High myopia is generally associated with an enlargement of the globe. The mechanical stretch forces responsible for enlarging the eyes induce morphological changes in the sclera. Many pathological myopia studies have documented fundus findings that include tigroid fundus, lacquer cracks, atrophy of the retinal pigment epithelium and choroid, posterior staphyloma, choroidal neovascularization, and the myopic configuration of the optic nerve head. In general, it is thought that a few changes occur in the anterior segment of myopic eyes. In recent years, however, new imaging technologies that are able to analyze the anterior segment of the eye have been introduced. This chapter summarizes changes that do occur in the anterior segment in high myopic eyes and discusses possible influential factors on the assessment and management of glaucoma.

Keywords Anterior segment • Cornea • Ciliary body

7.1 Myopic Ocular Morphological Changes

In 1977, Wiesel and Raviola reported an experimental animal model of myopia that was created by the lid fusion of monkey eyes. Lid fusion induces elongation of eyes, which causes myopia. Eyes in this model are characterized by distension of the postequatorial hemisphere and thinning of the posterior sclera [1]. However, these eyes do not expand symmetrically. Moreover, in contrast to the observed axial elongation and changes in the posterior sclera, no significant changes occur in the anterior segment of the eye (Fig. 7.1). These changes are accompanied by a general loss of collagen and proteoglycans in the sclera. Similar to that seen in animal models of myopia, human myopic eyes also exhibit expansion of the posterior sclera and the vitreous cavity. However, the scleral location where the ocular expansion occurs varies between individuals. The classification of myopic eyes is

T. Kameda, M.D., Ph.D. (✉) • Y. Kurimoto, M.D., Ph.D.
Department of Ophthalmology, Kobe City Medical Center General Hospital, 2-1-1, Minatojima-minamimachi, Chuo-ku, Kobe, Hyogo 650-0047, Japan
e-mail: kame@kcho.jp

K. Sugiyama, N. Yoshimura (eds.), *Myopia and Glaucoma*,
DOI 10.1007/978-4-431-55672-5_7

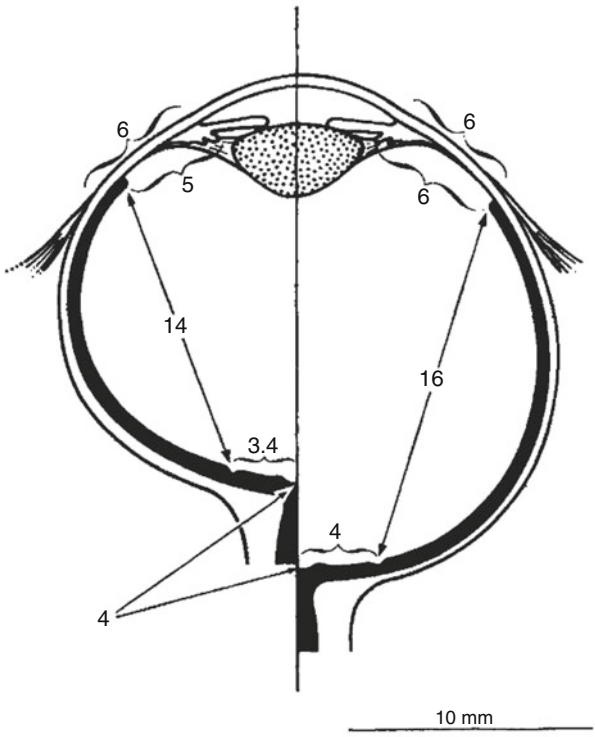

Fig. 7.1 Experimental myopia induced by monocular lid fusion of monkey eyes demonstrates the distension of the postequatorial hemisphere of the eye [1]

based on where the myopic changes actually occur and have been defined as axial elongation (which includes both equatorial stretching and posterior pole elongation) and global expansion. Magnetic resonance imaging (MRI) has proven to be a very useful tool when evaluating the shapes of the eye. Atchison et al. examined 88 participants and used MRI to measure the length, width, and height of both emmetropic and myopic eyes [2]. Their findings showed that as myopia worsened, the length increased more than the height, while the height increased more than the width. Based on the height and length dimensions, they found that 25 % of the myopic eyes fit the global expansion model, while 29 % fit the axial expansion model. When based on width and length dimensions, 17 % of the myopic eyes fit the global expansion model, while 39 % fit the axial elongation model. More recently, Moriyama et al. used high resolution 3D MRI and volume rendering to assess the ocular shapes of highly myopic eyes. Their findings demonstrated the presence of characteristic ocular shapes in the posterior segment of the myopic eyes [3]. Thus, the changes associated with myopia occur mostly behind the equator and few gross changes, if any, occur in the anterior segment of myopic eyes.

7.2 Myopic Changes in Cornea

Intraocular pressure (IOP) is the most important parameter used in determining glaucoma development and progression. However, measured IOP values can be influenced by various factors including central corneal thickness (CCT), corneal rigidity, Valsalva's maneuver, astigmatism, corneal curvature, and inappropriate amount of fluorescein. Among the techniques used to estimate IOP, Goldmann applanation tonometry (GAT) is the most commonly used device worldwide. GAT estimates IOP by flattening the corneal apex to a given area and then assessing the force needed. With this device, a flattened area with a diameter of 3.06 mm is empirically chosen to offset the surface tension of the tear film and both the corneal and ocular rigidity. GAT is designed to estimate IOP using the assumption that the CCT is 500 μm. However, it is has been shown that the CCT actually varies among individuals. The IOP will be overestimated in eyes having a thicker cornea, while it will be underestimated in eyes with a thinner cornea [4–7]. Meanwhile, thinner CCTs have been identified as a risk factor for both the development of primary open-angle glaucoma (POAG) in eyes with ocular hypertension [8] and for the observation of advanced glaucomatous damage at initial examinations [9]. According to the Ocular Hypertension Treatment Study, subjects with a corneal thickness of 555 μm or less had a threefold greater risk of developing POAG compared with subjects who had a corneal thickness of more than 588 μm. It has not been completely determined whether this increased risk of developing POAG is due to underestimating actual IOP in eyes with a thinner cornea or whether thinner corneas are a risk factor independent of IOP measurement. Furthermore, the corneal mechanical properties, such as elasticity, are known to have a greater effect on the tonometric IOP measurement errors than either the corneal curvature or thickness.

Several previous studies have examined the relationships between CCT and AL or myopic refractive error. Al-Mezaine et al. demonstrated that the AL was not correlated with the CCT in myopic eyes [10]. Fam et al. also found that there was no correlation between the degree of myopia and CCT in Singaporean Chinese subjects [11]. On the other hand, a significant correlation was found between CCT and refraction in a normal Japanese population [12].

The Ocular Response Analyzer (ORA) is a non-contact tonometer that is used to measure intraocular pressure and is the only instrument that can measure corneal hysteresis (CH), which is one of the biomechanical properties of cornea and a parameter of the viscoelastic properties of the cornea. The IOP will be overestimated in eyes having a stiffer cornea. The ORA determines the CH during the rapid motion of the cornea that occurs in response to a rapid air impulse. The air impulse causes deformation of the cornea, which is monitored by an electro-optical system. It has been previously reported that CH is lower in keratoconus, Fuchs' dystrophy, post-laser in situ keratomileusis (LASIK), and glaucoma [13–15].

Shen et al. demonstrated that the CH was significantly lower in high myopic eyes (spherical equivalent (SE) lower than −9.00 D) compared with subjects having a SE between −3.00 and 0 [16]. Moreover, CH was positively correlated with

refraction, while the refraction was negatively correlated with the IOP. Thus, mechanical strength in the anterior segment is compromised in high myopia [17]. Congdon et al. showed that the CH measured by the ORA was correlated with the CCT and was an independent risk factor for worsening of the glaucomatous visual field [14]. Therefore, the measurement of CH is important for high myopic eyes with glaucoma. In order to assess glaucoma risk and its clinical course, it will be important that detailed measurements of the physiological properties of the cornea be performed in high myopia.

7.3 Myopic Changes in Anterior Chamber

The anterior chamber depth (ACD) has been reported to be deeper in myopic eyes than emmetropic or hypertropic eyes [18, 19]. Use of anterior segment optical coherence tomography (ASOCT) makes it possible to determine measurements of novel parameters, including the anterior chamber width (ACW) and lens vault. ACW is defined as the horizontal scleral spur-to-spur distance. Nongpiur et al. [20] studied 1465 community-based subjects and 111 subjects with narrow angle in Singapore. They found that ACW and ACD were significantly correlated with the axial length (AL) and that shallow ACD and shorter AL were correlated with narrow angles. Lens vault is another parameter measured from the ASOCT images. Lens vault is defined as the perpendicular distance between the anterior pole of the crystalline lens and the horizontal line joining the two scleral spurs. Tan et al. showed that lens vault was negatively correlated with the axial length [21]. They found that greater lens vault was associated with narrow angles.

Established risk factors for primary angle closure include shallow ACD, thick and anteriorly displaced lens (increased lens vault), and short AL. In spite of these risk factors, some eyes with high myopia have been shown to have angle closure. In one retrospective study, 6 (1.9 %) out of 322 primary angle closure cases occurred in myopic eyes [22]. Barkana et al. additionally examined 17,938 patients with myopia of spherical equivalent (SE) of more than −6.0 diopters and reported finding nine cases of primary pupillary block and three cases of plateau iris configuration and syndrome [23].

7.4 Myopic Changes in Aqueous Humor Dynamics

The aqueous humor leaves the eye through two major pathways that include the trabecular or conventional pathway (via the trabecular meshwork, Schlemm's canal, collector channels, and aqueous veins into the episcleral veins) and the uveoscleral or unconventional pathway (via the iris root, uveal meshwork, anterior surface of the ciliary muscle, connective tissue between muscle bundles, suprachoroidal space, and finally through the sclera).

The coefficient of outflow (C) is determined by measuring increases of intraocular pressure caused by indentation with a tonometer, though the increase of intraocular pressure is influenced by ocular volume and rigidity. Tonographical data demonstrated lower outflow facility in high myopic eyes. In high myopic eyes, the increased ocular volume reduces the IOP elevation caused by the tonometer indentation. Thus, the tonographic data in high myopic eyes should be calculated with a correction for ocular rigidity. Only a limited number of studies demonstrated tonographic data in high myopic eyes. Study by Honmura found a decrease in the value of C in myopic eyes and a negative correlation between the value of C and the AL [24]. In the same study, Honmura also found there was lower aqueous production in the myopic eyes. Muto et al. compared hyperopic, emmetropic, and mild and high myopic eyes and found there was a reduced value of C in the high myopic eyes (−6.25 D to −20 D) [25].

7.5 Myopic Changes in Ciliary Body

The uveoscleral outflow pathway passes from the anterior chamber through the CB to the sclera. Prostaglandin analogues induce the expression of metalloproteinases and may reduce the extracellular matrix within the CB, iris root, and sclera, thereby increasing the uveoscleral outflow. The prostaglandin analogues are also involved in CB muscle relaxation, cell shape changes, and cytoskeletal alterations [26]. The proposed site of action of these prostaglandin analogues demonstrates the importance of the CB in IOP control. However, only a limited number of studies examining ciliary muscle morphology have been carried out in vivo due to its position posterior to the iris.

Several reports have used ultrasound biomicroscopy (UBM) or ASOCT to show that the ciliary muscle is thicker in myopic eyes [27–30]. Oliviera et al. reported that CB thickness measured with UBM was negatively correlated with the refractive error and positively correlated with the AL [30]. Thus, they postulated that a greater CB thickness might lead to a better response to the prostaglandin analogues.

7.6 Pigment Dispersion Syndrome

Pigment dispersion syndrome (PDS) is a disorder in which the pigment granules are released from the iris pigment epithelium. The diagnostic triad of clinical features consists of slit-like, mid-peripheral iris transillumination defects; diffuse and dense pigmentation on the trabecular meshwork; and pigment granules on the corneal endothelium (Krukenberg spindle). It is thought that pigmentary glaucoma is triggered by a progressive loading of pigment in the trabecular meshwork. Campbell observed a consistency between iris transillumination defects and the location of the zonular bundles. Therefore, the author proposed that posterior bowing of the

iris led to the contact and friction between the posterior pigmented iris epithelium and the zonular bundles [31]. In PDS, posterior insertion of the iris root into the ciliary body (CB) occurs. This anatomical variation predisposes the iridozonular contact and zonular pigment dispersion [32].

While PDS is frequently associated with myopia, pigmentary glaucoma eyes are more myopic than eyes with PDS. It has been reported that a higher degree of myopia is a risk factor for an earlier onset of pigmentary glaucoma [33]. In addition, posterior bowing of the iris can also occur in myopic eyes without PDS.

7.7 Recent Advances in Anterior Segment Visualization with ASOCT

Development of high-frequency UBM has made it possible for direct visualization of Schlemm's canal in vivo. Irshad et al. performed an in vivo UBM study of Schlemm's canal and reported that the average diameter of Schlemm's canal in 44 myopic eyes (122 ± 45 um) was significantly smaller than that observed in six hyperopic eyes (180 ± 69 um) [34]. They also reported that the location of the Schlemm's canal in black patients (659 ± 92 um) was posterior from the limbus as compared to white patients (624 ± 73 um), which indicates that there are potential differences in the position of Schlemm's canal depending upon the race of the patient.

Although limitations of visualization remain, recent advances of ASOCT technology have made it possible to perform more increasingly precise visualizations of the conventional outflow pathway [35–37]. Hong et al. used ASOCT and demonstrated that the area of the Schlemm's canal of POAG eyes was smaller than that observed in normal eyes [38]. However, the specific structural characteristics of eyes with high myopia, with or without glaucoma, have yet to be elucidated. As this new technology continues to develop, we will be able to collect further knowledge of these various structures that may ultimately deepen our understanding of the pathophysiology of myopic glaucoma.

References

1. Wiesel TN, Raviola E (1977) Myopia and eye enlargement after neonatal lid fusion in monkeys. Nature 266(5597):66–68
2. Atchison DA, Jones CE, Schmid KL, Pritchard N, Pope JM, Strugnell WE, Riley RA (2004) Eye shape in emmetropia and myopia. Invest Ophthalmol Vis Sci 45(10):3380–3386. doi:10.1167/iovs.04-0292
3. Moriyama M, Ohno-Matsui K, Modegi T, Kondo J, Takahashi Y, Tomita M, Tokoro T, Morita I (2012) Quantitative analyses of high-resolution 3D MR images of highly myopic eyes to determine their shapes. Invest Ophthalmol Vis Sci 53(8):4510–4518. doi:10.1167/iovs.12-9426

4. Doughty MJ, Zaman ML (2000) Human corneal thickness and its impact on intraocular pressure measures: a review and meta-analysis approach. Surv Ophthalmol 44(5):367–408
5. Stodtmeister R (1998) Applanation tonometry and correction according to corneal thickness. Acta Ophthalmol Scand 76(3):319–324
6. Singh RP, Goldberg I, Graham SL, Sharma A, Mohsin M (2001) Central corneal thickness, tonometry, and ocular dimensions in glaucoma and ocular hypertension. J Glaucoma 10 (3):206–210
7. Bhan A, Browning AC, Shah S, Hamilton R, Dave D, Dua HS (2002) Effect of corneal thickness on intraocular pressure measurements with the pneumotonometer, Goldmann applanation tonometer, and Tono-Pen. Invest Ophthalmol Vis Sci 43(5):1389–1392
8. Gordon MO, Beiser JA, Brandt JD, Heuer DK, Higginbotham EJ, Johnson CA, Keltner JL, Miller JP, Parrish RK 2nd, Wilson MR, Kass MA (2002) The Ocular Hypertension Treatment Study: baseline factors that predict the onset of primary open-angle glaucoma. Arch Ophthalmol 120(6):714–720; discussion 829–730
9. Herndon LW, Weizer JS, Stinnett SS (2004) Central corneal thickness as a risk factor for advanced glaucoma damage. Arch Ophthalmol 122(1):17–21. doi:10.1001/archopht.122.1.17
10. Al-Mezaine HS, Al-Obeidan S, Kangave D, Sadaawy A, Wehaib TA, Al-Amro SA (2009) The relationship between central corneal thickness and degree of myopia among Saudi adults. Int Ophthalmol 29(5):373–378. doi:10.1007/s10792-008-9249-8
11. Fam HB, How AC, Baskaran M, Lim KL, Chan YH, Aung T (2006) Central corneal thickness and its relationship to myopia in Chinese adults. Br J Ophthalmol 90(12):1451–1453. doi:10.1136/bjo.2006.101170
12. Suzuki S, Suzuki Y, Iwase A, Araie M (2005) Corneal thickness in an ophthalmologically normal Japanese population. Ophthalmology 112(8):1327–1336. doi:10.1016/j.ophtha.2005.03.022
13. Luce DA (2005) Determining in vivo biomechanical properties of the cornea with an ocular response analyzer. J Cataract Refract Surg 31(1):156–162. doi:10.1016/j.jcrs.2004.10.044
14. Congdon NG, Broman AT, Bandeen-Roche K, Grover D, Quigley HA (2006) Central corneal thickness and corneal hysteresis associated with glaucoma damage. Am J Ophthalmol 141 (5):868–875. doi:10.1016/j.ajo.2005.12.007
15. Shah S, Laiquzzaman M, Bhojwani R, Mantry S, Cunliffe I (2007) Assessment of the biomechanical properties of the cornea with the ocular response analyzer in normal and keratoconic eyes. Invest Ophthalmol Vis Sci 48(7):3026–3031. doi:10.1167/iovs.04-0694
16. Shen M, Fan F, Xue A, Wang J, Zhou X, Lu F (2008) Biomechanical properties of the cornea in high myopia. Vision Res 48(21):2167–2171. doi:10.1016/j.visres.2008.06.020
17. Jiang Z, Shen M, Mao G, Chen D, Wang J, Qu J, Lu F (2011) Association between corneal biomechanical properties and myopia in Chinese subjects. Eye (Lond) 25(8):1083–1089. doi:10.1038/eye.2011.104
18. Rabsilber TM, Becker KA, Frisch IB, Auffarth GU (2003) Anterior chamber depth in relation to refractive status measured with the Orbscan II Topography System. J Cataract Refract Surg 29(11):2115–2121
19. Park SH, Park KH, Kim JM, Choi CY (2010) Relation between axial length and ocular parameters. Ophthalmologica 224(3):188–193. doi:10.1159/000252982
20. Nongpiur ME, Sakata LM, Friedman DS, He M, Chan YH, Lavanya R, Wong TY, Aung T (2010) Novel association of smaller anterior chamber width with angle closure in Singaporeans. Ophthalmology 117(10):1967–1973. doi:10.1016/j.ophtha.2010.02.007
21. Tan GS, He M, Zhao W, Sakata LM, Li J, Nongpiur ME, Lavanya R, Friedman DS, Aung T (2012) Determinants of lens vault and association with narrow angles in patients from Singapore. Am J Ophthalmol 154(1):39–46. doi:10.1016/j.ajo.2012.01.015
22. Chakravarti T, Spaeth GL (2007) The prevalence of myopia in eyes with angle closure. J Glaucoma 16(7):642–643. doi:10.1097/IJG.0b013e318064c803
23. Barkana Y, Shihadeh W, Oliveira C, Tello C, Liebmann JM, Ritch R (2006) Angle closure in highly myopic eyes. Ophthalmology 113(2):247–254. doi:10.1016/j.ophtha.2005.10.006

24. Honmura S (1968) Studies on the relationship between ocular tension and myopia. II. Ocular tension, ocular rigidity, aqueous outflow and aqueous secretion in myopic eyes. Nihon Ganka Gakkai Zasshi 72(6):688–696
25. Muto K, Toyofuku H, Koshiyama H, Futa R (1968) Values of tonography in cases with refractive error. Nihon Ganka Kiyo 19(8):887–890
26. Weinreb RN, Toris CB, Gabelt BT, Lindsey JD, Kaufman PL (2002) Effects of prostaglandins on the aqueous humor outflow pathways. Surv Ophthalmol 47(Suppl 1):S53–S64
27. Buckhurst H, Gilmartin B, Cubbidge RP, Nagra M, Logan NS (2013) Ocular biometric correlates of ciliary muscle thickness in human myopia. Ophthalmic Physiol Opt 33 (3):294–304. doi:10.1111/opo.12039
28. Lewis HA, Kao CY, Sinnott LT, Bailey MD (2012) Changes in ciliary muscle thickness during accommodation in children. Optom Vis Sci 89(5):727–737. doi:10.1097/OPX.0b013e318253de7e
29. Muftuoglu O, Hosal BM, Zilelioglu G (2009) Ciliary body thickness in unilateral high axial myopia. Eye (Lond) 23(5):1176–1181. doi:10.1038/eye.2008.178
30. Oliveira C, Tello C, Liebmann JM, Ritch R (2005) Ciliary body thickness increases with increasing axial myopia. Am J Ophthalmol 140(2):324–325. doi:10.1016/j.ajo.2005.01.047
31. Campbell DG (1979) Pigmentary dispersion and glaucoma. A new theory. Arch Ophthalmol 97(9):1667–1672
32. Sokol J, Stegman Z, Liebmann JM, Ritch R (1996) Location of the iris insertion in pigment dispersion syndrome. Ophthalmology 103(2):289–293
33. Farrar SM, Shields MB, Miller KN, Stoup CM (1989) Risk factors for the development and severity of glaucoma in the pigment dispersion syndrome. Am J Ophthalmol 108(3):223–229
34. Irshad FA, Mayfield MS, Zurakowski D, Ayyala RS (2010) Variation in Schlemm's canal diameter and location by ultrasound biomicroscopy. Ophthalmology 117(5):916–920. doi:10.1016/j.ophtha.2009.09.041
35. Usui T, Tomidokoro A, Mishima K, Mataki N, Mayama C, Honda N, Amano S, Araie M (2011) Identification of Schlemm's canal and its surrounding tissues by anterior segment fourier domain optical coherence tomography. Invest Ophthalmol Vis Sci 52(9):6934–6939. doi:10.1167/iovs.10-7009
36. Kagemann L, Wollstein G, Ishikawa H, Bilonick RA, Brennen PM, Folio LS, Gabriele ML, Schuman JS (2010) Identification and assessment of Schlemm's canal by spectral-domain optical coherence tomography. Invest Ophthalmol Vis Sci 51(8):4054–4059. doi:10.1167/iovs.09-4559
37. Kagemann L, Wollstein G, Ishikawa H, Nadler Z, Sigal IA, Folio LS, Schuman JS (2012) Visualization of the conventional outflow pathway in the living human eye. Ophthalmology 119(8):1563–1568. doi:10.1016/j.ophtha.2012.02.032
38. Hong J, Xu J, Wei A, Wen W, Chen J, Yu X, Sun X (2013) Spectral-domain optical coherence tomographic assessment of Schlemm's canal in Chinese subjects with primary open-angle glaucoma. Ophthalmology 120(4):709–715. doi:10.1016/j.ophtha.2012.10.008

Chapter 8
Ocular Blood Flow in Myopic Glaucoma

Yu Yokoyama and Toru Nakazawa

Abstract Among various risk factors for the pathogenesis of glaucoma, intraocular pressure has been identified as playing a causative role in the process of axonal degeneration, and at present, it remains the only risk factor considered in glaucoma treatment. However, epidemiology studies have also shown that myopia is a risk factor for glaucoma, especially for normal tension glaucoma. Myopia is more common in Asia than in Western countries, and normal tension glaucoma is the most common type of open angle glaucoma in Asia. Normal tension glaucoma often causes central visual field loss, which can directly influence quality of life in patients.

In myopia, the axial length of the eye becomes elongated, which induces structural changes that are characteristic of myopia. These changes, which are particularly evident in patients with high myopia, include progressive temporal tilting of the optic nerve head and deformation of the lamina cribrosa. The resulting mechanical stress on the axons of the retinal ganglion cells leads to compromised ocular blood flow and ocular ischemia. Research on ocular circulation has produced a large body of evidence that decreased ocular blood flow in myopic eyes is associated with glaucoma.

Keywords Glaucoma • Myopia • Blood flow

8.1 Introduction

Data from population-based studies shows that the number of glaucoma patients over 40 years old has exceeded 60 million worldwide and will reach 80 million by 2020. Glaucoma is now the second leading cause of blindness, disproportionately affecting women and Asians [1]. Currently, the only standard treatment to prevent progression of the most common form of the disease, primary open angle glaucoma (POAG), is maintenance of low intraocular pressure (IOP) with the use of medication. However, although IOP is generally recognized as a major risk factor for

Y. Yokoyama • T. Nakazawa (✉)
Department of Ophthalmology, Tohoku University Graduate School of Medicine, 1-1 Seiryo-machi, Aoba-ku, Sendai, Miyagi 980-8574, Japan
e-mail: ntoru@oph.med.tohoku.ac.jp

K. Sugiyama, N. Yoshimura (eds.), *Myopia and Glaucoma*,
DOI 10.1007/978-4-431-55672-5_8

glaucoma [2], it is well known that the progression of glaucoma is related to multiple factors. Furthermore, previous investigations have revealed that reducing IOP does not halt glaucoma progression in all patients, including those with normal IOP [3, 4]. This has prompted investigation into factors independent of IOP that may be involved in the pathogenesis of glaucoma. These risk factors have been identified as myopia, family history, migraine, decreased perfusion pressure, race, and age [5–9]. In this chapter, the relationship between various morphological aspects of myopic change and the accompanying changes in ocular circulation and glaucoma are described with reference to current research.

8.2 Myopia as a Risk Factor for Glaucoma

A number of studies have investigated the role of myopia in the pathogenesis of glaucoma. The Blue Mountain Eye Study, a population study, identified a relationship between glaucoma and low myopia (between −1.0 and −3.0 diopters), finding that the odds ratio (OR) was 2.3 after adjusting for known glaucoma risk factors [7]. That study also found that eyes with moderate to high myopia had a higher risk (OR: 3.3).

Another population study, the Beijing Eye Study found that the prevalence of glaucoma did not vary significantly between a highly myopic group and a group with marked myopia. In both groups, however, glaucoma was more frequent (OR: 7.56) than in an emmetropic group [8]. In addition, they reported that there was a correlation between retinal nerve fiber layer thickness (RNFLT) and refractive error. An increase in myopia of one diopter correlated with a decrease in 1 μm of average RNFLT [10].

The role of myopia in the pathogenesis of glaucoma is not yet completely understood. However, eyes with myopia have a longer axial length than eyes with emmetropia, and structural changes in the eye caused by this elongation are regarded as an important element in the pathogenesis of myopia-associated glaucoma (Fig. 8.1) [11]. As myopia increases in severity, it is associated with progressive increases in cup to disc ratio, retinal nerve fiber layer loss, deformation of the lamina cribrosa, and susceptibility to glaucomatous damage [12].

8.3 Systemic Blood Flow and Glaucoma

Newman-Casey et al. reported that hypertension (hazard ratio, HR: 1.17) and diabetes (HR: 1.35) were risk factors for OAG in a large cohort epidemiological study that ran from 2001 to 2007 [13]. Their findings have since been reinforced [14–17], although the identification of conditions associated with metabolic syndrome, such as hypertension and diabetes, as risk factors for glaucoma remains controversial [18–20]. Additionally, low systemic blood pressure has been reported

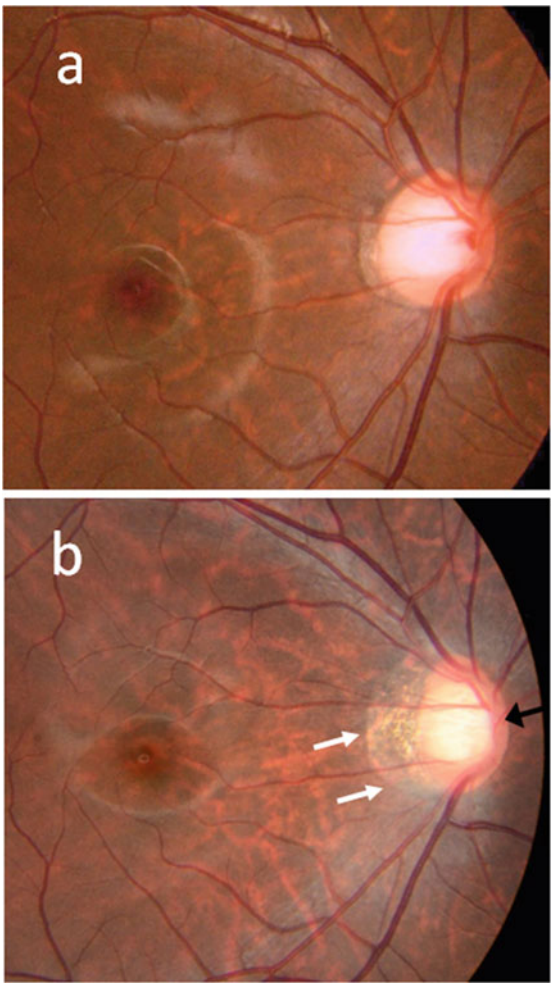

Fig. 8.1 Morphological changes in the optic nerve head with progression of myopia. (**a**) Fundus photograph of a myopic eye in a 14-year-old male patient. (**b**) Fundus photograph of the same eye when the patient was 19 years old. The enlargement of the area of crescent peripapillary atrophy (*white arrow*), straightening of the vessels, and distinctly visible choroidal vessels (tigroid fundus) are evident. The origin of the retinal artery is obscured by the rim because of the steeply tilted disc (*black arrow*)

to be a major risk factor for glaucoma [4, 19, 17]. Individuals who experience nightly dips in systemic blood pressure and fluctuation in systemic blood pressure are thought to be particularly vulnerable [21–23]. These irregularities in blood pressure can result in low ocular perfusion pressure and insufficient ocular blood supply [24, 25].

8.4 Ocular Blood Supply

The ophthalmic artery is the major vascular vessel providing blood to the inner retina and optic nerve. The central retinal artery, which branches off the ophthalmic artery and enters the optic nerve approximately 12 mm posterior to the globe,

supplies blood to the retinal ganglion cell bodies in the inner retina and nerve fibers. The central retinal artery also provides partial perfusion to the superficial optic disc. The pre-laminar region and lamina cribrosa are mainly supplied from branches of the posterior ciliary arteries (PCA), branching off from the ophthalmic artery and also from other vessels originating from the arterial circle of Zinn-Haller (ZHAC). In addition, fine centripetal branches from the peripapillary choroid provide blood to the pre-laminar region [26–28]. The blood supply in this region is sectorial in nature, similar to distribution of the PCA circulation. These branches from the PCA pierce the sclero-optic junction and enter the lamina cribrosa through the border tissue of Elschnig at the choroid [29]. It is generally assumed that microvessels throughout the optic nerve have characteristics of the blood-brain barrier (BBB), since tracers such as peroxidase do not pass out of the optic nerve capillaries [30]. However, a study of immunohistochemistry using non-BBB markers showed that microvessels in the pre-laminar region of the optic nerve head (ONH) lack typical BBB characteristics and display nonspecific permeability [31], possibly mediated by vesicular transport.

8.4.1 Devices to Measure Ocular Circulation

The identification of a relationship between ocular blood flow and the pathogenesis of glaucoma has inspired much recent research. Accurate methods to measure ocular blood flow are critical to these investigations, and various quantitative and qualitative techniques have been introduced to achieve the necessary accuracy [32, 33]. These include fluorescein angiography, laser or ultrasound Doppler shift, and devices based on the laser speckle phenomenon. These techniques each have characteristic advantages in measuring glaucoma-related tissues, such as the retinal vessels, optic nerve, short PCA, the ZHAC, ocular artery, and choroid, and their complementary use allows an overall understanding of ocular blood flow. Here, we provide an outline of the major techniques currently used in ophthalmological research to measure ocular blood flow.

8.4.1.1 Angiography

Fluorescein angiography allows for the visualization of morphological structures passing a fluorescent dye through them. The mean circulation time is used as a measure of blood velocity. However, the relationship between retinal blood flow and transit time in fluorescein angiography is weak [34]. Angiography can be used to evaluate the perfusion of microvascular beds and to identify the failure of vessels, which is indicated by hyperfluorescence, defects in fluorescence, and leakage [35]. A scanning laser ophthalmoscope can also be used to quantify macular blood flow velocity by tracking hyperfluorescent and hypofluorescent dots as they pass through the perifoveal capillaries [36]. This approach, does, however, require

excellent image quality, because otherwise these hyperfluorescent and hypofluorescent dots cannot be identified unequivocally in consecutive images [32]. Angiography with indocyanin green (ICG) has a peak spectral absorption at about 800 nm and is often used to assess choroidal vessels and circulation. The major advantages of ICG-based methods for the assessment of choroidal blood flow are superior penetration of near infrared light into pigmented ocular structures and improved binding to plasma proteins, which prevents marked leakage from vessels to the surrounding tissue [33].

8.4.1.2 Laser Doppler Velocimetry

Laser Doppler velocimetry (LDV) is used to determine the velocity of blood cells in the larger retinal vessels [37]. This technique uses the optical Doppler shift of light, which is directly proportional to the velocity of blood cells. LDV combined with measurements of vessel diameter at the same site enables the determination of volumetric flow rate in the major retinal vessels. However, LDV cannot be used to measure ONH blood flow [33].

8.4.1.3 Color Doppler Imaging

Color Doppler imaging (CDI) is used to assess blood velocity, especially in the retrobulbar vessels, including the ophthalmic artery, central retinal artery, and short posterior ciliary arteries. CDI facilitates the determination of blood flow velocity by color-coding the Doppler frequency shift of ultrasonic waves and super imposing the resulting color map on a B-scan image [38]. The measurement parameters of CDI are peak systolic velocity (PSV), end diastolic velocity (EDV), and mean velocity. The resistive index (RI) can also be calculated with the following formula: $RI = (PSV - EDV)/PSV$. However, the usefulness of the RI as an indicator of vessel resistance in the central retinal artery remains controversial [39]. CDI produces highly reproducible measurements of blood velocity in the ophthalmic artery, but in narrower vessels, such as the short PCA, measurement values tend to fluctuate [40].

8.4.1.4 Laser Doppler Flowmetry

Laser Doppler flowmetry (LDF) is based on the scattering effect of light in tissue and can measure both relative blood velocity and blood flow. This technique uses a laser beam to illuminate a small volume of tissue that does contain any large visible vessels. Some of the light scattered by the tissue and moving red blood cells is then detected by a photo detector [41], and based on the scattering effect, relative

measurements of the mean velocity of the erythrocytes and the volume of blood can be obtained. A relative value for blood flow can then be determined by calculating the product of the velocity and volume measurements. However, the tissues which have influence on the light scattering vary considerably between individuals. Therefore, when comparing interindividually, this character of LDF should be taken into account.

8.4.1.5 Laser Speckle Flowgraphy

Laser speckle flowgraphy (LSFG) uses the laser speckle phenomenon. This phenomenon occurs when surfaces are illuminated by coherent laser light. When the ocular fundus is illuminated by laser light, the scattering of the light by the tissue gives rise to a speckle pattern. Changes in the velocity of blood flow cause blurring of the speckle pattern, and this blurring can be quantified by specialized software. The main measurement parameter of LSFG is mean blur rate, an arbitrary unit calculated from the light intensity of the speckle pattern on a point-by-point basis.

8.4.1.6 Pulsatile Ocular Blood Flow

Pneumotonometric methods are used to estimate pulsatile ocular blood flow (POBF) on the basis of changes in measurement of IOP during the cardiac cycle [42]. This provides a non-invasive, continuous measurement of IOP, which, when compared to the rate of change of IOP, can be used to estimate the pulsatile component of ocular blood flow [43]. POBF analysis includes the determination of fundus pulsation amplitude and pulse amplitude. The main limitation of this technique arises from the lack of information it provides on the non-pulsatile component of ocular blood flow [32].

8.5 Ocular Circulation as a Risk Factor for Glaucoma

Population-based studies have revealed that low blood pressure and low ocular perfusion pressure (OPP) increase the prevalence of glaucoma. Adequate irrigation of ocular tissues can only be ensured by adequate OPP, which depends on a complex regulation process to balance BP and IOP. The vascular hypothesis of glaucoma pathogenesis is thus based on the premise that abnormal perfusion, with the subsequent deterioration in ONH circulation, plays a major role in the pathophysiology of damage in glaucoma. Many studies performed with a variety of techniques have found that glaucoma is associated with altered ocular blood flow, particularly ocular blood flow in the posterior pole of the eye [44–48]. In eyes with

glaucomatous visual field deterioration, retrobulbar blood velocity decreases significantly, and the resistance of the vessels increases significantly [45–49]. In severe glaucoma, deterioration of ocular circulation also increases with the progression of glaucoma and visual field loss [50]. In glaucoma patients with asymmetric visual field loss, the more affected eye also has lower blood velocity in the central retinal artery than the less affected eye [51]. CDI data shows that retrobulbar blood velocity in eyes with glaucoma is significantly correlated with mean blood pressure [52]. In comparison, healthy eyes show a lower, although still significant, correlation. This implies that the vascular autoregulation system in ocular arteries, which acts in response to changes in perfusion pressure [53], is compromised in eyes with glaucoma. LSFG studies of pre-laminar tissue in the ONH of eyes with glaucoma have shown that blood flow in this area is significantly lower than normal and that it correlates to the severity of glaucoma. This is consistent with histological studies, indicating that dropout of the capillaries within the pre-laminar and laminar lesions in the ONH may be occurring.

8.6 Ocular Circulation Studies in Myopia

In myopic eyes, elongation of the axial length leads to stretching of the sclera, and the optic disc becoming elliptical and tilted temporally, changes which are associated with enlarged crescent PPA [54]. Temporal crescent PPA is a common consequence of scleral stretching [55]. Furthermore, there is evidence that myopia leads to the deterioration of ocular circulation. With myopic change, the diameter of the retinal arteries becomes smaller and retinal blood flow in the retinal arteries decreases [56–58]. Retrobulbar blood flow and choroidal circulation also decrease in severe myopia [58, 59].

This leads to the question of whether there is an association between glaucoma and myopic changes in ocular circulation. Nicolela's classification system of ONH morphology categorizes elliptical ONHs with temporal crescent PPA as the "myopic glaucomatous type" [60, 61]. Myopic eyes with glaucoma tend to significantly younger at the time of diagnosis, with the central vision frequently threatened by glaucomatous scotoma. There are also a higher number of patients of Asian origin. Moreover, in the four glaucomatous optic disc types, retrobulbar circulation in the myopic glaucomatous type shows lower PSV, determined by CDI, in the ophthalmic artery than the focal ischemic type [62]. In the LSFG, tissue circulation in the optic nerve area in myopic glaucoma has also been reported to decrease, in correlation with visual field defects [63]. Figure 8.2 shows the difference in blood circulation between a glaucomatous ONH with myopic deformation and one with focal rim notch. Changes in ocular circulation in myopic eyes thus appear to be one of the mechanisms of glaucoma pathogenesis.

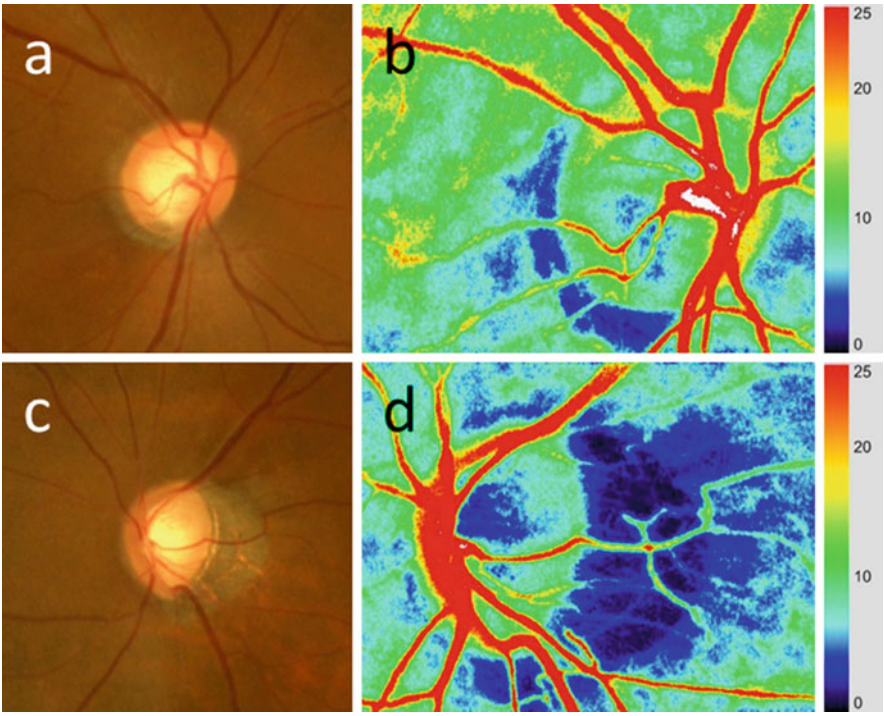

Fig. 8.2 (**a**) Blood flow in optic nerve head of a patient with asymmetric refractive error (color-coded map, laser speckle flowgraphy: LSFG). (**b**) Fundus photograph of right eye with normal refractive error (0.15 diopters). (**c**) Color-coded LSFG map of right eye. Warmer colors indicate higher mean blur rate (MBR: arbitrary unit used by LSFG). (**d**) Fundus photograph of left eye with high refractive error (−3.38 diopters). (**e**) Color-coded LSFG map of left eye. The proportion of warm colors in the optic nerve head is lower than in the right eye (**b**)

8.6.1 Retinal Circulation in Myopic Eyes

Quigley and Cohen showed that perfusion pressure in the retinal artery becomes attenuated with elongation of the axial length, a finding that arose from the observation that the frequency of diabetic retinopathy is lower in myopic eyes than emmetropic eyes [64]. The attenuation of perfusion pressure in arteriole segments is measured by the pressure attenuation index (PAI), which is proportional to the length and inversely proportional to the diameter of the segment. There is a positive correlation between PAI and axial length. The protective effect of myopia against diabetic retinopathy thus seems to arise from axial elongation causing pressure attenuation in the retinal artery. However, decreased perfusion pressure in the retinal arteries may also eventually lead to glaucomatous damage, because the retinal artery feeds the inner retina, including the ganglion cells and their axons [65, 66]. In addition, as myopia progresses, the diameter of the retinal arteries becomes smaller [57]. Measurement of retinal arterial velocity and the

diameter of major superotemporal or inferotemporal arteries indicate that retinal blood flow decreases in high myopia, mainly due to the narrowing of the retinal vessel diameter [56]. This structural change in myopia may have a negative effect on retinal irrigation.

8.6.2 Hemodynamics of the Choroid in Myopia

Choroidal circulation, especially in the peripapillary area, is important to the study of POAG because the blood supply of the pre-laminar section of the ONH depends on the peripapillary choroid [67]. The elongated axial length of highly myopic eyes causes stretching of the sclera between the disc and the posterior pole, often leading to thinning of the peripapillary choroid. Although it is difficult to directly measure choroidal circulation, choroidal thinning is thought to indicate reduced choroidal circulation [68]. Disturbances in choroidal circulation and stretching of the sclera in highly myopic eyes are also thought to be associated with enlarged areas of peripapillary atrophy [69]. The vascular/hemodynamic theory may also help in understanding choroidal hemodynamics in myopia, as it describes glaucomatous optic neuropathy as an ischemic injury resulting in reduced ocular blood flow at the level of the lamina cribrosa [70].

A number of studies have investigated the association between choroidal hemodynamics and the pathogenesis of glaucoma. Histologic studies have found only an inconsistent association between glaucoma and choroidal thickness [71]. *In vivo* studies of choroidal thickness with optical coherence tomography (OCT) have also had conflicting results. Hirooka et al. reported that peripapillary choroidal thickness was associated with glaucoma, and Usui et al. reported that highly myopic eyes with normal tension glaucoma had greater thinning of the choroid than controls matched for age, spherical equivalent refractive error, and axial length [72]. In contrast, Mwanza et al. reported that there was no association between glaucoma and choroidal thickness, in a study that used enhanced-depth imaging techniques and spectral domain OCT [73]. These conflicting results may be due to differences between the studies in measurement location, the distribution of subjects, and the incidence in the subjects of different types of glaucoma, especially myopic glaucoma. In addition, despite the considerable improvements in ocular posterior segment imaging offered by OCT, *in vivo* assessment of the choroid remains difficult. Data in support of the association between choroidal blood flow and glaucoma is also available from an eye bank histological study showing that eyes with advanced glaucoma have lower capillary density in the choriocapillaris of the macula, temporal peripapillary, and equatorial choroid than control eyes [74]. This may reflect the fact that the pre-laminar region of the ONH is fed by the peripapillary choroid [26–28].

8.6.3 Circulation in the Posterior Ciliary Arteries and the Arterial Circle of Zinn-Haller in Myopic Eyes

The PCAs are the main vessels supplying the ONH and are particularly important sources of circulation supplying the pre-laminar tissue and lamina cribrosa. The status of the PCAs is thus an important indicator of blood flow in glaucoma. CDI data shows that blood velocity in the PCAs is decreased in highly myopic eyes [58]. The occlusion of the para-optic branches of the short PCAs could induce time-dependent deterioration in the area of anoxic segmental degeneration. Thus, the circulation of PCAs is important for understanding the pathogenesis of glaucoma [75].

The peripapillary ZHAC which is fed by the PCAs branches into the intra-laminar region of the ONH and is the major arterial contributor to the vascular system in the lamina cribrosa [28, 76]. In high myopia, the ZHAC is located within the myopic crescent, with the vessels appearing as a hyporeflective circle within the peripapillary sclera. The ZHAC usually has a rhomboid configuration [77].

In a histomorphometric study, the distance of the ZHAC from the peripapillary ring (located at the optic disc border) was found to increase significantly with axial elongation and other related parameters [78, 79]. The distance of the ZHAC from the lamina cribrosa, for which it is the main source of arterial blood, would thus also increase. Although the relationship of alterations to the ZHAC caused by axial elongation and glaucoma is thus not yet fully understood, it is possible that these changes affect the blood supply to the ONH and could serve as an indicator of the onset of glaucoma.

8.7 Impact of Ischemia on Retinal Ganglion Cells

The results of many studies show that ischemia has multiple detrimental effects on the retinal ganglion cells (RGCs) and their axons [80–82]. Mechanisms implicated in RGC death include hypoxia-induced reactive oxygen species (ROS) [83], excitotoxicity, nitric oxide (NO) [84, 85], and the inflammation reaction [86]. There is strong evidence that chronic retinal ischemia also results in a variety of harmful intra-retinal events.

Ischemia and reperfusion induce ROS generation in three phases: in the first phase, mitochondria generate ROS; in the second phase, xanthine oxidase is activated; and in the third phase, Ca2+- dependent ROS generation begins [87]. Investigations of ischemia in RGCs have included ROS generation and cytotoxicity [83] and NO [88]. NO, synthesized by nitric oxide synthase (NOS), has been shown to have neuroprotective and neurotoxic roles [89], and some experiments have shown that NO production contributes to cytotoxicity resulting

in cell death [84, 85]. Excitatory amino acids have been also reported to play an important role in the development of hypoxic-ischemic retinal injury [90, 91]. Glutamate excitotoxicity may also facilitate primary and/or secondary degeneration of the RGCs in glaucoma [92, 93].

Ischemia causes increased permeability of the blood-retinal barrier due to vascular endothelial growth factor, NO, free radicals, and aquaporin-4 protein expression resulting in serum leakage into retinal tissue [94]. The compression induced by tissue edema is thought to occur secondarily and to also be a cause of RGC degeneration [95].

8.8 Conclusion

Glaucoma is a multifactorial disease with a pathogenesis that remains unclear. However, myopia is known to be a major risk factor for glaucoma, and an understanding of myopia's role in glaucoma is important. A number of studies have reported that there is an association between ocular circulation deterioration and myopic morphological change. Elucidation of the effect of myopia on ocular circulation might lead to improved knowledge of the pathogenesis of myopic glaucoma (Fig. 8.3, the summary of this chapter).

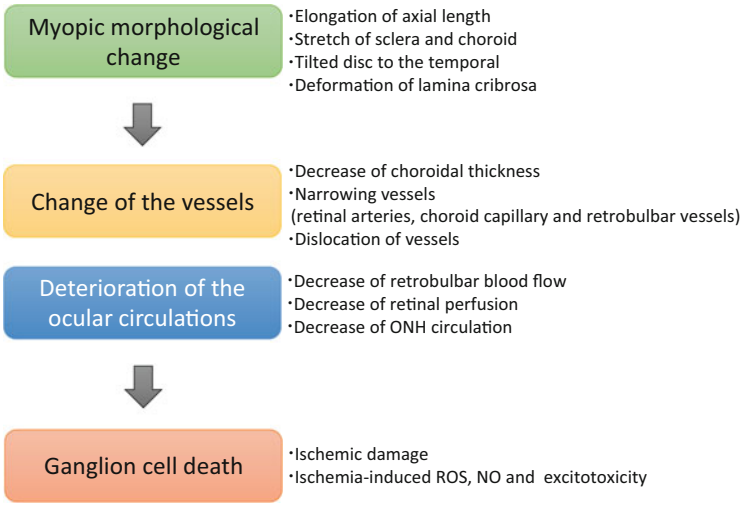

Fig. 8.3 Summary of this chapter: Ocular blood flow in myopic glaucoma

References

1. Quigley HA, Broman AT (2006) The number of people with glaucoma worldwide in 2010 and 2020. Br J Ophthalmol 90(3):262–267. doi:90/3/262 [pii] 10.1136/bjo.2005.081224
2. Kass MA, Heuer DK, Higginbotham EJ, Johnson CA, Keltner JL, Miller JP, Parrish RK 2nd, Wilson MR, Gordon MO (2002) The Ocular Hypertension Treatment Study: a randomized trial determines that topical ocular hypotensive medication delays or prevents the onset of primary open-angle glaucoma. Arch Ophthalmol 120(6):701–713; discussion 829–730. doi: ecs20045 [pii]
3. Comparison of glaucomatous progression between untreated patients with normal-tension glaucoma and patients with therapeutically reduced intraocular pressures. Collaborative Normal-Tension Glaucoma Study Group (1998). Am J Ophthalmol 126 (4):487–497. doi: S0002939498002232 [pii]
4. Leske MC, Heijl A, Hyman L, Bengtsson B, Dong L, Yang Z (2007) Predictors of long-term progression in the early manifest glaucoma trial. Ophthalmology 114(11):1965–1972. doi: S0161-6420(07)00241-2 [pii] 10.1016/j.ophtha.2007.03.016
5. Phelps CD, Corbett JJ (1985) Migraine and low-tension glaucoma. A case-control study. Invest Ophthalmol Vis Sci 26(8):1105–1108
6. Sommer A, Tielsch JM, Katz J, Quigley HA, Gottsch JD, Javitt JC, Martone JF, Royall RM, Witt KA, Ezrine S (1991) Racial differences in the cause-specific prevalence of blindness in east Baltimore. N Engl J Med 325(20):1412–1417. doi:10.1056/NEJM199111143252004
7. Mitchell P, Hourihan F, Sandbach J, Wang JJ (1999) The relationship between glaucoma and myopia: the Blue Mountains Eye Study. Ophthalmology 106(10):2010–2015
8. Xu L, Wang Y, Wang S, Jonas JB (2007) High myopia and glaucoma susceptibility the Beijing Eye Study. Ophthalmology 114(2):216–220. doi:S0161-6420(06)01059-1 [pii] 10.1016/j.ophtha.2006.06.050
9. Leske MC, Wu SY, Hennis A, Honkanen R, Nemesure B (2008) Risk factors for incident open-angle glaucoma: the Barbados Eye Studies. Ophthalmology 115(1):85–93. doi:S0161-6420(07)00242-4 [pii] 10.1016/j.ophtha.2007.03.017
10. Zhao L, Wang Y, Chen CX, Xu L, Jonas JB (2014) Retinal nerve fibre layer thickness measured by Spectralis spectral-domain optical coherence tomography: The Beijing Eye Study. Acta Ophthalmol 92(1):e35–e41. doi:10.1111/aos.12240
11. Scott R, Grosvenor T (1993) Structural model for emmetropic and myopic eyes. Ophthalmic Physiol Opt 13(1):41–47
12. Fong DS, Epstein DL, Allingham RR (1990) Glaucoma and myopia: are they related? Int Ophthalmol Clin 30(3):215–218
13. Newman-Casey PA, Talwar N, Nan B, Musch DC, Stein JD (2011) The relationship between components of metabolic syndrome and open-angle glaucoma. Ophthalmology 118 (7):1318–1326. doi:10.1016/j.ophtha.2010.11.022 S0161-6420(10)01262-5 [pii]
14. Kahn HA, Milton RC (1980) Alternative definitions of open-angle glaucoma. Effect on prevalence and associations in the Framingham eye study. Arch Ophthalmol 98 (12):2172–2177
15. Klein BE, Klein R, Jensen SC (1994) Open-angle glaucoma and older-onset diabetes. The Beaver Dam Eye Study. Ophthalmology 101(7):1173–1177
16. Mitchell P, Smith W, Chey T, Healey PR (1997) Open-angle glaucoma and diabetes: the Blue Mountains eye study, Australia. Ophthalmology 104(4):712–718
17. Bonomi L, Marchini G, Marraffa M, Bernardi P, Morbio R, Varotto A (2000) Vascular risk factors for primary open angle glaucoma: the Egna-Neumarkt Study. Ophthalmology 107 (7):1287–1293. doi:S0161-6420(00)00138-X [pii]
18. de Voogd S, Ikram MK, Wolfs RC, Jansonius NM, Witteman JC, Hofman A, de Jong PT (2006) Is diabetes mellitus a risk factor for open-angle glaucoma? The Rotterdam Study. Ophthalmology 113(10):1827–1831. doi:S0161-6420(06)00692-0 [pii] 10.1016/j.ophtha.2006.03.063

19. Leske MC, Connell AM, Wu SY, Hyman LG, Schachat AP (1995) Risk factors for open-angle glaucoma. The Barbados Eye Study. Arch Ophthalmol 113(7):918–924
20. Tan GS, Wong TY, Fong CW, Aung T (2009) Diabetes, metabolic abnormalities, and glaucoma. Arch Ophthalmol 127(10):1354–1361. doi:10.1001/archophthalmol.2009.268 127/10/1354 [pii]
21. Hayreh SS (1999) The role of age and cardiovascular disease in glaucomatous optic neuropathy. Surv Ophthalmol 43(Suppl 1):S27–S42
22. Graham SL, Drance SM (1999) Nocturnal hypotension: role in glaucoma progression. Surv Ophthalmol 43(Suppl 1):S10–S16
23. Plange N, Kaup M, Daneljan L, Predel HG, Remky A, Arend O (2006) 24-h blood pressure monitoring in normal tension glaucoma: night-time blood pressure variability. J Hum Hypertens 20(2):137–142. doi:1001959 [pii] 10.1038/sj.jhh.1001959
24. Topouzis F, Wilson MR, Harris A, Founti P, Yu F, Anastasopoulos E, Pappas T, Koskosas A, Salonikiou A, Coleman AL (2013) Association of open-angle glaucoma with perfusion pressure status in the Thessaloniki Eye Study. Am J Ophthalmol 155(5):843–851. doi:10.1016/j.ajo.2012.12.007 S0002-9394(12)00861-6 [pii]
25. Sung KR, Lee S, Park SB, Choi J, Kim ST, Yun SC, Kang SY, Cho JW, Kook MS (2009) Twenty-four hour ocular perfusion pressure fluctuation and risk of normal-tension glaucoma progression. Invest Ophthalmol Vis Sci 50(11):5266–5274. doi:10.1167/iovs.09-3716 iovs.09-3716 [pii]
26. Hayreh SS (1975) Segmental nature of the choroidal vasculature. Br J Ophthalmol 59 (11):631–648
27. Hayreh SS (2009) Ischemic optic neuropathy. Prog Retin Eye Res 28(1):34–62. doi:10.1016/j.preteyeres.2008.11.002 S1350-9462(08)00076-1 [pii]
28. Hayreh SS (2001) The blood supply of the optic nerve head and the evaluation of it – myth and reality. Prog Retin Eye Res 20(5):563–593. doi:S1350-9462(01)00004-0 [pii]
29. Lieberman MF, Maumenee AE, Green WR (1976) Histologic studies of the vasculature of the anterior optic nerve. Am J Ophthalmol 82(3):405–423
30. Peyman GA, Apple D (1972) Peroxidase diffusion processes in the optic nerve. Arch Ophthalmol 88(6):650–654
31. Hofman P, Hoyng P, van der Werf F, Vrensen GF, Schlingemann RO (2001) Lack of blood-brain barrier properties in microvessels of the prelaminar optic nerve head. Invest Ophthalmol Vis Sci 42(5):895–901
32. Schmetterer L, Garhofer G (2007) How can blood flow be measured? Surv Ophthalmol 52 (Suppl 2):S134–S138. doi:S0039-6257(07)00185-3 [pii] 10.1016/j.survophthal.2007.08.008
33. Caprioli J, Coleman AL (2010) Blood pressure, perfusion pressure, and glaucoma. Am J Ophthalmol 149(5):704–712. doi:10.1016/j.ajo.2010.01.018 S0002-9394(10)00034-6 [pii]
34. Tomic L, Maepea O, Sperber GO, Alm A (2001) Comparison of retinal transit times and retinal blood flow: a study in monkeys. Invest Ophthalmol Vis Sci 42(3):752–755
35. Schwartz B (1994) Circulatory defects of the optic disk and retina in ocular hypertension and high pressure open-angle glaucoma. Surv Ophthalmol 38(Suppl):S23–S34
36. Wolf S, Arend O, Toonen H, Bertram B, Jung F, Reim M (1991) Retinal capillary blood flow measurement with a scanning laser ophthalmoscope. Preliminary results. Ophthalmology 98 (6):996–1000
37. Feke GT (2006) Laser Doppler instrumentation for the measurement of retinal blood flow: theory and practice. Bull Soc Belge Ophtalmol 302:171–184
38. Liu CJ, Chou YH, Chou JC, Chiou HJ, Chiang SC, Liu JH (1997) Retrobulbar haemodynamic changes studied by colour Doppler imaging in glaucoma. Eye (Lond) 11(Pt 6):818–826. doi:10.1038/eye.1997.212
39. Polska E, Kircher K, Ehrlich P, Vecsei PV, Schmetterer L (2001) RI in central retinal artery as assessed by CDI does not correspond to retinal vascular resistance. Am J Physiol Heart Circ Physiol 280(4):H1442–H1447

40. Harris A, Williamson TH, Martin B, Shoemaker JA, Sergott RC, Spaeth GL, Katz JL (1995) Test/Retest reproducibility of color Doppler imaging assessment of blood flow velocity in orbital vessels. J Glaucoma 4(4):281–286. doi:00061198-199508000-00011 [pii]
41. Riva CE, Harino S, Petrig BL, Shonat RD (1992) Laser Doppler flowmetry in the optic nerve. Exp Eye Res 55(3):499–506. doi:0014-4835(92)90123-A [pii]
42. Krakau CE (1992) Calculation of the pulsatile ocular blood flow. Invest Ophthalmol Vis Sci 33 (9):2754–2756
43. Yang YC, Hulbert MF, Batterbury M, Clearkin LG (1997) Pulsatile ocular blood flow measurements in healthy eyes: reproducibility and reference values. J Glaucoma 6(3):175–179
44. Michelson G, Langhans MJ, Harazny J, Dichtl A (1998) Visual field defect and perfusion of the juxtapapillary retina and the neuroretinal rim area in primary open-angle glaucoma. Graefes Arch Clin Exp Ophthalmol 236(2):80–85
45. Kaiser HJ, Schoetzau A, Stumpfig D, Flammer J (1997) Blood-flow velocities of the extraocular vessels in patients with high-tension and normal-tension primary open-angle glaucoma. Am J Ophthalmol 123(3):320–327
46. Nicolela MT, Hnik P, Drance SM (1996) Scanning laser Doppler flowmeter study of retinal and optic disk blood flow in glaucomatous patients. Am J Ophthalmol 122(6):775–783
47. Harris A, Sergott RC, Spaeth GL, Katz JL, Shoemaker JA, Martin BJ (1994) Color Doppler analysis of ocular vessel blood velocity in normal-tension glaucoma. Am J Ophthalmol 118 (5):642–649
48. Butt Z, McKillop G, O'Brien C, Allan P, Aspinall P (1995) Measurement of ocular blood flow velocity using colour Doppler imaging in low tension glaucoma. Eye (Lond) 9(Pt 1):29–33. doi:10.1038/eye.1995.4
49. Galassi F, Nuzzaci G, Sodi A, Casi P, Vielmo A (1992) Color Doppler imaging in evaluation of optic nerve blood supply in normal and glaucomatous subjects. Int Ophthalmol 16 (4–5):273–276
50. Yamazaki Y, Drance SM (1997) The relationship between progression of visual field defects and retrobulbar circulation in patients with glaucoma. Am J Ophthalmol 124(3):287–295
51. Nicolela MT, Drance SM, Rankin SJ, Buckley AR, Walman BE (1996) Color Doppler imaging in patients with asymmetric glaucoma and unilateral visual field loss. Am J Ophthalmol 121 (5):502–510
52. Garhofer G, Fuchsjager-Mayrl G, Vass C, Pemp B, Hommer A, Schmetterer L (2010) Retrobulbar blood flow velocities in open angle glaucoma and their association with mean arterial blood pressure. Invest Ophthalmol Vis Sci 51(12):6652–6657. doi:10.1167/iovs.10-5490 iovs.10-5490 [pii]
53. Shiga Y, Shimura M, Asano T, Tsuda S, Yokoyama Y, Aizawa N, Omodaka K, Ryu M, Yokokura S, Takeshita T, Nakazawa T (2013) The influence of posture change on ocular blood flow in normal subjects, measured by laser speckle flowgraphy. Curr Eye Res 38(6):691–698. doi:10.3109/02713683.2012.758292
54. Kim TW, Kim M, Weinreb RN, Woo SJ, Park KH, Hwang JM (2012) Optic disc change with incipient myopia of childhood. Ophthalmology 119(1):21–26. doi:S0161-6420(11)00736-6 [pii] 10.1016/j.ophtha.2011.07.051
55. Nakazawa M, Kurotaki J, Ruike H (2008) Longterm findings in peripapillary crescent formation in eyes with mild or moderate myopia. Acta Ophthalmol 86(6):626–629. doi:10.1111/j.1600-0420.2007.01139.x AOS1139 [pii]
56. Shimada N, Ohno-Matsui K, Harino S, Yoshida T, Yasuzumi K, Kojima A, Kobayashi K, Futagami S, Tokoro T, Mochizuki M (2004) Reduction of retinal blood flow in high myopia. Graefes Arch Clin Exp Ophthalmol 242(4):284–288. doi:10.1007/s00417-003-0836-0
57. Wong TY, Knudtson MD, Klein R, Klein BE, Meuer SM, Hubbard LD (2004) Computer-assisted measurement of retinal vessel diameters in the Beaver Dam Eye Study: methodology, correlation between eyes, and effect of refractive errors. Ophthalmology 111(6):1183–1190. doi:10.1016/j.ophtha.2003.09.039 S0161-6420(04)00124-1 [pii]

58. Akyol N, Kukner AS, Ozdemir T, Esmerligil S (1996) Choroidal and retinal blood flow changes in degenerative myopia. Can J Ophthalmol 31(3):113–119
59. Samra WA, Pournaras C, Riva C, Emarah M (2013) Choroidal hemodynamic in myopic patients with and without primary open-angle glaucoma. Acta Ophthalmol 91(4):371–375. doi:10.1111/j.1755-3768.2012.02386.x
60. Broadway DC, Nicolela MT, Drance SM (1999) Optic disk appearances in primary open-angle glaucoma. Surv Ophthalmol 43(Suppl 1):S223–S243
61. Nicolela MT, Drance SM (1996) Various glaucomatous optic nerve appearances: clinical correlations. Ophthalmology 103(4):640–649
62. Nicolela MT, Walman BE, Buckley AR, Drance SM (1996) Various glaucomatous optic nerve appearances. A color Doppler imaging study of retrobulbar circulation. Ophthalmology 103 (10):1670–1679
63. Yokoyama Y, Aizawa N, Chiba N, Omodaka K, Nakamura M, Otomo T, Yokokura S, Fuse N, Nakazawa T (2011) Significant correlations between optic nerve head microcirculation and visual field defects and nerve fiber layer loss in glaucoma patients with myopic glaucomatous disk. Clin Ophthalmol 5:1721–1727. doi:10.2147/OPTH.S23204 opth-5-1721 [pii]
64. Quigley M, Cohen S (1999) A new pressure attenuation index to evaluate retinal circulation. A link to protective factors in diabetic retinopathy. Arch Ophthalmol 117(1):84–89
65. Jonas JB, Nguyen XN, Naumann GO (1989) Parapapillary retinal vessel diameter in normal and glaucoma eyes. I. Morphometric data. Invest Ophthalmol Vis Sci 30(7):1599–1603
66. Jonas JB, Naumann GO (1989) Parapapillary retinal vessel diameter in normal and glaucoma eyes. II. Correlations. Invest Ophthalmol Vis Sci 30(7):1604–1611
67. Anderson DR (1970) Vascular supply to the optic nerve of primates. Am J Ophthalmol 70 (3):341–351
68. Kim M, Kim SS, Kwon HJ, Koh HJ, Lee SC (2012) Association between choroidal thickness and ocular perfusion pressure in young, healthy subjects: enhanced depth imaging optical coherence tomography study. Invest Ophthalmol Vis Sci 53(12):7710–7717. doi:10.1167/iovs.12-10464 iovs.12-10464 [pii]
69. Yasuzumi K, Ohno-Matsui K, Yoshida T, Kojima A, Shimada N, Futagami S, Tokoro T, Mochizuki M (2003) Peripapillary crescent enlargement in highly myopic eyes evaluated by fluorescein and indocyanine green angiography. Br J Ophthalmol 87(9):1088–1090
70. Grunwald JE, Piltz J, Hariprasad SM, DuPont J (1998) Optic nerve and choroidal circulation in glaucoma. Invest Ophthalmol Vis Sci 39(12):2329–2336
71. Nemeth J (1990) The posterior coats of the eye in glaucoma. An echobiometric study. Graefes Arch Clin Exp Ophthalmol 228(1):33–35
72. Usui S, Ikuno Y, Miki A, Matsushita K, Yasuno Y, Nishida K (2012) Evaluation of the choroidal thickness using high-penetration optical coherence tomography with long wavelength in highly myopic normal-tension glaucoma. Am J Ophthalmol 153(1):10–16. doi:10.1016/j.ajo.2011.05.037 S0002-9394(11)00464-8 [pii]
73. Mwanza JC, Hochberg JT, Banitt MR, Feuer WJ, Budenz DL (2011) Lack of association between glaucoma and macular choroidal thickness measured with enhanced depth-imaging optical coherence tomography. Invest Ophthalmol Vis Sci 52(6):3430–3435. doi:10.1167/iovs.10-6600 iovs.10-6600 [pii]
74. Spraul CW, Lang GE, Lang GK, Grossniklaus HE (2002) Morphometric changes of the choriocapillaris and the choroidal vasculature in eyes with advanced glaucomatous changes. Vision Res 42(7):923–932. doi:S0042698902000226 [pii]
75. Hiraoka M, Inoue K, Ninomiya T, Takada M (2012) Ischaemia in the Zinn-Haller circle and glaucomatous optic neuropathy in macaque monkeys. Br J Ophthalmol 96(4):597–603. doi:10.1136/bjophthalmol-2011-300831 bjophthalmol-2011-300831 [pii]
76. Hayreh SS (1969) Blood supply of the optic nerve head and its role in optic atrophy, glaucoma, and oedema of the optic disc. Br J Ophthalmol 53(11):721–748

77. Ohno-Matsui K, Kasahara K, Moriyama M (2013) Detection of Zinn-Haller arterial ring in highly myopic eyes by simultaneous indocyanine green angiography and optical coherence tomography. Am J Ophthalmol 155(5):920–926. doi:10.1016/j.ajo.2012.12.010 S0002-9394(12)00864-1 [pii]
78. Jonas JB, Holbach L, Panda-Jonas S (2013) Peripapillary arterial circle of zinn-haller: location and spatial relationships with myopia. PLoS One 8(11):e78867. doi:10.1371/journal.pone.0078867 PONE-D-13-31070 [pii]
79. Jonas JB, Holbach L, Panda-Jonas S (2014) Peripapillary ring: histology and correlations. Acta Ophthalmol 92(4):e273–e279. doi:10.1111/aos.12324
80. Lafuente MP, Villegas-Perez MP, Selles-Navarro I, Mayor-Torroglosa S, Miralles de Imperial J, Vidal-Sanz M (2002) Retinal ganglion cell death after acute retinal ischemia is an ongoing process whose severity and duration depends on the duration of the insult. Neuroscience 109(1):157–168. doi:S0306452201004584 [pii]
81. Adachi M, Takahashi K, Nishikawa M, Miki H, Uyama M (1996) High intraocular pressure-induced ischemia and reperfusion injury in the optic nerve and retina in rats. Graefes Arch Clin Exp Ophthalmol 234(7):445–451
82. Danylkova NO, Pomeranz HD, Alcala SR, McLoon LK (2006) Histological and morphometric evaluation of transient retinal and optic nerve ischemia in rat. Brain Res 1096(1):20–29. doi:S0006-8993(06)01105-X [pii] 10.1016/j.brainres.2006.04.061
83. Nakayama M, Aihara M, Chen YN, Araie M, Tomita-Yokotani K, Iwashina T (2011) Neuroprotective effects of flavonoids on hypoxia-, glutamate-, and oxidative stress-induced retinal ganglion cell death. Mol Vis 17:1784–1793. doi:195 [pii]
84. Tajes M, Ill-Raga G, Palomer E, Ramos-Fernandez E, Guix FX, Bosch-Morato M, Guivernau B, Jimenez-Conde J, Ois A, Perez-Asensio F, Reyes-Navarro M, Caballo C, Galan AM, Alameda F, Escolar G, Opazo C, Planas A, Roquer J, Valverde MA, Munoz FJ (2013) Nitro-oxidative stress after neuronal ischemia induces protein nitrotyrosination and cell death. Oxid Med Cell Longev 2013:826143. doi:10.1155/2013/826143
85. Mishra OP, Zubrow AB, Ashraf QM, Delivoria-Papadopoulos M (2006) Nuclear Ca(++)-influx, Ca (++)/calmodulin-dependent protein kinase IV activity and CREB protein phosphorylation during post-hypoxic reoxygenation in neuronal nuclei of newborn piglets: the role of nitric oxide. Neurochem Res 31(12):1463–1471. doi:10.1007/s11064-006-9204-x
86. Jo N, Wu GS, Rao NA (2003) Upregulation of chemokine expression in the retinal vasculature in ischemia-reperfusion injury. Invest Ophthalmol Vis Sci 44(9):4054–4060
87. Abramov AY, Scorziello A, Duchen MR (2007) Three distinct mechanisms generate oxygen free radicals in neurons and contribute to cell death during anoxia and reoxygenation. J Neurosci 27(5):1129–1138. doi:27/5/1129 [pii] 10.1523/JNEUROSCI.4468-06.2007
88. Liu B, Neufeld AH (2000) Expression of nitric oxide synthase-2 (NOS-2) in reactive astrocytes of the human glaucomatous optic nerve head. Glia 30(2):178–186. doi:10.1002/(SICI)1098-1136(200004)30:2<178::AID-GLIA7>3.0.CO;2-C
89. Iadecola C (1997) Bright and dark sides of nitric oxide in ischemic brain injury. Trends Neurosci 20(3):132–139. doi:S0166-2236(96)10074-6 [pii]
90. Niyadurupola N, Sidaway P, Ma N, Rhodes JD, Broadway DC, Sanderson J (2013) P2X7 receptor activation mediates retinal ganglion cell death in a human retina model of ischemic neurodegeneration. Invest Ophthalmol Vis Sci 54(3):2163–2170. doi:10.1167/iovs.12-10968 iovs.12-10968 [pii]
91. Lee D, Kim KY, Noh YH, Chai S, Lindsey JD, Ellisman MH, Weinreb RN, Ju WK (2012) Brimonidine blocks glutamate excitotoxicity-induced oxidative stress and preserves mitochondrial transcription factor a in ischemic retinal injury. PLoS One 7(10):e47098. doi:10.1371/journal.pone.0047098 PONE-D-12-10031 [pii]
92. Dreyer EB, Zurakowski D, Schumer RA, Podos SM, Lipton SA (1996) Elevated glutamate levels in the vitreous body of humans and monkeys with glaucoma. Arch Ophthalmol 114(3):299–305

93. Vorwerk CK, Gorla MS, Dreyer EB (1999) An experimental basis for implicating excitotoxicity in glaucomatous optic neuropathy. Surv Ophthalmol 43(Suppl 1):S142–S150
94. Kaur C, Foulds WS, Ling EA (2008) Blood-retinal barrier in hypoxic ischaemic conditions: basic concepts, clinical features and management. Prog Retin Eye Res 27(6):622–647. doi:10.1016/j.preteyeres.2008.09.003 S1350-9462(08)00055-4 [pii]
95. Kaur C, Foulds WS, Ling EA (2008) Hypoxia-ischemia and retinal ganglion cell damage. Clin Ophthalmol 2(4):879–889